Supplementary Information

S.1 Soil properties, soil content, & vegetation biomass

The intact soil cores were initially weighed before incubation and then sieved (2 mm) to separate roots, rocks, and soil material after incubation. Each fraction was weighed, after which the roots and soil were oven-dried at 55 °C to obtain dry weights (Figure S1).

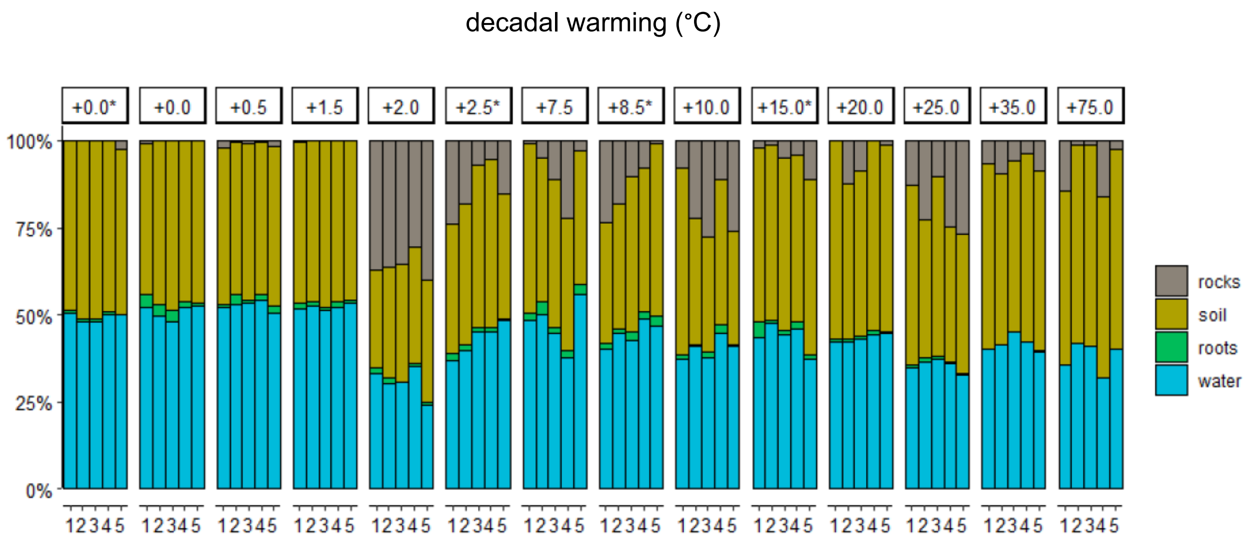

Figure S1. Percentages of water (cyan), roots (green), soil (gold), and rocks (dark grey) per five replicates within each decadal warming level. Decadal warming levels included: ambient (+0.0, 0.0, and 0.5 °C), low (+1.5, 2.0, and 2.5 °C), mid (+7.5, 8.5, and 10.0 °C), mid-high (+15.0 and 20.0 °C), high (+25.0 and 35.0 °C), and hotspot (+75.0 °C).

Composition of intact soil cores is shown as percentages of water, roots, soil, and rocks across the decadal warming gradient (Figure S1). Each bar represents one of five replicate cores per plot per decadal warming level: ambient (+0 °C), low (+1–3 °C), mid (+7–10 °C), mid-high (+15–20 °C), high (+25–35 °C), and hotspot (+75 °C). Root content declined under higher warming, especially at the hotspot, indicating reduced belowground plant biomass. Rock content varied most strongly among levels and between replicates, with one (+2 °C) core containing > 20% rock and < 20% soil.

Methods for determining SOC concentration (%C; Figure 2A) and soil bulk density (g cm^{-3}; Figure 2B) are described in section 2.4 of the main text. Corresponding post-hoc test results provided in Supplementary Tables 1 and 2, respectively.

Table S1. Dunn post-hoc test for SOC content (%C) using Holm adjustments for p-values with pairwise comparisons between decadal warming levels. Adjusted p-values, unadjusted p-values, and standardized Z-values are shown for significant Kruskal–Wallis (chi-squared = 173.7, p = 1.2e-35) ranked data. Comparisons are displayed under the decadal warming level indicated in the table headers.

Dunn Post-hoc Test for SOC Content (%C)						
Pairwise Comparison (p-value, adjusted)						
		Decadal Warming Level				
		Ambient	Low	Mid	Mid-High	High
Decadal Warming Level	Low	1.19e-08	--	--	--	--
Decadal Warming Level	Mid	1.55e-08	9.82e-01	--	--	--
Decadal Warming Level	Mid-High	3.92e-06	1.00e+00	1.00e+00	--	--
Decadal Warming Level	High	2.33e-24	5.29e-07	4.95e-07	1.34e-06	--
Decadal Warming Level	Hotspot	2.80e-25	4.90e-09	4.85e-09	1.40e-08	6.56e-01
Pairwise Comparison (p-value, unadjusted)						
		Decadal Warming Level				
		Ambient	Low	Mid	Mid-High	High
Decadal Warming Level	Low	1.08e-09	--	--	--	--
Decadal Warming Level	Mid	1.72e-09	9.82e-01	--	--	--
Decadal Warming Level	Mid-High	7.84e-07	7.38e-01	7.54e-01	--	--
Decadal Warming Level	High	1.66e-25	6.61e-08	7.08e-08	2.23e-07	--
Decadal Warming Level	Hotspot	1.87e-26	3.77e-10	4.04e-10	1.40e-09	1.64e-01
Standardized Test Statistic (Z-value)						
		Decadal Warming Level				
		Ambient	Low	Mid	Mid-High	High
Decadal Warming Level	Low	6.10	--	--	--	--
Decadal Warming Level	Mid	6.02	-0.022	--	--	--
Decadal Warming Level	Mid-High	4.94	-0.335	-0.313	--	--
Decadal Warming Level	High	10.44	5.40	5.39	5.18	--
Decadal Warming Level	Hotspot	10.64	6.26	6.25	6.06	1.39

Table S2. Dunn post-hoc test for soil bulk density (g cm^{-3}) using Holm adjustments for p-values with pairwise comparisons between decadal warming levels. Adjusted p-values, unadjusted p-values, and standardized Z-values are shown for significant Kruskal–Wallis (chi-squared = 118.3, p = 7.1e-24) ranked data. Comparisons are displayed under the decadal warming level indicated in the table headers.

Dunn Post-hoc Test for Soil Bulk Density (g cm^{-3})						
Pairwise Comparison (p-value, adjusted)						
		Decadal Warming Level				
		Ambient	Low	Mid	Mid-High	High
Decadal Warming Level	Low	1.91e-12	--	--	--	--
	Mid	6.36e-05	3.15e-02	--	--	--
	Mid-High	1.40e-05	3.74e-01	7.31e-01	--	--
	High	3.80e-17	3.83e-02	8.92e-06	1.53e-03	--
	Hotspot	5.53e-14	3.87e-02	4.60e-05	2.53e-03	0.81e-01
Pairwise Comparison (p-value, unadjusted)						
		Decadal Warming Level				
		Ambient	Low	Mid	Mid-High	High
Decadal Warming Level	Low	1.47e-13	--	--	--	--
	Mid	7.07e-06	5.25e-03	--	--	--
	Mid-High	1.28e-06	1.25e-01	3.65e-01	--	--
	High	2.53e-18	7.65e-03	7.43e-07	1.92e-04	--
	Hotspot	3.95e-15	9.67e-03	4.60e-06	3.61e-04	0.81 e-01
Standardized Test Statistic (Z-value)						
		Decadal Warming Level				
		Ambient	Low	Mid	Mid-High	High
Decadal Warming Level	Low	-7.39	--	--	--	--
	Mid	-4.49	2.79	--	--	--
	Mid-High	-4.84	1.54	-9.05	--	--
	High	-8.73	-2.67	-4.95	-3.73	--
	Hotspot	-7.86	-2.59	-4.58	-3.57	-0.23

Medians with standard error (SE) were calculated for SOC concentration (kg C m^{-3}), above ground and total vegetation biomass stock (kg m^{-2}), soil total nitrogen (%N), soil total phosphorus (mg P kg^{-1} soil), soil carbon to nitrogen (%C:%N), and soil pH, respectively. To test for differences among decadal warming levels, each variable was analyzed using a Kruskal–Wallis rank sum omnibus test with five degrees of freedom, implemented through the "kruskal.test" function in the R stats (version 3.6.2) package. When significant outcomes were detected, pairwise comparisons were conducted with Dunn's post-hoc test via the "dunnTest" function in the FSA (version 0.9.5) package, applying Holm-adjusted p-values to account for family-wise error. The test provided standardized Z-statistics and adjusted p-values for each comparison, which were then used to assign compact letter displays (CLDs) to indicate statistically distinct groups in the figures.

SOC concentrations (kg C m^{-3}; Figure S2) were calculated by correcting SOC concentrations (%C; Figure 2A) with soil bulk density (g cm^{-3}; Figure 2B) by converting %C concentrations to g C 100 g dry $soil^{-1}$ and then multiplying by the soil bulk density. This correction excluded the fixed 3 cm core depth used in SOC stock (kg C m^{-2}; Figure 2C) estimates. Because the only distinction between SOC concentration (kg C m^{-3}) and stock (kg C m^{-2}) calculation was the exclusion or inclusion of a constant core depth, their pairwise statistics were identical (Table S3). However, these statistics differed from those of the uncorrected SOC concentrations (%C; Table S1), as both SOC and soil bulk density co-varied in the corrected estimates.

SOC concentrations (kg C m^{-3}) retained a statistically significant decline with increasing decadal warming level (Figure S2 & Table S3; chi-squared = 171.90, p = 2.9e-35). Median SOC concentration in ambient plots (+0 °C) was 44.3 ± 0.7 kg C m^{-3}, which dropped to 42.2 ± 0.9 kg C m^{-3} in the +1–3 °C decadal warming level. A more pronounced decline occurred at +7–10 °C (35.8 ± 0.4 kg C m^{-3}), but concentrations exhibited a slight resurgence at +15–20 °C (37.4 ± 0.6 kg C m^{-3}). Although raw SOC concentrations in %C continued to decline, the concurrent rise in bulk density at the +15–20 °C marginally offset this loss, resulting in this modest rebound in SOC concentration (kg C m^{-3}) at this mid-high decadal warming level. These then dropped further at +25–35 °C to 26.3 ± 0.5 kg C m^{-3}, before reaching the minimum at the geothermal hotspot (+75 °C) with a median of 15.7 ± 0.6 kg C m^{-3}.

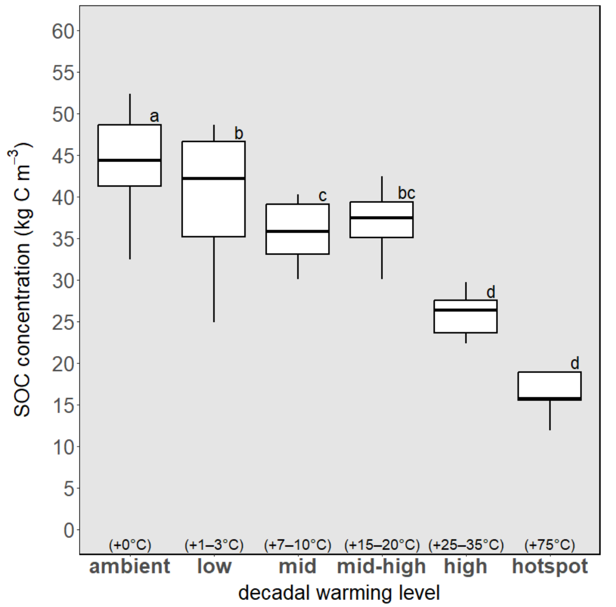

Figure S2. SOC concentrations (kg C m^{-3}) for each decadal warming level. Medians per level indicated by a black line across each box with the interquartile range of point distribution from 25 to 75 percent from the median as box upper and lower limits, and 95% upper and lower standard errors shown as black bars above and below each box. Data outliers that fall outside the bounds of the standard errors are plotted as independent black points. Kruskal-Wallis rank sum omnibus tests gave a chi-squared = 171.9 and a p-value = 2.9e-35. Compact letter display (CLD) in the top right of boxes indicate significant differences ($p \leq 0.05$) between groups.

Table S3. Dunn post-hoc test for SOC concentration (kg C m^{-3}) and stock (kg C m^{-2}) using Holm adjustments for p-values with pairwise comparisons between decadal warming levels. Adjusted p-values, unadjusted p-values, and standardized Z-values are shown for significant Kruskal–Wallis (chi-squared = 171.9, p = 2.9e-35) ranked data with a one-factorial layout for non-normally distributed residuals. Comparisons are displayed under the decadal warming level indicated in the table headers.

Dunn Post-hoc Test for SOC Concentration (kg C m^{-3}) and Stock (kg C m^{-2})

Pairwise Comparison (p-value, adjusted)

Decadal Warming Level		Decadal Warming Level: Ambient	Low	Mid	Mid-High	High
	Low	3.51e-03	--	--	--	--
	Mid	6.28e-10	6.68e-03	--	--	--
	Mid-High	4.94e-05	3.95e-01	4.31e-01	--	--
	High	7.56e-23	4.71e-12	2.56e-05	1.01e-06	--
	Hotspot	3.85e-23	1.68e-13	5.52e-07	2.14e-08	2.17e-01

Pairwise Comparison (p-value, unadjusted)

Decadal Warming Level		Decadal Warming Level: Ambient	Low	Mid	Mid-High	High
	Low	7.02e-04	--	--	--	--
	Mid	5.71e-11	1.67e-03	--	--	--
	Mid-High	8.23e-06	1.32e-01	2.16e-01	--	--
	High	5.40e-24	3.92e-13	3.66e-06	1.26e-07	--
	Hotspot	2.57e-24	1.29e-14	6.14e-08	2.14e-09	2.17e-01

Standardized Test Statistic (Z-value)

Decadal Warming Level		Decadal Warming Level: Ambient	Low	Mid	Mid-High	High
	Low	3.39	--	--	--	--
	Mid	6.55	3.14	--	--	--
	Mid-High	4.46	1.51	-1.24	--	--
	High	1.01	7.26	4.63	5.28	--
	Hotspot	1.02	7.71	5.41	5.99	1.23

Prior to soil core collection, all aboveground vegetation within the 6 cm diameter soil sample ring area was clipped at the soil surface and placed directly into 20 × 25 cm paper sampling bags for later biomass determination. After sampling was finished, sample bags containing the aboveground vegetation were oven-dried at 55 °C for a minimum of 96 h. The dried samples were then weighed to log their dry masses. During soil core extraction, any roots extending below the base of the 3 cm high sample ring were trimmed off ensuring that only the root biomass and other soil constituents within the intact core were retained. Details on the storage of the intact cores before incubation and their maintenance during the experiments are provided in Sections 2.2 of the main text. Following incubation, the roots that were separated from the rest of the soil core samples in the sieving (2 mm) process were placed in 15 x 20 cm paper sampling bags. These root sample bags were then oven-dried at 55 °C for a minimum of 96 h, and once removed from the oven they were weighed. Total vegetation biomass was attained by summing each sample's aboveground and belowground (root) dry masses. Aboveground and total biomass values in g were then normalized to the sampled area to derive vegetation biomass stocks in kg m^{-2}.

Vegetation biomass stock (kg m^{-2}) increased significantly with decadal warming up to +15–20 °C, before declining below ambient at the high and hotspot levels (Figure S3; chi-squared = 162.0, p = 3.8e-33). Median total biomass rose from 3.6 ± 0.1 kg m^{-2} in ambient plots to 5.7 ± 0.2 kg m^{-2} at +15–20 °C, while aboveground biomass increased from 3.5 ± 0.2 to 5.5 ± 0.3 kg m^{-2} over the same range. Total and aboveground biomass actually peaked in the +1–3 °C decadal warming level with median stocks of 6.7 ± 0.2 and 6.5 ± 0.2 kg m^{-2}, respectively. At the hotspot, both total and aboveground biomass declined sharply to 1.6 ± 0.1 kg m^{-2}. These values were significantly lower than all other treatments, and were actually the lowest for all decadal warming levels. Post-hoc tests confirmed that vegetation biomass at +15–20 °C was significantly higher than at ambient, low, and hotspot levels, but not distinguishable from +7–10 °C (Table S4). This pattern suggests that moderate warming enhanced plant growth and biomass accumulation, but extreme warming suppressed vegetation productivity, likely due to shifts toward stress-tolerant, low-biomass plant communities. Importantly, the increase in biomass at intermediate warming levels did not translate into higher SOC stock, indicating that decomposition processes outpaced OM inputs under prolonged warming.

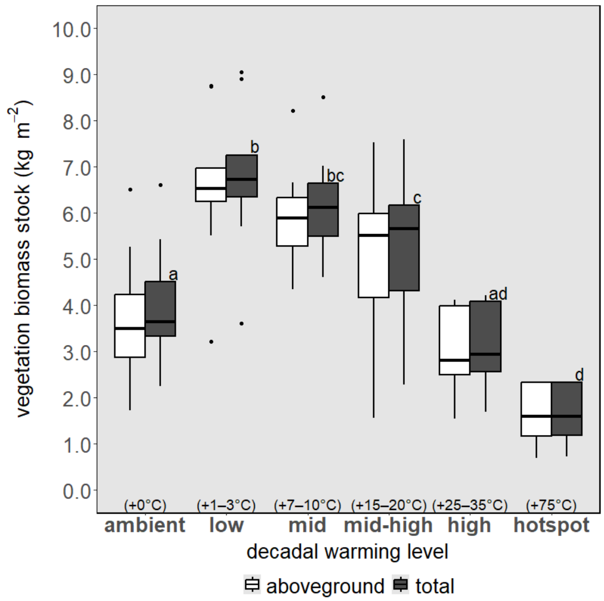

Figure S3. Vegetation biomass stock (kg m^{-2}) for each decadal warming level. Above ground stock show in light grey and total (above and below ground) stock shown in dark grey. Medians per level indicated by a black line across each box with the interquartile range of point distribution from 25 to 75 percent from the median as box upper and lower limits, and 95% upper and lower standard errors shown as black bars above and below each box. Data outliers that fall outside the bounds of the standard errors are plotted as independent black points. Kruskal-Wallis rank sum omnibus tests gave a chi-squared = 162.0 and a *p*-value = 3.8e-33. Compact letter display (CLD) in the top right of boxes indicate significant differences ($p \leq 0.05$) between groups.

Table S4. Dunn post-hoc test for vegetation biomass stock (kg m^{-2}) using Holm adjustments for p-values with pairwise comparisons between decadal warming levels. Adjusted p-values, unadjusted p-values, and standardized Z-values are shown for significant Kruskal–Wallis (chi-squared = 162.0, p = 3.8e-33) ranked data with a one-factorial layout for non-normally distributed residuals. Comparisons are displayed under the decadal warming level indicated in the table headers.

Dunn Post-hoc Test for Vegetation Biomass Stock (kg m^{-2})

Pairwise Comparison (p-value, adjusted)

		Decadal Warming Level				
		Ambient	Low	Mid	Mid-High	High
Decadal Warming Level	Low	5.14e-14	--	--	--	--
	Mid	2.10e-11	3.04e-01	--	--	--
	Mid-High	9.11e-04	3.33e-03	6.79e-02	--	--
	High	2.61e-01	3.40e-13	9.48e-11	1.75e-04	--
	Hotspot	7.82e-04	7.24e-20	2.69e-17	1.41e-09	4.57e-02

Pairwise Comparison (p-value, unadjusted)

		Decadal Warming Level				
		Ambient	Low	Mid	Mid-High	High
Decadal Warming Level	Low	3.96e-15	--	--	--	--
	Mid	1.91e-12	1.52e-01	--	--	--
	Mid-High	1.30e-04	6.65e-04	2.26e-02	--	--
	High	2.61e-01	2.84e-14	9.48e-12	2.19e-05	--
	Hotspot	1.30e-04	4.83e-21	1.92e-18	1.56e-10	1.14e-02

Standardized Test Statistic (Z-value)

		Decadal Warming Level				
		Ambient	Low	Mid	Mid-High	High
Decadal Warming Level	Low	-7.86	--	--	--	--
	Mid	-7.04	1.43	--	--	--
	Mid-High	-3.83	3.40	2.28	--	--
	High	1.13	7.61	6.81	4.25	--
	Hotspot	3.83	9.41	8.76	6.40	2.53

The milled sub-sample of dry soil (3 g; Planetary Ball Mill PM 400, RETSCH, Germany) for SOC concentration analysis was also used to determine soil total nitrogen (N) concentrations (%N). For this analysis, 50 mg of milled soil was analyzed with a FlashEA Nitrogen and Carbon Analyzer (Thermo Scientific, Denmark), again, using the same standard combustion procedure employed in the SOC concentration (%C) assessments.

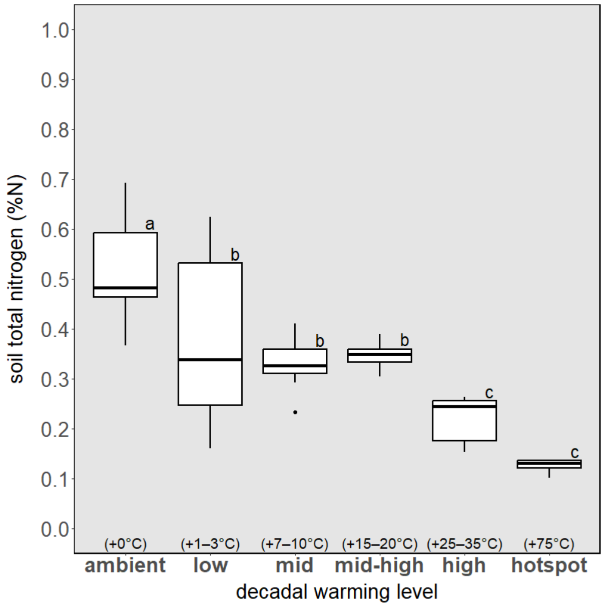

Figure S4. Soil total nitrogen (%N) for each decadal warming level. Medians per level indicated by a black line across each box with the interquartile range of point distribution from 25 to 75 percent from the median as box upper and lower limits, and 95% upper and lower standard errors shown as black bars above and below each box. Data outliers that fall outside the bounds of the standard errors are plotted as independent black points. Kruskal-Wallis rank sum omnibus tests gave a chi-squared = 173.0 and a *p*-value = 1.8e-35. Compact letter display (CLD) in the top right of boxes indicate significant differences ($p \leq 0.05$) between groups.

Soil total nitrogen concentrations (%N) declined significantly (chi-squared = 173.0, p = 1.8e-35) with increasing decadal warming (Figure S4 & Table S5). Median values decreased from 0.48 ± 0.01% in ambient plots (+0 °C) to 0.34 ± 0.02% at the low (+1–3 °C), 0.33 ± 0.01% at the mid (+7–10 °C), and 0.34 ± 0.01% at the mid-high (+15–20 °C) decadal warming levels. Concentrations then declined further at the high warming level (+25–35 °C) to 0.24 ± 0.01% before reaching the minimum at the hotspot (+75 °C) with 0.13 ± 0.00%. Post-hoc comparisons confirmed that soil total nitrogen concentrations (%N) in hotspot plots were significantly lower than all other warming levels, while mid and mid-high plots did not differ from one another (Table S5).

Table S5. Dunn post-hoc test for soil total nitrogen (%N) using Holm adjustments for p-values with pairwise comparisons between decadal warming levels. Adjusted p-values, unadjusted p-values, and standardized Z-values are shown for significant Kruskal–Wallis (chi-squared = 173.0, p = 1.8e-35) ranked data with a one-factorial layout for non-normally distributed residuals. Comparisons are displayed under the decadal warming level indicated in the table headers.

Dunn Post-hoc Test for Soil Total Nitrogen (%N)

Pairwise Comparison (p-value, adjusted)

Decadal Warming Level		Ambient	Low	Mid	Mid-High	High
	Low	1.13e-09	--	--	--	--
	Mid	5.03e-11	1.00e+00	--	--	--
	Mid-High	1.36e-06	7.10e-01	1.00e+00	--	--
	High	9.76e-23	1.51e-05	9.0e-05	2.41e-05	--
	Hotspot	2.72e-26	5.85e-09	5.50e-08	1.60e-08	2.51e-01

Pairwise Comparison (p-value, unadjusted)

Decadal Warming Level		Ambient	Low	Mid	Mid-High	High
	Low	9.38e-11	--	--	--	--
	Mid	3.87e-12	6.08e-01	--	--	--
	Mid-High	1.70e-07	7.10e-01	4.14e-01	--	--
	High	6.97e-24	2.16e-06	1.80e-05	4.02e-06	--
	Hotspot	1.81e-27	5.32e-10	6.11e-09	1.60e-09	6.27e-02

Standardized Test Statistic (Z-value)

Decadal Warming Level		Ambient	Low	Mid	Mid-High	High
	Low	6.48	--	--	--	--
	Mid	6.94	0.51	--	--	--
	Mid-High	5.23	-0.37	-0.82	--	--
	High	10.08	4.74	4.29	4.61	--
	Hotspot	10.86	6.21	5.81	6.03	1.86

With declines in soil total nitrogen concentration (%N; Figure S4) more-or-less paralleling the rate of loss in SOC concentration (%C; Figure 2A), soil total carbon to nitrogen ratios (%C:%N) remained comparatively balanced under increasing decadal warming (Figure S5 & Table S6; chi-squared = 68.7, p = 1.9e-13). Across most warming levels, median total carbon to nitrogen ratios fell within a range of 12.7 to 13.9 (i.e., just above or below ~13). An exception occurred at high decadal warming (+25–35 °C) where the most ratios at this level landed below the otherwise stable total carbon to nitrogen range. Under these conditions the median was actually 11.7 ± 0.2, indicating SOC concentrations (%C) were being depleted slightly faster than soil total nitrogen concentrations (%N). Conversely, at the mid decadal warming level (+7–10 °C) total nitrogen concentrations (%N) were maintained despite a modest rebound in SOC concentrations (%C). This produced the highest median ratio of 13.9 ± 0.1, although values from this level still mainly aligned with the consistent, relative ratio of ~13 observed across the decadal warming gradient.

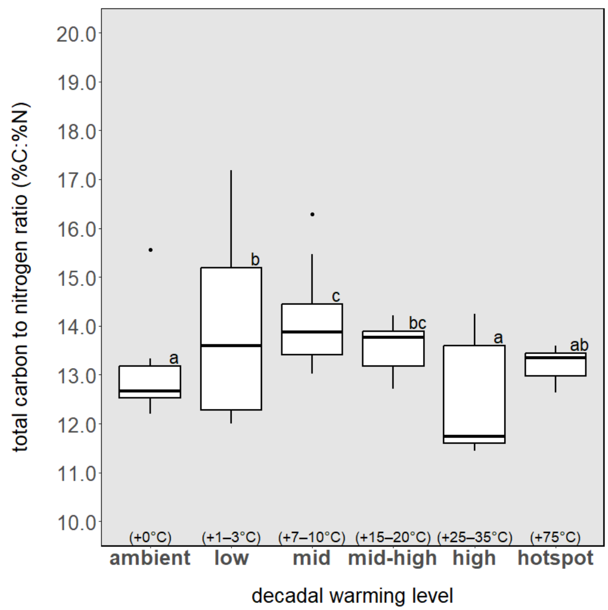

Figure S5. Soil total carbon to nitrogen (%C:%N) for each decadal warming level. Medians per level indicated by a black line across each box with the interquartile range of point distribution from 25 to 75 percent from the median as box upper and lower limits, and 95% upper and lower standard errors shown as black bars above and below each box. Data outliers that fall outside the bounds of the standard errors are plotted as independent black points. Kruskal-Wallis rank sum omnibus tests gave a chi-squared = 68.7 and a p-value = 1.9e-13. Compact letter display (CLD) in the top right of boxes indicate significant differences ($p \leq 0.05$) between groups.

Table S6. Dunn post-hoc test for soil total carbon to nitrogen (%C:%N) using Holm adjustments for p-values with pairwise comparisons between decadal warming levels. Adjusted p-values, unadjusted p-values, and standardized Z-values are shown for significant Kruskal–Wallis (chi-squared = 68.7, p = 1.9e-13) ranked data with a one-factorial layout for non-normally distributed residuals. Comparisons are displayed under the decadal warming level indicated in the table headers.

Dunn Post-hoc Test for Soil Total Carbon to Nitrogen (%C:%N)

Pairwise Comparison (p-value, adjusted)

Decadal Warming Level	Ambient	Low	Mid	Mid-High	High
Low	1.72e-03	--	--	--	--
Mid	4.18e-11	1.14e-02	--	--	--
Mid-High	1.25e-04	7.64e-01	3.99e-01	--	--
High	6.16e-01	3.82e-03	1.03e-08	3.30e-04	--
Hotspot	4.66e-01	6.37e-01	9.13e-03	4.38e-01	4.22e-01

Pairwise Comparison (p-value, unadjusted)

Decadal Warming Level	Ambient	Low	Mid	Mid-High	High
Low	1.56e-04	--	--	--	--
Mid	2.79e-12	1.42e-03	--	--	--
Mid-High	9.63e-06	2.55e-01	9.97e-02	--	--
High	6.16e-01	3.82e-04	7.33e-10	2.75e-05	--
Hotspot	9.32e-02	3.18e-01	1.01e-03	7.30e-02	6.02e-02

Standardized Test Statistic (Z-value)

Decadal Warming Level	Ambient	Low	Mid	Mid-High	High
Low	-3.78	--	--	--	--
Mid	-6.99	-3.19	--	--	--
Mid-High	-4.43	-1.14	1.65	--	--
High	0.50	3.55	6.16	4.19	--
Hotspot	-1.68	1.00	3.29	1.79	-1.88

Soil total phosphorus concentrations (mg P kg soil^{-1}) were also measured by separating 1.2 mg of dried, 2 mm sieved soil from each sample. After this, 30 ml of 0.1 M H_2SO_4 solution was added, and samples were agitated for 2 hours before they were transferred to a centrifuge for 10 minutes at 2000 RPM. They were then filtered through a 0.45µ membrane filter before being analyzed through a color detection process using a SEAL AA500 AutoAnalyzer (Seal Analytical, Global) to extract the total phosphorus concentration within the sample.

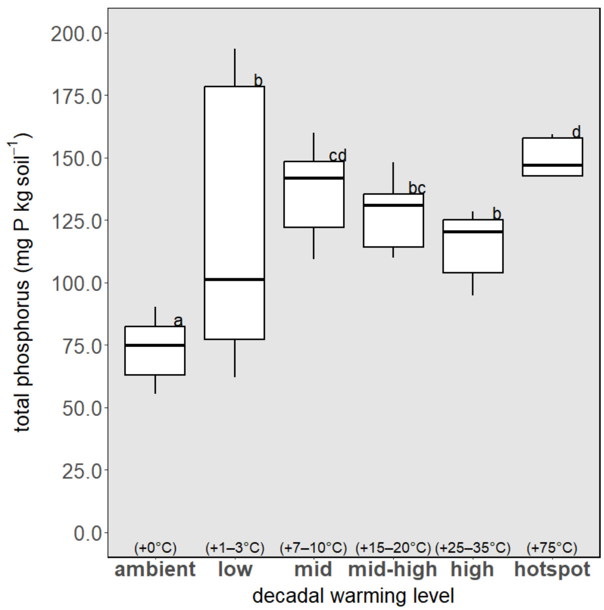

Figure S6. Soil total phosphorus (mg P kg soil^{-1}) for each decadal warming level. Medians per level indicated by a black line across each box with the interquartile range of point distribution from 25 to 75 percent from the median as box upper and lower limits, and 95% upper and lower standard errors shown as black bars above and below each box. Data outliers that fall outside the bounds of the standard errors are plotted as independent black points. Kruskal-Wallis rank sum omnibus tests gave a chi-squared = 147.7 and a *p*-value = 4.1e-30. Compact letter display (CLD) in the top right of boxes indicate significant differences ($p \leq 0.05$) between groups.

Total soil phosphorus concentrations in mg P kg soil^{-1} showed an increase with decadal warming level signifying up-concentration as the other elements are lost (Figure S6 & Table S7). Soil total phosphorus concentrations (mg P kg soil^{-1}) increased significantly with decadal warming (chi-squared = 147.7, p = 4.1e-30). Median concentrations rose from 74.6 ± 1.5 mg P kg^{-1} in ambient soils (+0 °C) to 101.0 ± 6.6 mg P kg^{-1} at the low decadal warming level (+1–3 °C), and further to 141.9 ± 2.2 mg P kg^{-1} at the mid (+7–10 °C) decadal warming level. Concentrations then fell at the mid-high decadal warming level (+15–20 °C) with 130.9 ± 2.1 mg P kg^{-1} before declining further at the high level (+25–35 °C; 120.2 ± 2.1 mg P kg^{-1}). The highest median concentration was observed at the geothermal hotspot (+75 °C) with 147.0 ± 1.6 mg P kg^{-1}. Post-hoc comparisons indicated that ambient plots were significantly lower than all warming treatments, while the hotspot differed significantly from the mid-high and high levels but not from the mid treatment (Table S7). These results suggest that phosphorus accumulated progressively along the warming gradient, with strongest concentrations at the hotspot. Together with the concurrent declines in SOC and total soil nitrogen concentrations, the increase in soil total phosphorus highlights divergent nutrient responses to decadal warming exposure, pointing toward a slight enrichment of P as C and N are lost through decomposition and other soil processes.

Table S7. Dunn post-hoc test for soil total phosphorus (mg P kg $soil^{-1}$) using Holm adjustments for p-values with pairwise comparisons between decadal warming levels. Adjusted p-values, unadjusted p-values, and standardized Z-values are shown for significant Kruskal–Wallis (chi-squared = 147.7, p = 4.1e-30) ranked data with a one-factorial layout for non-normally distributed residuals. Comparisons are displayed under the decadal warming level indicated in the table headers.

Dunn Post-hoc Test for Soil Total Phosphorus (mg P kg $soil^{-1}$)						
Pairwise Comparison (p-value, adjusted)						
		Decadal Warming Level				
		Ambient	Low	Mid	Mid-High	High
Decadal Warming Level	Low	4.38e-10	--	--	--	--
	Mid	4.04e-24	1.29e-03	--	--	--
	Mid-High	6.25e-12	2.75e-01	3.52e-01	--	--
	High	2.70e-06	8.09e-01	5.74e-03	4.09e-01	--
	Hotspot	1.25e-18	1.26e-04	4.07e-01	2.16e-02	3.77e-04
Pairwise Comparison (p-value, unadjusted)						
		Decadal Warming Level				
		Ambient	Low	Mid	Mid-High	High
Decadal Warming Level	Low	3.65e-11	--	--	--	--
	Mid	2.69e-25	1.61e-04	--	--	--
	Mid-High	4.81e-13	1.38e-01	7.03e-02	--	--
	High	2.46e-07	8.09e-01	8.21e-04	1.36e-01	--
	Hotspot	8.95e-20	1.26e-05	1.02e-01	3.60e-03	4.19e-05
Standardized Test Statistic (Z-value)						
		Decadal Warming Level				
		Ambient	Low	Mid	Mid-High	High
Decadal Warming Level	Low	-6.62	--	--	--	--
	Mid	-10.39	-3.77	--	--	--
	Mid-High	-7.23	-1.49	1.81	--	--
	High	-5.16	0.24	3.35	1.49	--
	Hotspot	-9.10	-4.37	-1.64	-2.91	-4.10

Soil pH of each sample was measured by mixing 10 grams of < 2 mm, dry soil from each sample with 50 milliliters of 0.01M $CaCl_2$ solution. After shaking for two hours, the pH was measured using a computer operated 855 Robotic Titrosampler (Metrohm, Denmark).

Soil pH exhibited statistically significant differences across the warming gradient (Figure S7; chi-squared = 158.1, p = 2.5e-32), but the absolute changes were minor. Median values increased only slightly from 5.16 ± 0.02 in ambient plots (+0 °C) to 5.96 ± 0.02 at the hotspot (+75 °C), with most intermediate treatments falling within a narrow range of 5.3–5.6. While post-hoc tests (Table S8) detected significant contrasts between some decadal warming levels, these differences reflect subtle shifts of ≤ 1 pH unit, indicating that soil acidity was largely stable despite pronounced differenced in decadal warming.

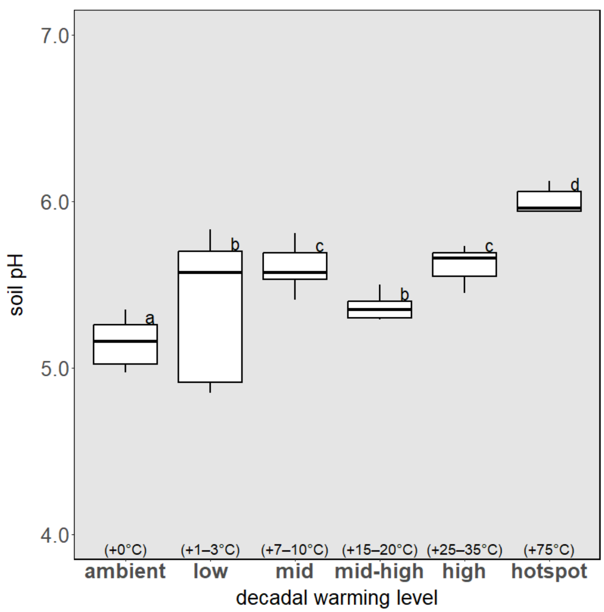

Figure S7. Soil pH for each decadal warming level. Medians per level indicated by a black line across each box with the interquartile range of point distribution from 25 to 75 percent from the median as box upper and lower limits, and 95% upper and lower standard errors shown as black bars above and below each box. Data outliers that fall outside the bounds of the standard errors are plotted as independent black points. Kruskal-Wallis rank sum omnibus tests gave a chi-squared = 158.1 and a p-value = 2.5e-32. Compact letter display (CLD) in the top right of boxes indicate significant differences ($p \leq 0.05$) between groups.

Table S8. Dunn post-hoc test for soil pH using Holm adjustments for p-values with pairwise comparisons between decadal warming levels. Adjusted p-values, unadjusted p-values, and standardized Z-values are shown for significant Kruskal–Wallis (chi-squared = 158.1, p = 2.5e-32) ranked data with a one-factorial layout for non-normally distributed residuals. Comparisons are displayed under the decadal warming level indicated in the table headers.

Dunn Post-hoc Test for Soil pH

Pairwise Comparison (p-value, adjusted)

Decadal Warming Level	Decadal Warming Level: Ambient	Low	Mid	Mid-High	High
Low	2.87e-08	--	--	--	--
Mid	1.32e-17	1.45e-02	--	--	--
Mid-High	1.59e-02	6.07e-02	2.52e-05	--	--
High	4.12e-12	4.91e-02	9.94e-01	3.94e-04	--
Hotspot	1.11e-24	4.61e-09	2.91e-04	1.35e-12	1.20e-03

Pairwise Comparison (p-value, unadjusted)

Decadal Warming Level	Decadal Warming Level: Ambient	Low	Mid	Mid-High	High
Low	2.87e-09	--	--	--	--
Mid	9.44e-19	3.63e-03	--	--	--
Mid-High	3.18e-03	3.04e-02	2.80e-06	--	--
High	3.43e-13	1.64e-02	9.94e-01	5.63e-05	--
Hotspot	7.41e-26	4.19e-10	3.64e-05	1.04e-13	2.00e-04

Standardized Test Statistic (Z-value)

Decadal Warming Level	Decadal Warming Level: Ambient	Low	Mid	Mid-High	High
Low	-5.94	--	--	--	--
Mid	-8.84	-2.91	--	--	--
Mid-High	-2.95	2.17	4.69	--	--
High	-7.28	-2.40	0.01	-4.03	--
Hotspot	-10.51	-6.25	-4.13	-7.44	-3.72

S.2 Observed and modeled R_s

How fluxes were calculated can be found in section 2.5 of the main text. Soil respiration per gram dry soil (F_S; µg CO_2–C g soil^{-1} h^{-1}) followed the same trend as area-based soil respiration (F_A; µmol CO_2 m^{-2} s^{-1}) and not soil respiration normalized by SOC content (F_C; µg CO_2–C g SOC^{-1} h^{-1}). These findings are consistent with bulk SOC depletion being the primary factor underlying reduced respiration.

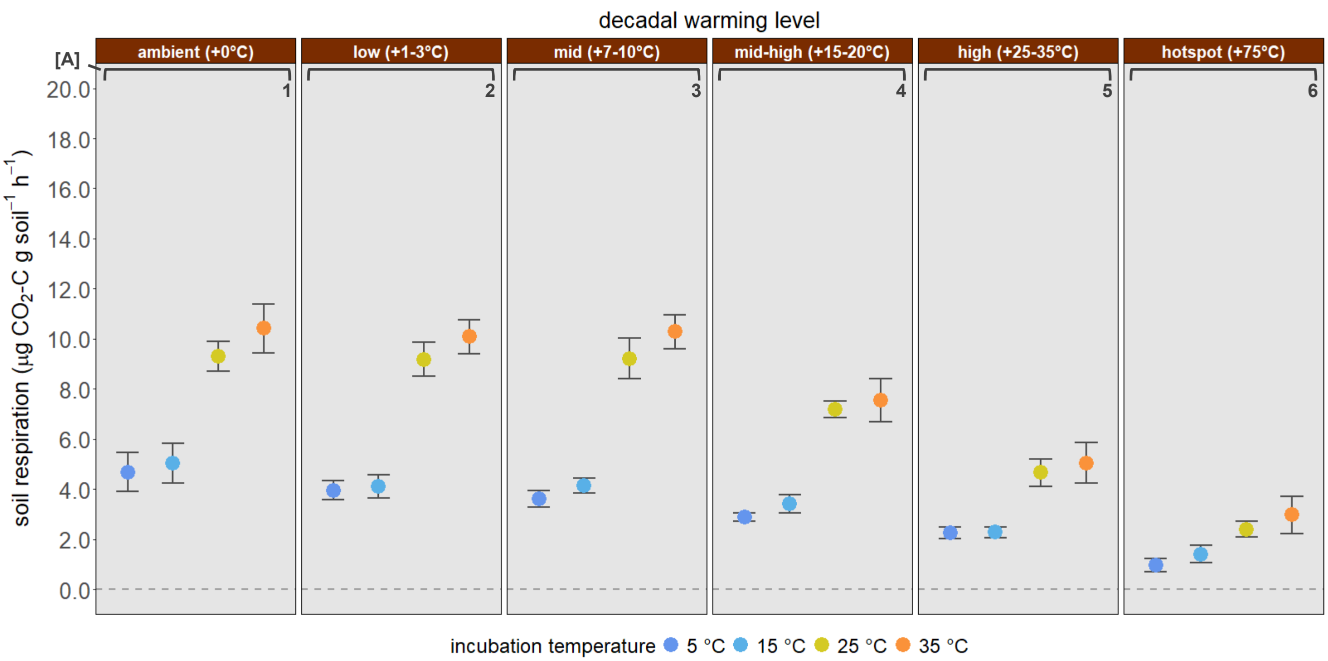

Figure S8. Mean soil respiration rates by gram soil in µg CO_2–C g soil^{-1} h^{-1} for each incubation temperature (indigo = 5 °C, blue = 15 °C, lime-green = 25 °C, orange = 35 °C) with standard error indicated by the black bars.

Area-based and SOC-normalized soil respiration was modeled, with specific model parameter values given in Table S9 for area-based estimates and Supplementary 10 for SOC-normalized estimates.

Table S9. Model parameter values for the Van't Hoff, Lloyd-Taylor and sigmoidal models for soil respiration by area (µmol CO_2 m^{-2} s^{-1}) response to direct, stepwise temperature increase. In the global (i.e. site-level) Van't Hoff, Lloyd-Taylor, and sigmoidal models, all parameters were fitted using all the data(white) and for group parameter fitted models (i.e. fitted by treatment) parameters were fitted by decadal warming level indicated in greyscale from ambient (lightest) to hotspot (darkest). Best model for each of the three model types, i.e. with lowest AICc, indicated in bold and the best of all three, i.e. lowest AICc for all models preformed, indicated by asterisks (**) next to model number.

Van't Hoff Fitted Model Parameters

model no.	***R₀***						***β***					
1	1.403						0.033					
2	**1.874**	**1.688**	**1.632**	**1.525**	**1.040**	**0.663**	**0.033**					
3	1.492						0.040	0.037	0.036	0.033	0.020	0.004
4	1.984	1.599	1.532	1.551	1.156	0.610	0.031	0.035	0.035	0.032	0.029	0.036

Lloyd-Taylor Fitted Model Parameters

model no.	***R₀***						***β***						***d***					
1	35.531						-186.973						219.336					
2	**47.918**	**43.187**	**41.749**	**39.049**	**26.589**	**16.971**	**-188.621**						**219.001**					
3	86.208						-303.260	-314.352	-317.830	-324.416	-363.821	-410.910	196.282					
4	2116.321						-1270.429						93.040	96.599	97.686	99.720	111.017	123.007
5	39.326	49.275	48.625	36.931	19.091	20.596	-171.080	-197.296	-198.938	-182.347	-160.487	-202.223	219.771					
6	42.824	45.194	44.063	37.649	22.227	18.271	-184.457						216.867	222.219	222.490	219.524	214.384	223.112
7	41.638						-180.563	-172.846	-176.515	-199.075	-298.004	-320.446	217.578	224.469	223.996	216.827	193.109	200.851
8	79.058	44.298	48.222	20.213	45.907	15.313	-291.322	-181.570	-197.686	-102.944	-318.058	-160.107	197.347	222.775	220.003	237.975	189.802	227.872

Sigmoidal Fitted Model Parameters

model no.	***b***						***c***						***d***						***a***
1	1.662						2.568						20.583						-7.609
2	2.655	2.218	2.101	1.913	0.950	0.134	2.568						20.583						-7.609
3	1.540						4.126	3.641	3.450	3.092	1.471	0.299	19.271						-6.077
4	1.546						3.855						17.647	20.081	20.954	22.219	36.022	52.909	-4.644
5**	**2.368**	**1.893**	**1.836**	**1.796**	**1.346**	**0.762**	**3.176**	**3.259**	**3.132**	**2.816**	**1.725**	**1.231**	**20.594**						**-7.762**
6	2.338	1.874	1.783	1.538	1.561	0.960	3.331						20.730	20.395	20.718	20.022	33.804	38.507	-5.570
7	1.537						3.927	3.646	3.486	3.049	1.613	1.255	17.691	19.466	19.748	18.948	21.699	37.016	-6.343
8	2.406	1.908	1.868	1.739	1.350	0.796	3.186	3.235	3.133	2.765	1.709	1.282	21.233	20.701	21.130	19.287	20.556	22.593	-8.075

Table S10. Model parameter values for the Van't Hoff, Lloyd-Taylor and sigmoidal models for soil respiration by SOC (μg CO_2-C g SOC^{-1} h^{-1}) response to direct, stepwise temperature increase. In the global (i.e. site-level) Van't Hoff, Lloyd-Taylor, and sigmoidal models, all parameters were fitted using all the data(white) and for group parameter fitted models (i.e. fitted by treatment) parameters were fitted by decadal warming level indicated in greyscale from ambient (lightest) to hotspot (darkest). For the Lloyd-Taylor model (model no. 8) that would not converge, absent fitted parameters R_0, β, and d are indicated by "--". Best model for each of the three model types, i.e. with lowest AICc, indicated in bold and the best of all three, i.e. lowest AICc for all models preformed, indicated by asterisks (**) next to model number.

Van't Hoff Fitted Model Parameters

model no.	R_0						β					
1	**52.984**						**0.033**					
2	55.505	53.595	55.423	50.239	49.641	52.882	0.033					
3	52.978						0.034	0.033	0.034	0.031	0.030	0.033
4	58.170	50.338	52.735	53.646	56.484	47.185	0.031	0.035	0.034	0.030	0.028	0.037

Lloyd-Taylor Fitted Model Parameters

model no.	R_0						β						d					
1	**1061.994**						**-153.099**						**226.430**					
2	1131.654	1094.335	1131.285	1027.074	1012.578	1079.850	-155.033						226.085					
3	1163.792						-161.694	-164.633	-162.120	-168.885	-169.686	-165.765	223.910					
4	1280.496						-179.183						219.389	220.873	219.766	222.460	222.645	221.420
5	966.515	1278.540	1263.245	879.114	713.782	1402.235	-142.532	-165.312	-162.013	-142.687	-128.649	-173.027	226.571					
6	1036.412	1165.472	1178.918	954.103	845.707	1206.179	-152.888						224.021	229.127	228.432	224.531	220.542	230.607
7	1100.786						-162.063	-145.610	-144.225	-172.314	-194.018	-141.392	221.857	230.637	230.219	220.587	221.441	232.992
8	--	--	--	--	--	--	--	--	--	--	--	--	--	--	--	--	--	--

Sigmoidal Fitted Model Parameters

model no.	b						c						d						a
1**	**158.270**						**-96.142**						**20.214**						**8.057**
2	164.462	158.790	162.738	153.550	153.422	156.661	-96.142						20.214						8.057
3	158.300						-88.089	-99.602	-94.953	-99.364	-95.493	-99.836	20.204						8.024
4	158.442						-96.145						19.079	20.016	19.329	20.409	21.655	21.400	8.300
5	163.227	164.002	167.667	151.139	146.005	159.229	-93.610	-105.976	-105.430	-91.353	-81.750	-100.902	20.240						7.939
6	167.094	157.391	162.278	148.440	154.183	159.683	-94.600						22.158	20.093	20.618	18.052	21.263	22.332	9.656
7	158.725						-88.084	-100.942	-97.121	-99.727	-93.291	-98.234	20.372	19.676	19.286	20.132	21.898	21.286	8.300
8	166.420	161.801	167.929	145.796	143.326	165.771	-93.489	-101.619	-102.644	-87.940	-78.044	-103.054	22.206	20.568	21.386	18.297	20.000	22.926	10.023

Table S11. Model fit statistics for the Van't Hoff, Lloyd-Taylor, and sigmoidal models describing SOC-normalized soil respiration (μg CO_2-C g SOC^{-1} h^{-1}) in response to stepwise instantaneous temperature increases. Model type is listed in the "Model" column, while the corresponding fit statistics are presented under the columns labeled "R^2", "RMSE", and "AICc", respectively. Models that used all data, from ambient (+0 °C) to hotspot (+75 °C) decadal warming levels, are marked with "†" next to the respective fit statistics. For models that exclude the hotspot (+75 °C), only including data from ambient (+0 °C) to high (+25–35 °C) decadal warming levels, respective fit statistics are indicated by "‡". In globally (i.e., site-level) parameterized models, parameters were fit to all data, either including or excluding the hotspot (+75 °C), regardless of decadal warming level. These models are labeled "*global*" in the "Parameter Adjusted" column. For decadal warming level (i.e., treatment-level) parameterized models, the parameters listed in italics "*by treatment*" under this column were adjusted separately by decadal warming level. Any parameters not listed "*by treatment*" here were fit globally. Due to model non-convergence, fit statistics for the Lloyd-Taylor model where all parameters were adjusted by decadal warming level (i.e., "*R_0, β & d by treatment*") are not reported ("--"). For each model type, the best-performing parameterization with the lowest AICc is shown in bold. The best overall model with the lowest AICc across all model types and parameterizations is indicated by asterisks ("**").

Soil Respiration (μg CO_2-C g SOC^{-1} h^{-1}) Model Fit Statistics							
Model	Parameter Adjusted	$R^2_{†}$	RMSE†	AICc†	$R^2_{‡}$	RMSE‡	AICc‡
Van't Hoff	***global***	**0.842**	**16.787**	**210.70**	**0.818**	**17.741**	**179.29**
Van't Hoff	*R_0 by treatment*	0.856	16.031	226.89	0.835	16.886	193.15
Van't Hoff	*β by treatment*	0.858	15.896	226.48	0.838	16.744	192.81
Van't Hoff	*R_0 & β by treatment*	0.862	15.667	262.58	0.841	16.622	224.19
Lloyd-Taylor	***global***	**0.863**	**15.633**	**210.19**	**0.838**	**16.707**	**180.06**
Lloyd-Taylor	*R_0 by treatment*	0.876	14.829	228.40	0.855	15.808	196.27
Lloyd-Taylor	*β by treatment*	0.875	14.917	228.69	0.853	15.908	196.52
Lloyd-Taylor	*d by treatment*	0.873	15.014	229.00	0.851	16.022	196.81
Lloyd-Taylor	*R_0 & β by treatment*	0.883	14.423	270.88	0.861	15.507	234.98
Lloyd-Taylor	*R_0 & d by treatment*	0.883	14.416	270.86	0.861	15.503	234.97
Lloyd-Taylor	*β & d by treatment*	0.883	14.424	270.88	0.861	15.513	235.00
Lloyd-Taylor	*R_0, β & d by treatment*	--	--	--	--	--	--
Sigmoidal**	***global***	**0.970**	**7.346**	**177.16**	**0.972**	**6.901**	**148.31**
Sigmoidal	*b by treatment*	0.980	6.011	191.13	0.984	5.183	158.57
Sigmoidal	*c by treatment*	0.974	6.782	196.92	0.977	6.279	166.25
Sigmoidal	*d by treatment*	0.974	6.846	197.37	0.976	6.403	167.03
Sigmoidal	*b & c by treatment*	0.988	4.681	232.20	0.994	3.321	191.44
Sigmoidal	*b & d by treatment*	0.983	5.434	239.36	0.989	4.323	201.98
Sigmoidal	*c & d by treatment*	0.978	6.307	246.51	0.981	5.747	213.37
Sigmoidal	*b, c & d by treatment*	0.992	3.764	451.73	0.998	1.780	419.81

At the hotspot (+75 °C), reduced replication increased uncertainty. To evaluate whether this influenced model selection for SOC-normalized fluxes, we reran the analyses with hotspot data excluded. This allowed us to test whether model parameterization continued to favor global (site-level) fitting once the potentially high-uncertainty treatment was removed. Fit statistics for this are provided in Table S11.

With hotspot (+75 °C) data excluded, the best overall fit (AICc = 148.31, R^2 = 0.972, and RMSE = 6.901) was the sigmoidal model with parameters *a*, *b*, *c*, and *d* were adjusted globally (Table 2). The best fits from the Van't Hoff (AICc = 179.29, R^2 = 0.818, and RMSE = 17.741) and Lloyd-Taylor (AICc = 180.06, R^2 = 0.838, and RMSE = 16.707) models were also parameterized globally. Although fit statistics improved with the removal of hotspot data, AICc still favored global over treatment-specific models (Table S11). This suggests that, once differences in SOC availability were accounted for, temperature responses of SOC-normalized respiration were broadly consistent across decadal warming levels. A slight decline in normalized respiration with warming was observed, but the effect was not strong enough to warrant treatment-specific parameterization.

Flux modeling methods are described in Section 2.5 of the main text. Data visualizations of area-based flux model runs, including temperature (°C) vs. soil respiration (CO_2 m^{-2} s^{-1}) and observed vs. modeled soil respiration (CO_2 m^{-2} s^{-1}), are provided in Supplementary Figures 9–12 (Van't Hoff function), 13–20 (Lloyd–Taylor function), and 21–28 (sigmoidal function). Supplementary Figures 29–32 (Van't Hoff function), 33–39 (Lloyd–Taylor function), and 40–47 (sigmoidal function) present data visualizations of SOC-normalized flux model runs, showing both temperature (°C) vs. soil respiration (µg CO_2–C g SOC^{-1} h^{-1}) and observed vs. modeled soil respiration (µg CO_2–C g SOC^{-1} h^{-1}). Due to non-convergence, the Lloyd–Taylor model with all parameters (i.e., R_0, β, and *d*) adjusted by decadal warming level could not be fit to the SOC-normalized soil flux data and is therefore not reported.

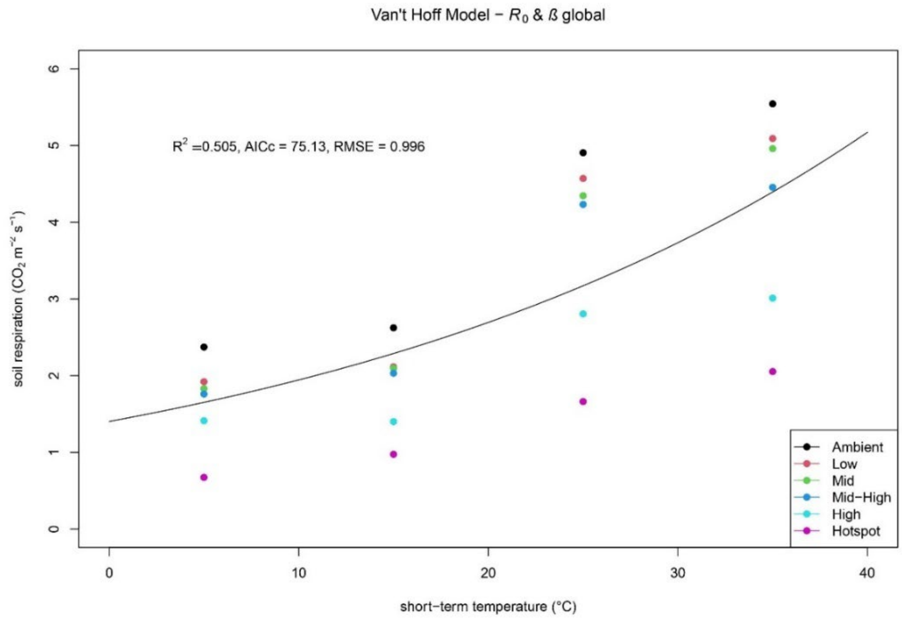

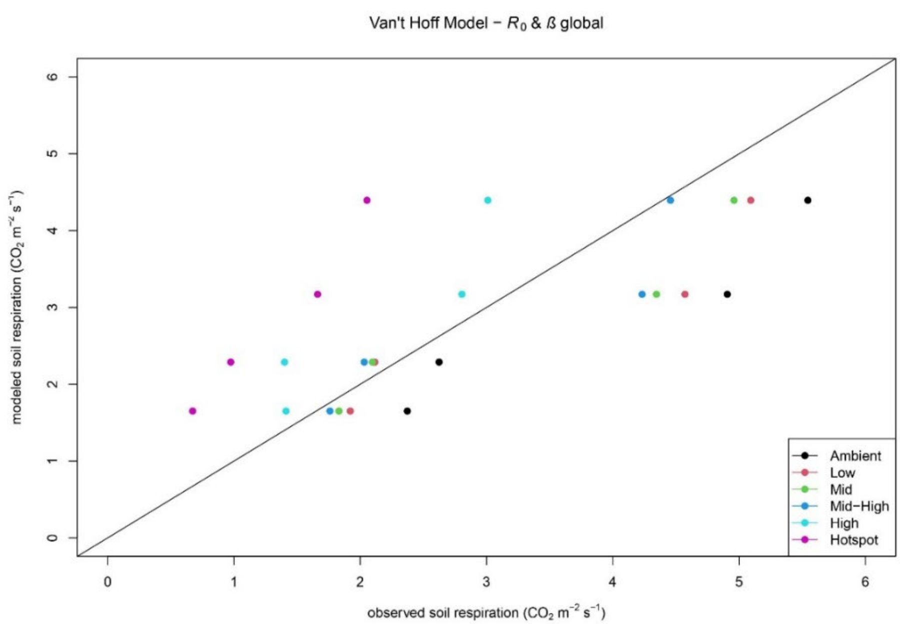

Figure S9. Van't Hoff model 1 with R_0 and β parameters adjusted globally, fit to soil respiration in µmol CO_2 m^{-2} s^{-1} against short-term temperature in °C (above). Model fit R^2, RMSE, and AICc found in top-right corner of top sub-plot. Mean modeled soil respiration in µmol CO_2 m^{-2} s^{-1} against mean observed respiration in µmol CO_2 m^{-2} s^{-1} (below). Ambient in black, low in red, mid in green, mid-high in blue, high in cyan, and hotspot in magenta for decadal warming levels.

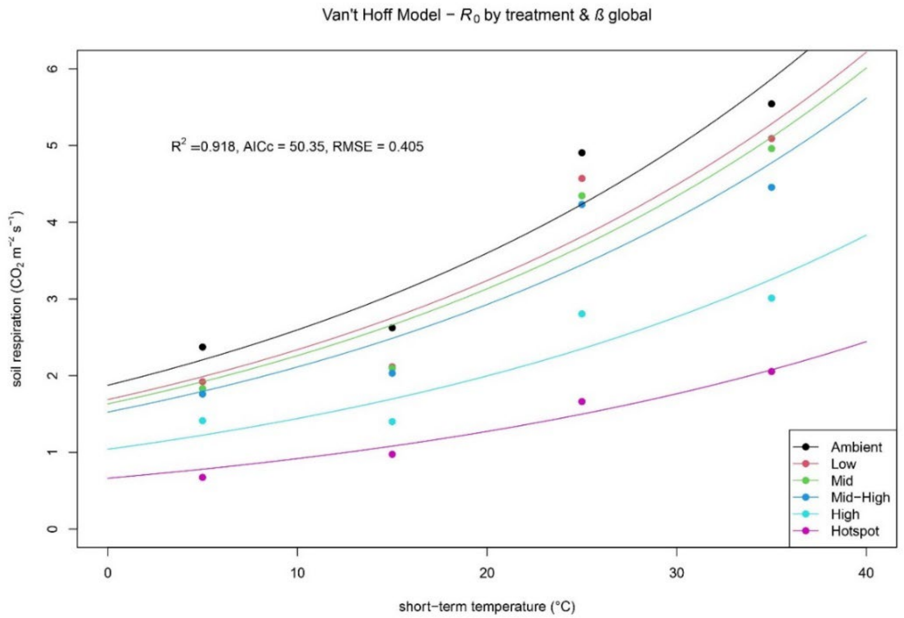

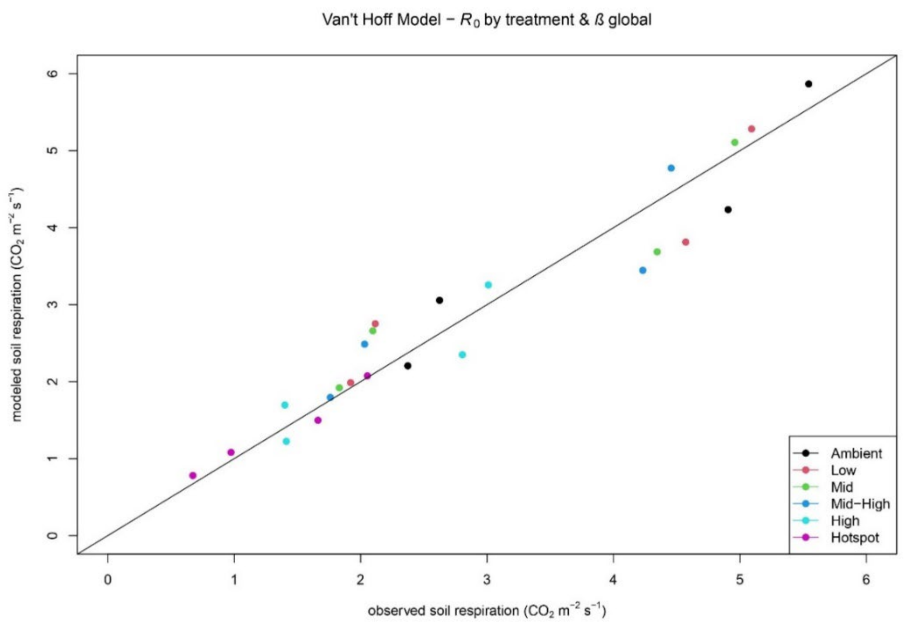

Figure S10. Van't Hoff model 2 with R_0 adjusted by decadal warming level and β adjusted globally, fit to soil respiration in μmol CO_2 m^{-2} s^{-1} against short-term temperature in °C (above). Model fit R^2, RMSE, and AICc found in top-right corner of top sub-plot. Mean modeled soil respiration in μmol CO_2 m^{-2} s^{-1} against mean observed respiration in μmol CO_2 m^{-2} s^{-1} (below). Ambient in black, low in red, mid in green, mid-high in blue, high in cyan, and hotspot in magenta for decadal warming levels.

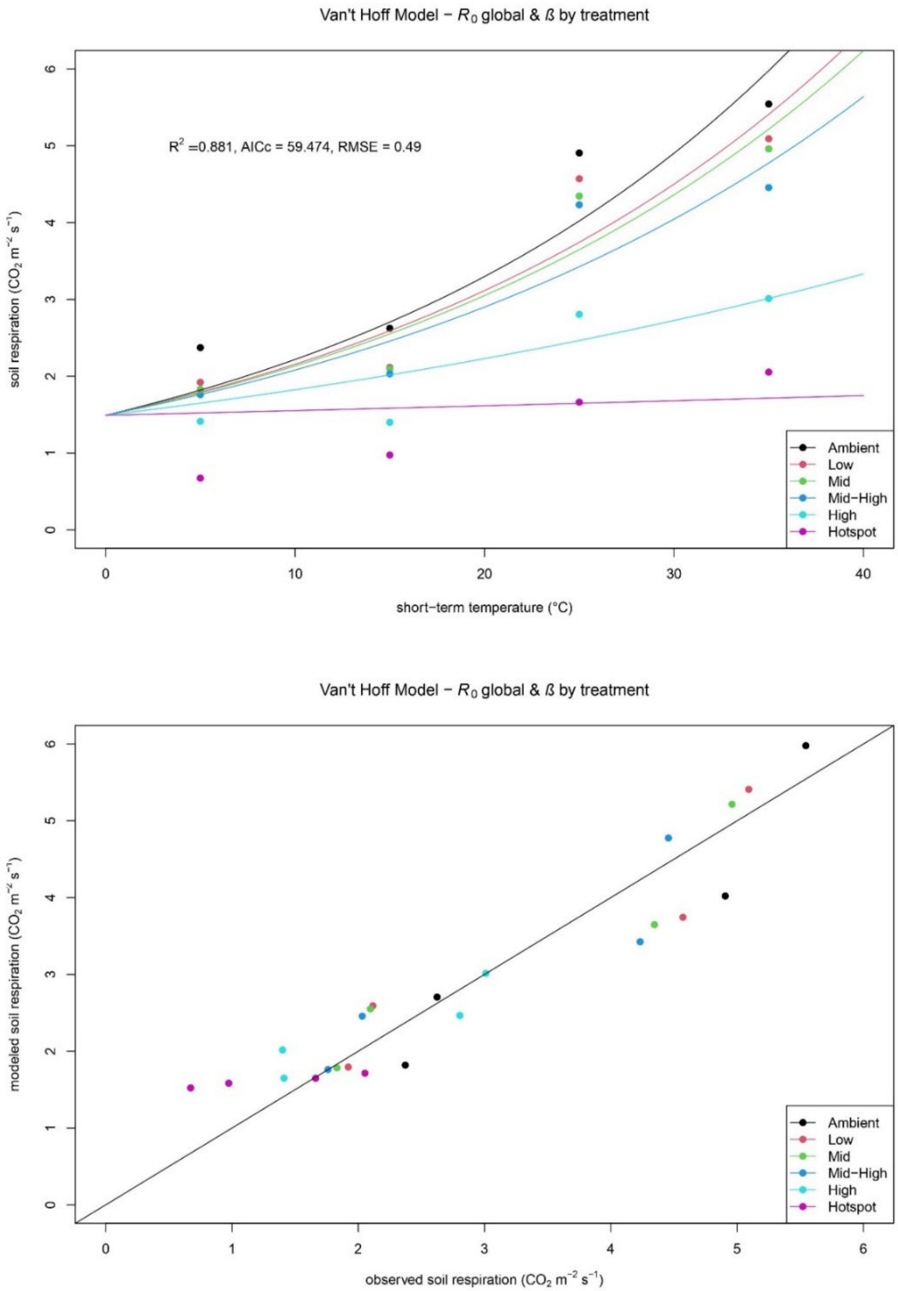

Figure S11. Van't Hoff model 3 with β adjusted by decadal warming level and R_0 adjusted globally, fit to soil respiration in µmol CO_2 m^{-2} s^{-1} against short-term temperature in °C (above). Model fit R^2, RMSE, and AICc found in top-right corner of top sub-plot. Mean modeled soil respiration in µmol CO_2 m^{-2} s^{-1} against mean observed respiration in µmol CO_2 m^{-2} s^{-1} (below). Ambient in black, low in red, mid in green, mid-high in blue, high in cyan, and hotspot in magenta for decadal warming levels.

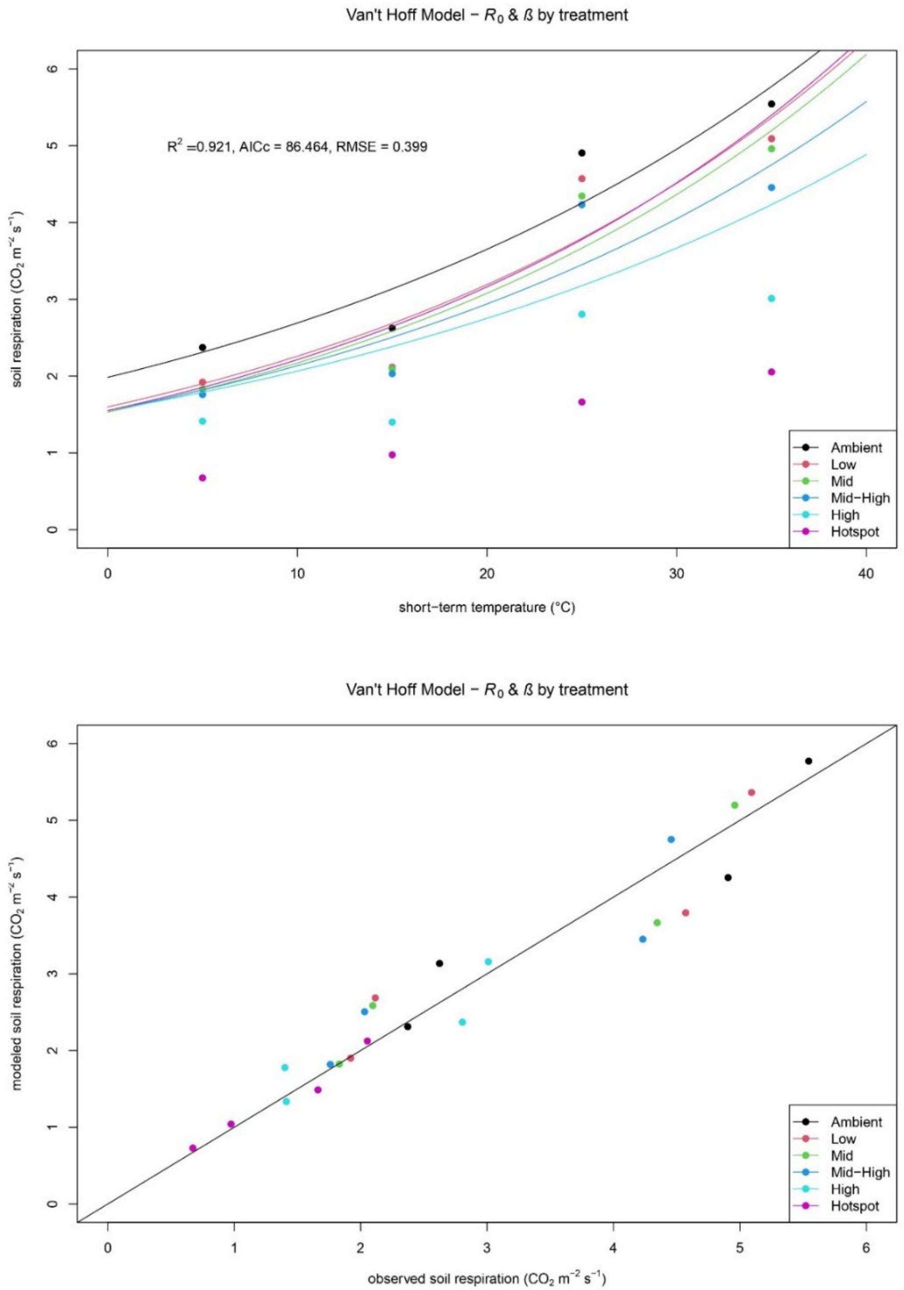

Figure S12. Van't Hoff model 4 with R_0 and β adjusted by decadal warming level, fit to soil respiration in µmol CO_2 m^{-2} s^{-1} against short-term temperature in °C (above). Model fit R^2, RMSE, and AICc found in top-right corner of top sub-plot. Mean modeled soil respiration in µmol CO_2 m^{-2} s^{-1} against mean observed respiration in µmol CO_2 m^{-2} s^{-1} (below). Ambient in black, low in red, mid in green, mid-high in blue, high in cyan, and hotspot in magenta for decadal warming levels.

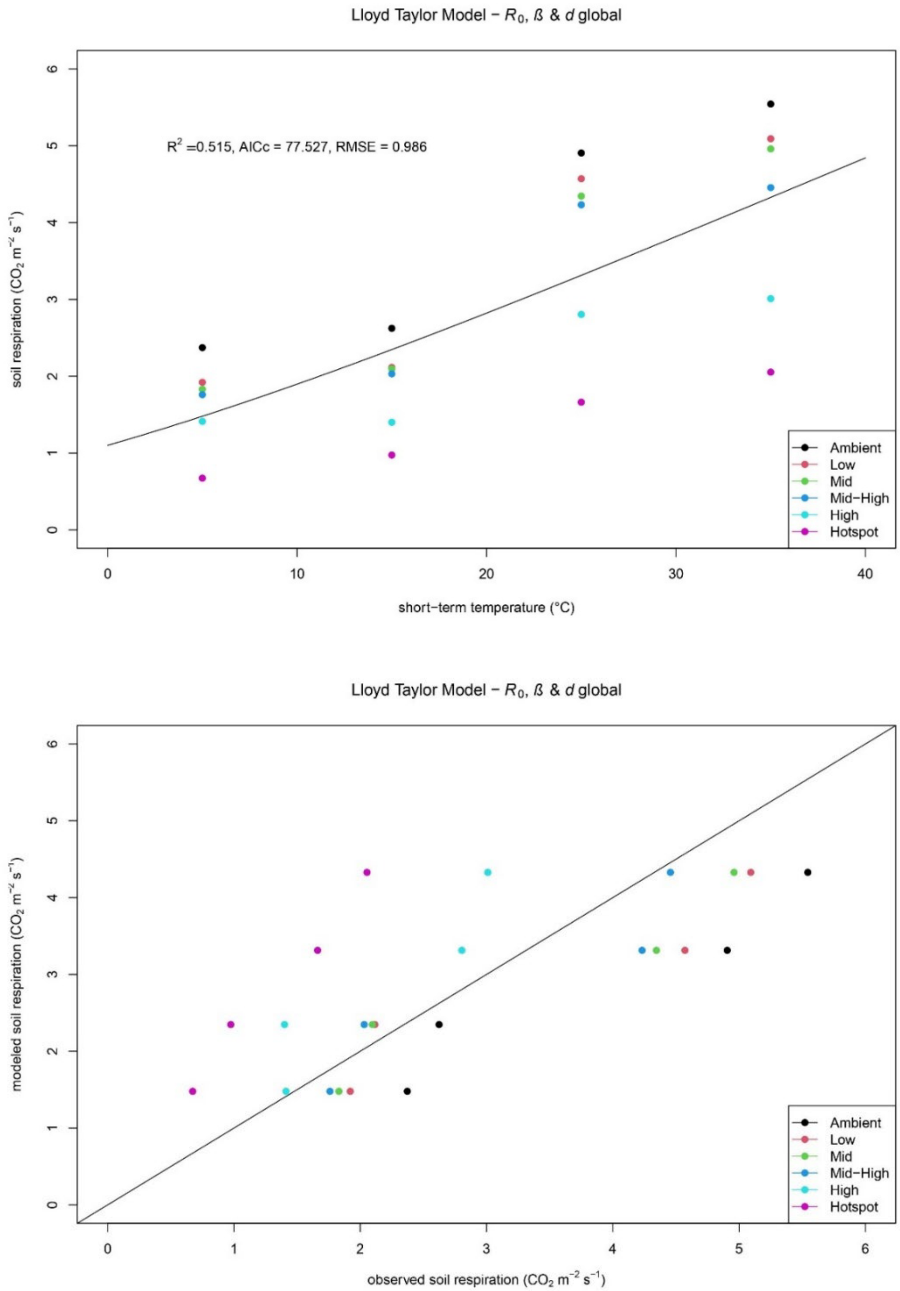

Figure S13. Lloyd-Taylor model 1 with R_0, β, and d parameters adjusted globally, fit to soil respiration in µmol CO_2 m^{-2} s^{-1} against short-term temperature in °C (above). Model fit R^2, RMSE, and AICc found in top-right corner of top sub-plot. Mean modeled soil respiration in µmol CO_2 m^{-2} s^{-1} against mean observed respiration in µmol CO_2 m^{-2} s^{-1} (below). Ambient in black, low in red, mid in green, mid-high in blue, high in cyan, and hotspot in magenta for decadal warming levels.

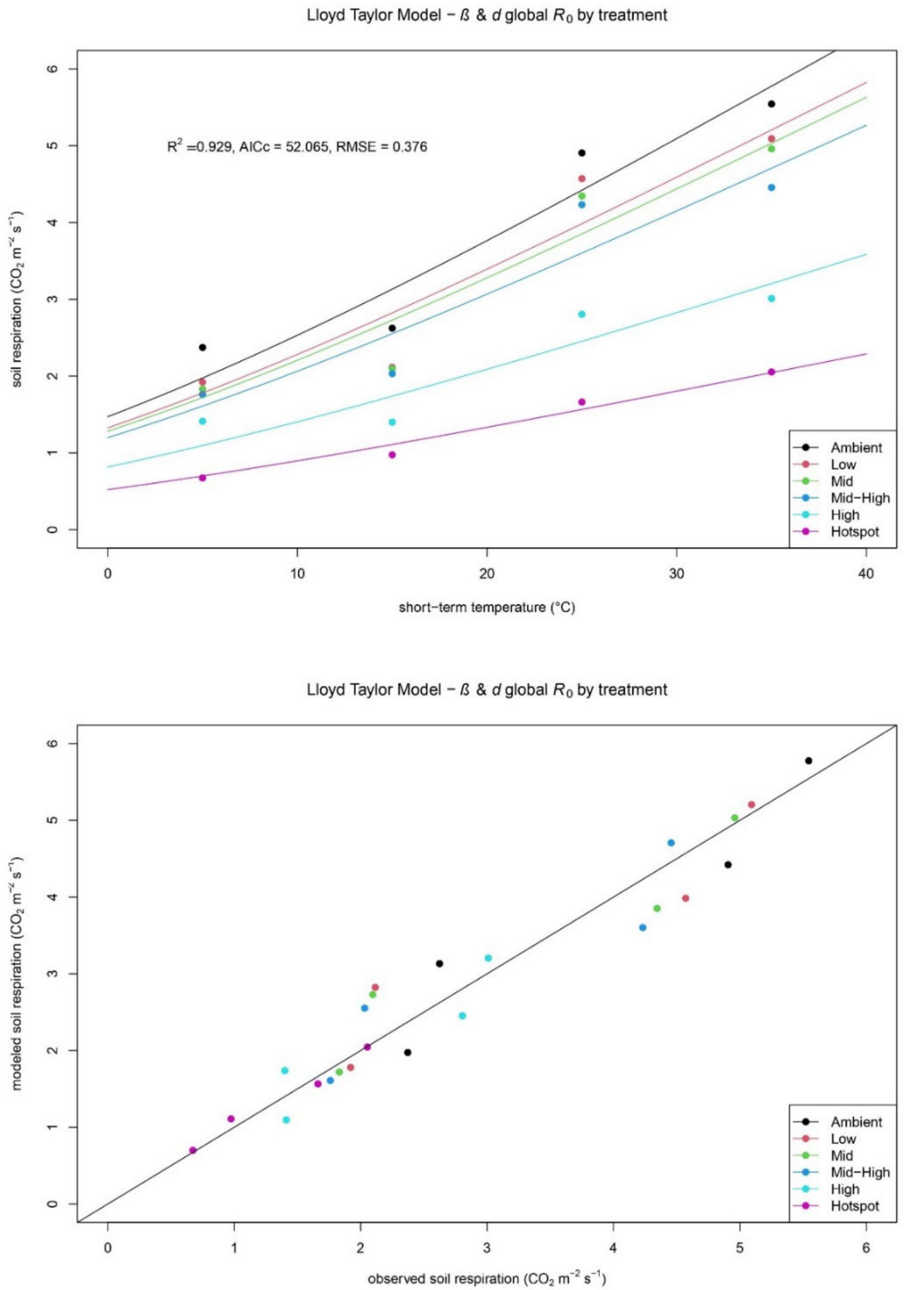

Figure S14. Lloyd-Taylor model 2 with R_0 adjusted by decadal warming level β and d adjusted globally, fit to soil respiration in μmol CO_2 m^{-2} s^{-1} against short-term temperature in °C (above). Model fit R^2, RMSE, and AICc found in top-right corner of top sub-plot. Mean modeled soil respiration in μmol CO_2 m^{-2} s^{-1} against mean observed respiration in μmol CO_2 m^{-2} s^{-1} (below). Ambient in black, low in red, mid in green, mid-high in blue, high in cyan, and hotspot in magenta for decadal warming levels.

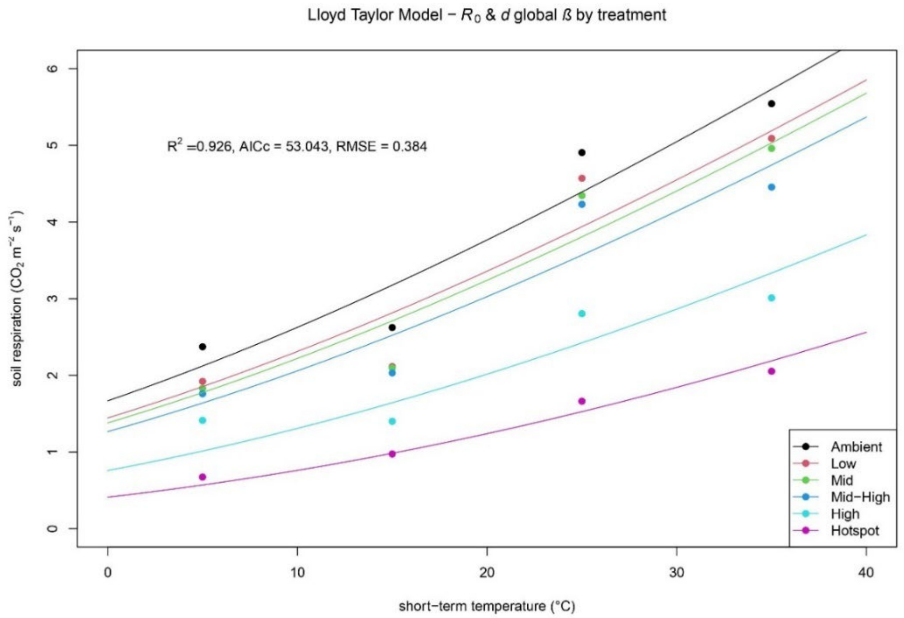

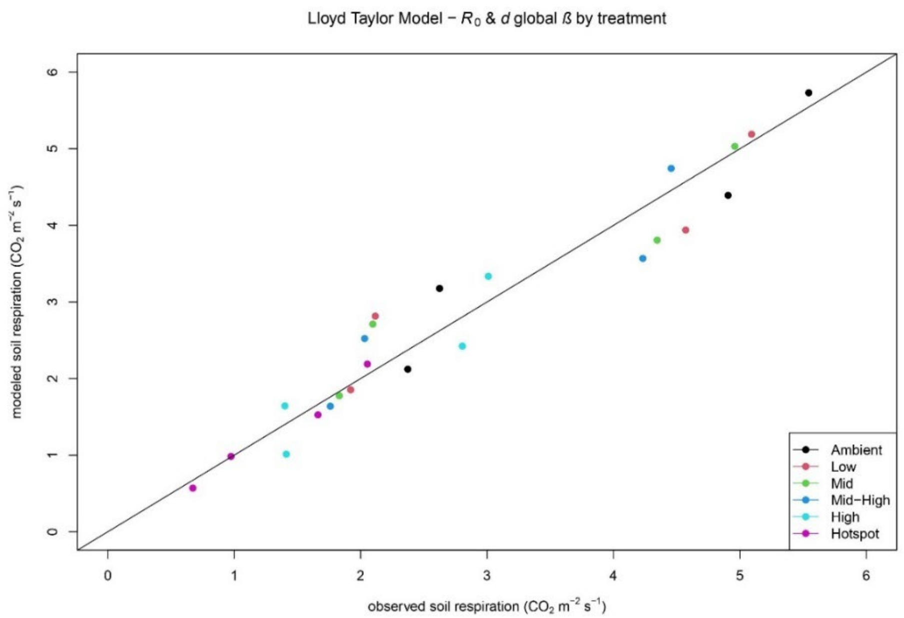

Figure S15. Lloyd-Taylor model 3 with β adjusted by decadal warming level R_0 and d adjusted globally, fit to soil respiration in µmol CO_2 m^{-2} s^{-1} against short-term temperature in °C (above). Model fit R^2, RMSE, and AICc found in top-right corner of top sub-plot. Mean modeled soil respiration in µmol CO_2 m^{-2} s^{-1} against mean observed respiration in µmol CO_2 m^{-2} s^{-1} (below). Ambient in black, low in red, mid in green, mid-high in blue, high in cyan, and hotspot in magenta for decadal warming levels.

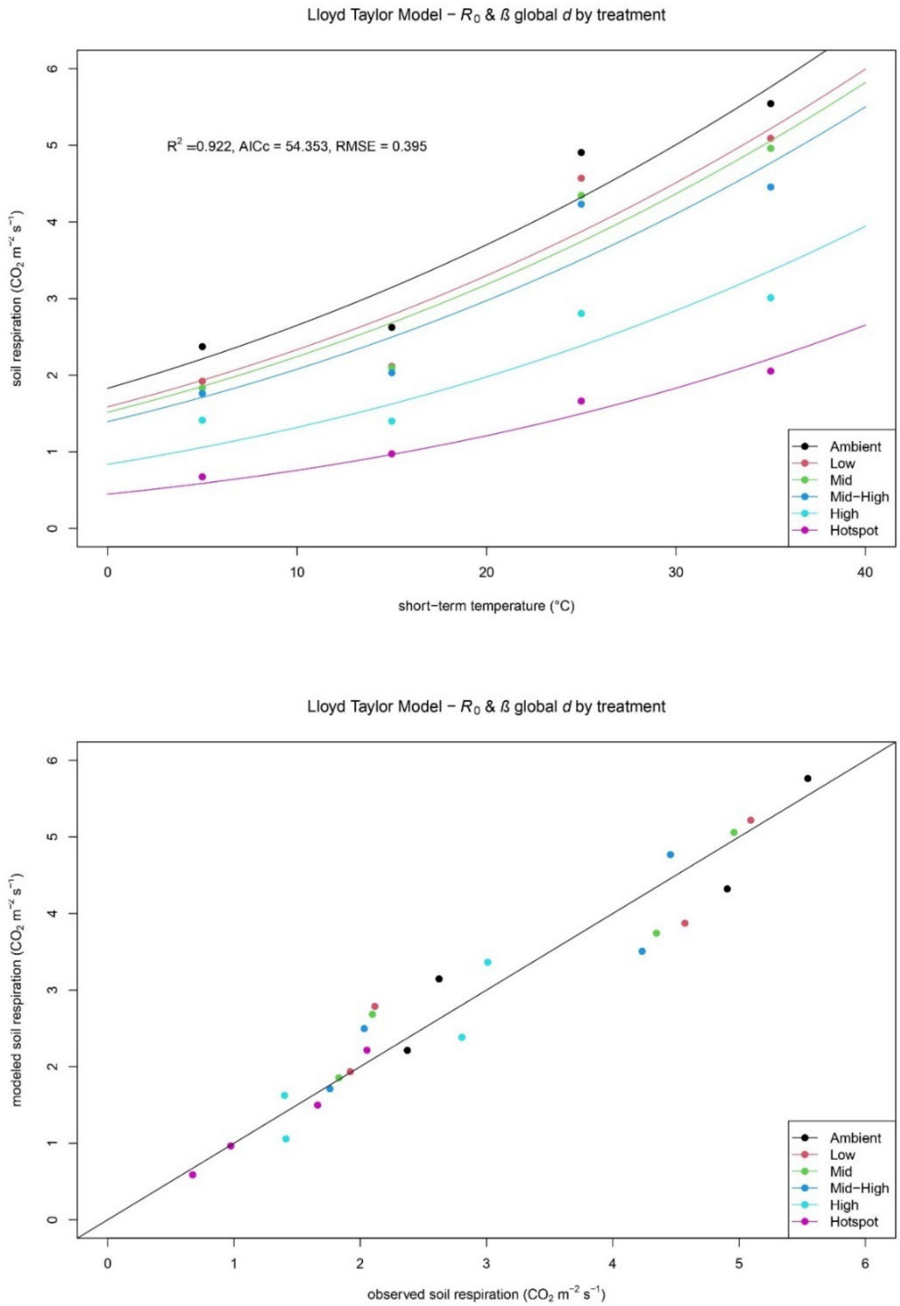

Figure S16. Lloyd-Taylor model 4 with d adjusted by decadal warming level R_0 and β adjusted globally, fit to soil respiration in µmol CO_2 m^{-2} s^{-1} against short-term temperature in °C (above). Model fit R^2, RMSE, and AICc found in top-right corner of top sub-plot. Mean modeled soil respiration in µmol CO_2 m^{-2} s^{-1} against mean observed respiration in µmol CO_2 m^{-2} s^{-1} (below). Ambient in black, low in red, mid in green, mid-high in blue, high in cyan, and hotspot in magenta for decadal warming levels.

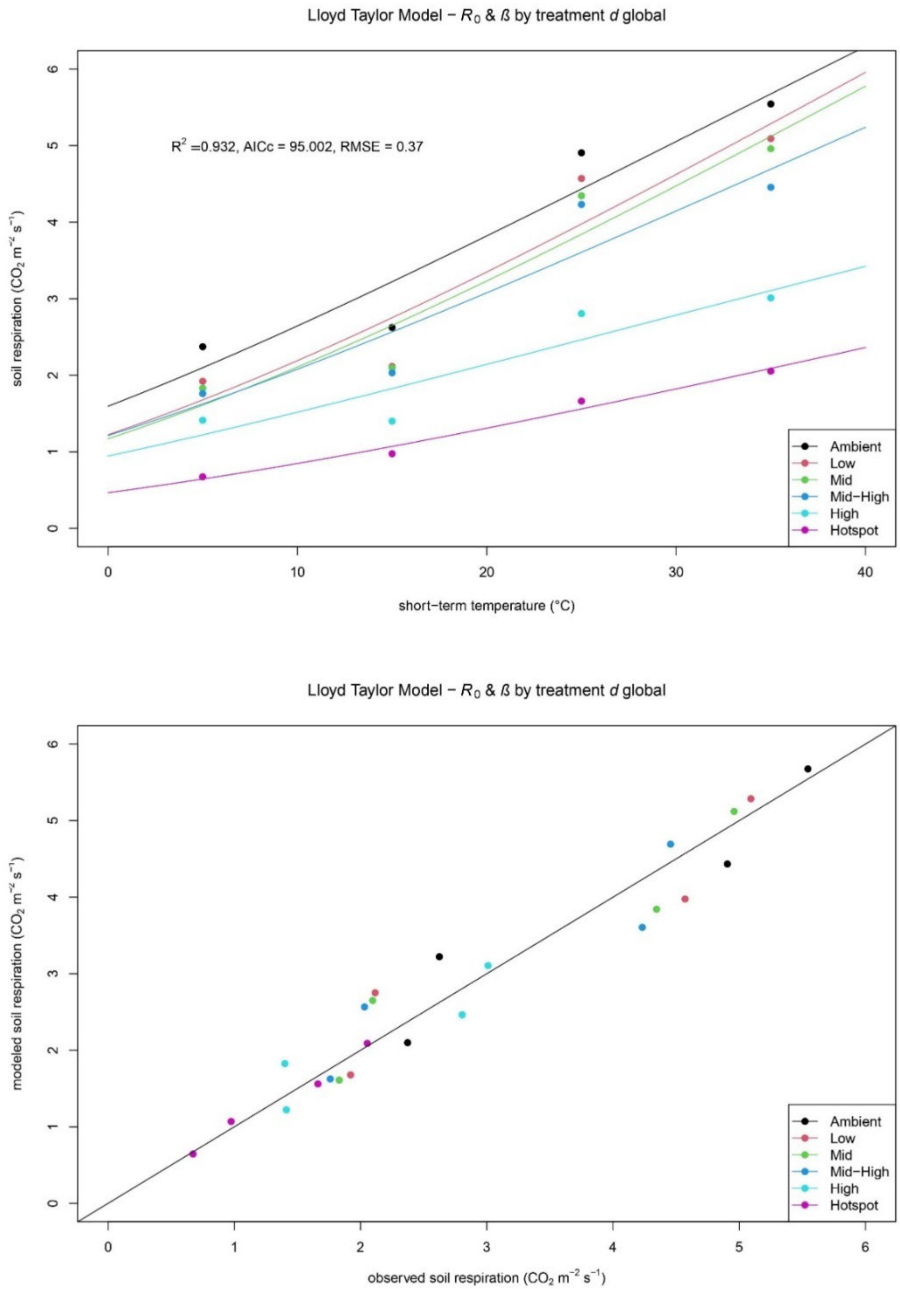

Figure S17. Lloyd-Taylor model 5 with R_0 and β adjusted by decadal warming level d adjusted globally, fit to soil respiration in µmol CO_2 m^{-2} s^{-1} against short-term temperature in °C (above). Model fit R^2, RMSE, and AICc found in top-right corner of top sub-plot. Mean modeled soil respiration in µmol CO_2 m^{-2} s^{-1} against mean observed respiration in µmol CO_2 m^{-2} s^{-1} (below). Ambient in black, low in red, mid in green, mid-high in blue, high in cyan, and hotspot in magenta for decadal warming levels.

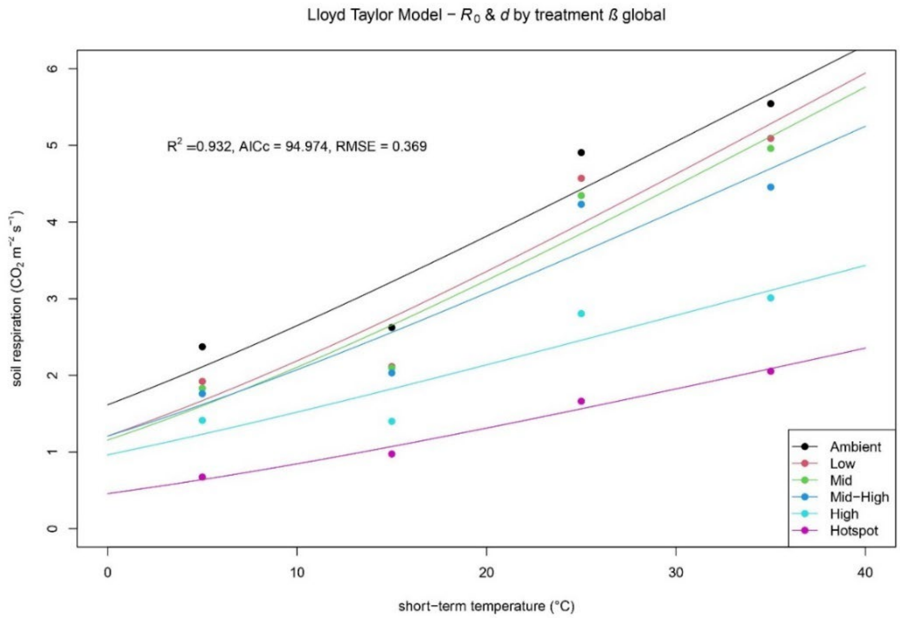

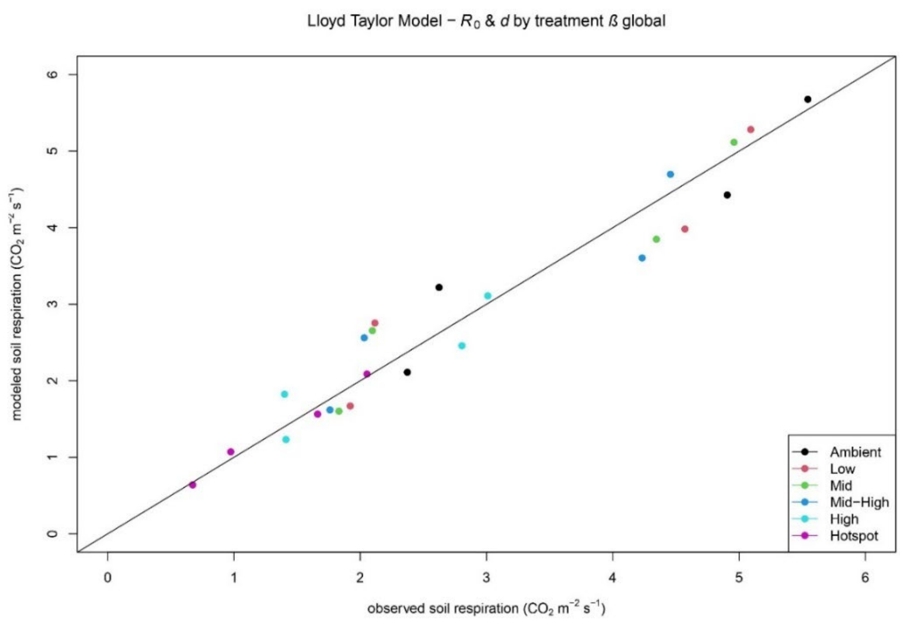

Figure S18. Lloyd-Taylor model 6 with R_0 and d adjusted by decadal warming level β adjusted globally, fit to soil respiration in µmol CO_2 m^{-2} s^{-1} against short-term temperature in °C (above). Model fit R^2, RMSE, and AICc found in top-right corner of top sub-plot. Mean modeled soil respiration in µmol CO_2 m^{-2} s^{-1} against mean observed respiration in µmol CO_2 m^{-2} s^{-1} (below). Ambient in black, low in red, mid in green, mid-high in blue, high in cyan, and hotspot in magenta for decadal warming levels.

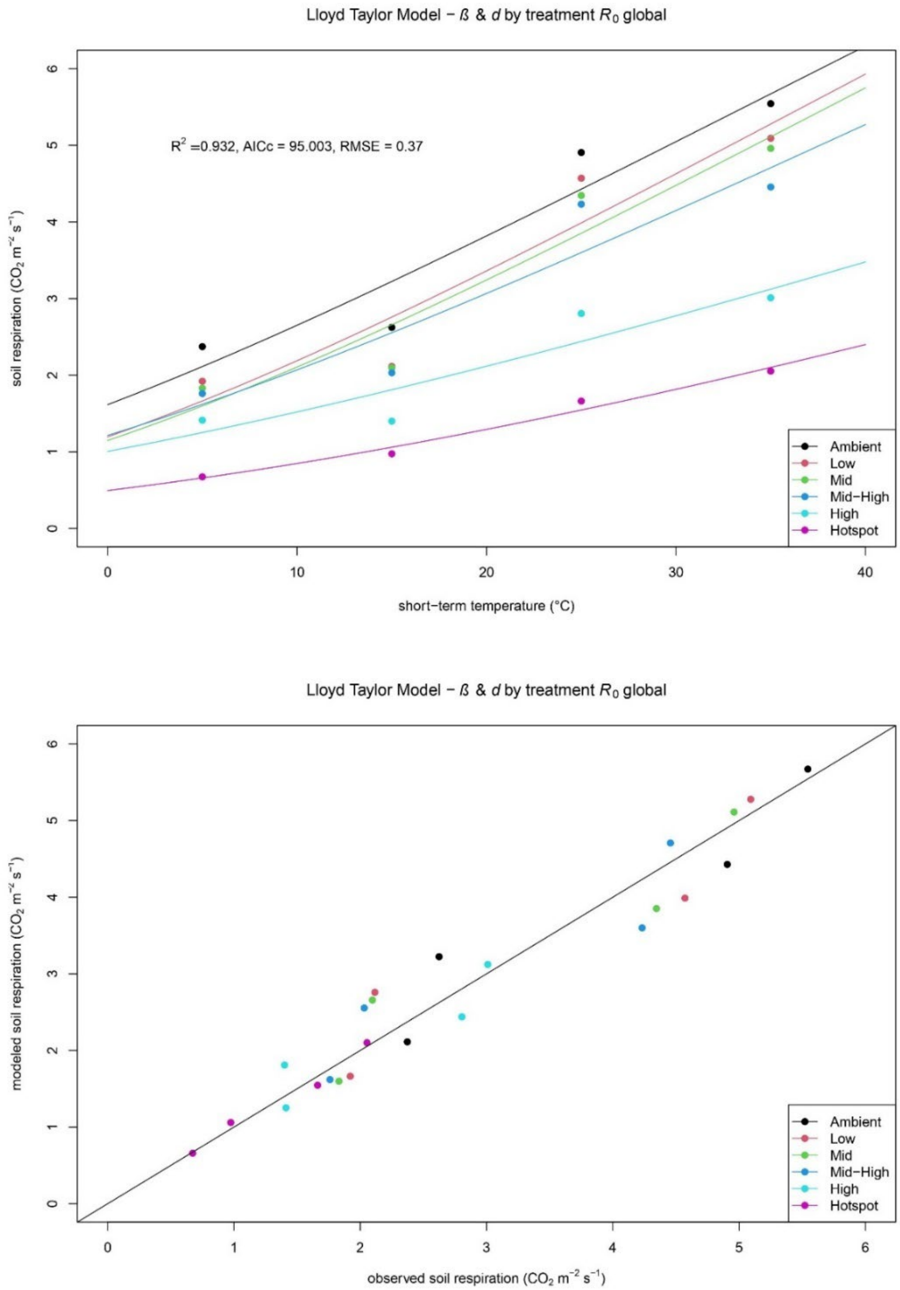

Figure S19. Lloyd-Taylor model 7 with β and d adjusted by decadal warming level R_0 adjusted globally, fit to soil respiration in µmol CO_2 m^{-2} s^{-1} against short-term temperature in °C (above). Model fit R^2, RMSE, and AICc found in top-right corner of top sub-plot. Mean modeled soil respiration in µmol CO_2 m^{-2} s^{-1} against mean observed respiration in µmol CO_2 m^{-2} s^{-1} (below). Ambient in black, low in red, mid in green, mid-high in blue, high in cyan, and hotspot in magenta for decadal warming levels.

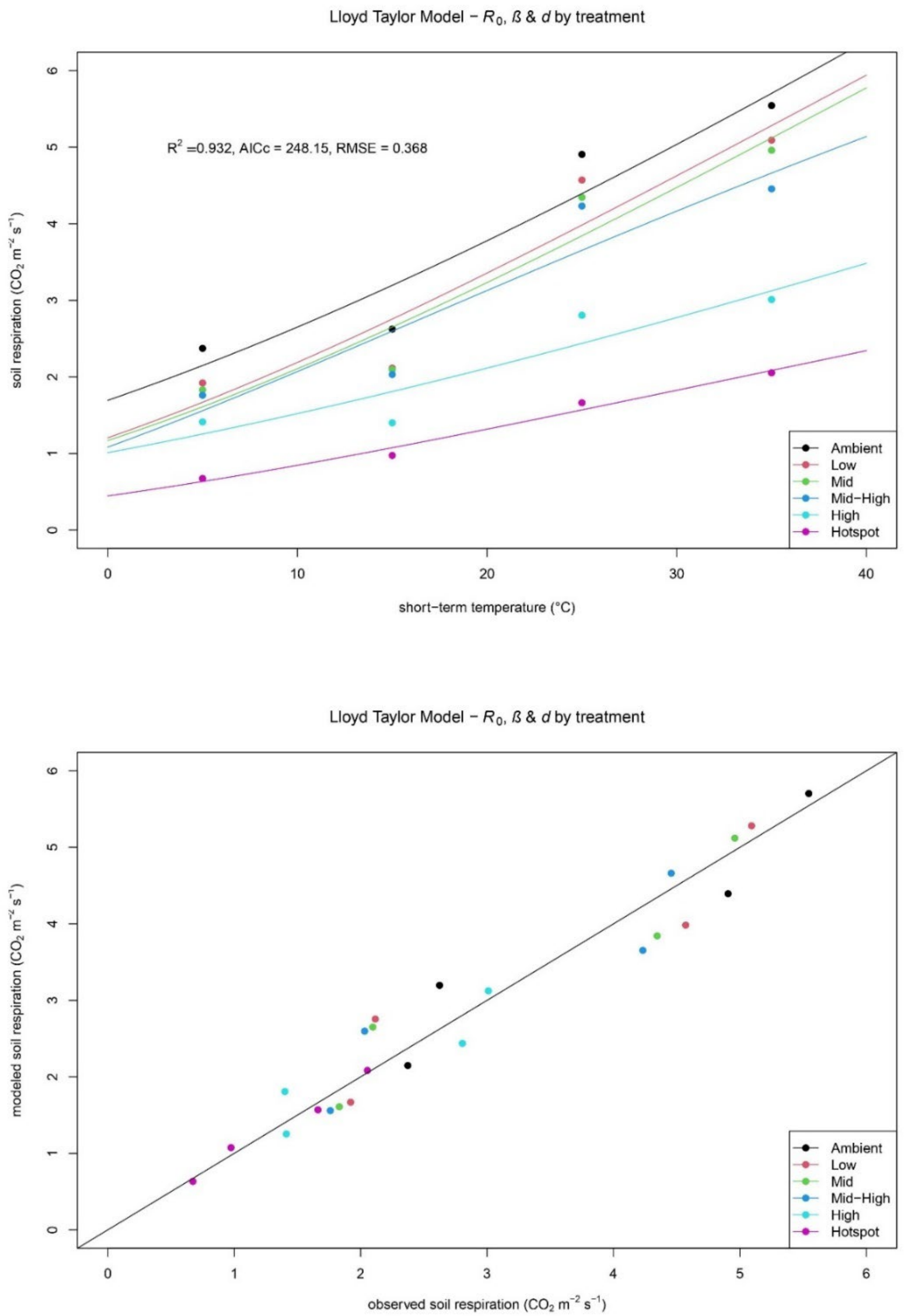

Figure S20. Lloyd-Taylor model 8 with R_0, β, and d adjusted by decadal warming level, fit to soil respiration in µmol CO_2 m^{-2} s^{-1} against short-term temperature in °C (above). Model fit R^2, RMSE, and AICc found in top-right corner of top sub-plot. Mean modeled soil respiration in µmol CO_2 m^{-2} s^{-1} against mean observed respiration in µmol CO_2 m^{-2} s^{-1} (below). Ambient in black, low in red, mid in green, mid-high in blue, high in cyan, and hotspot in magenta for decadal warming levels.

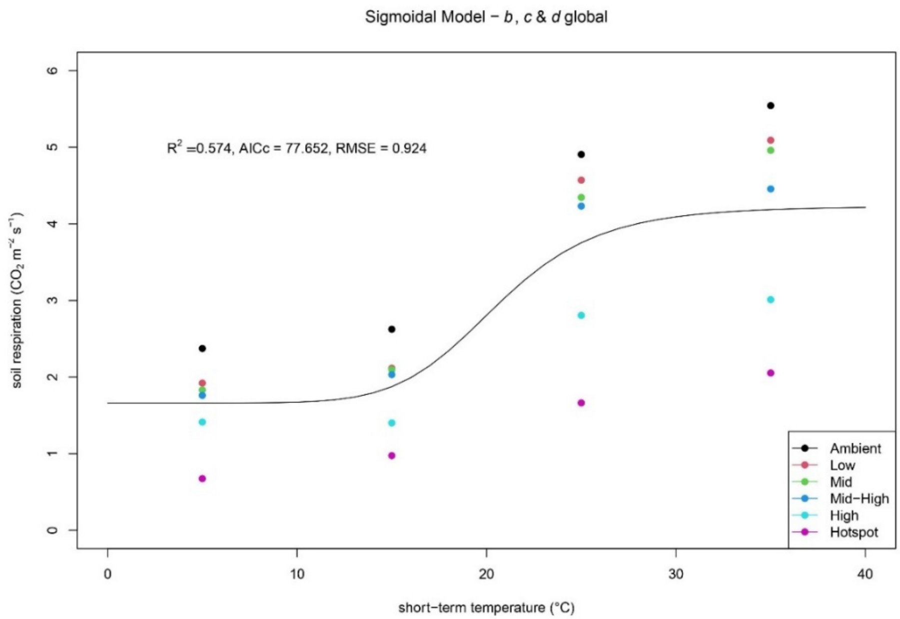

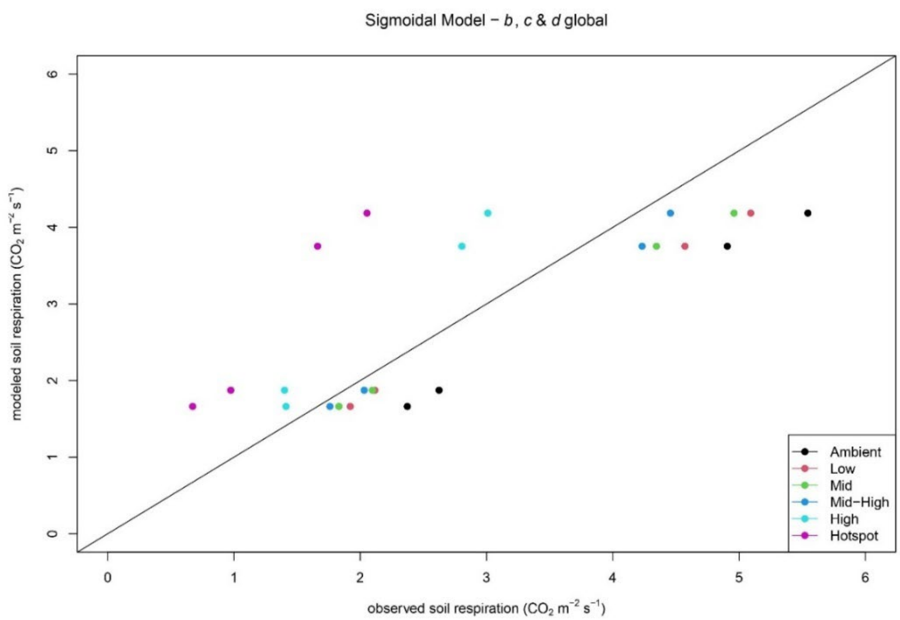

Figure S21. Sigmoidal model 1 with *b*, *c*, and *d* parameters adjusted globally and *a* as a global constant, fit to soil respiration in µmol CO_2 m^{-2} s^{-1} against short-term temperature in °C (above). Model fit R^2, RMSE, and AICc found in top-right corner of top sub-plot. Mean modeled soil respiration in µmol CO_2 m^{-2} s^{-1} against mean observed respiration in µmol CO_2 m^{-2} s^{-1} (below). Ambient in black, low in red, mid in green, mid-high in blue, high in cyan, and hotspot in magenta for decadal warming levels.

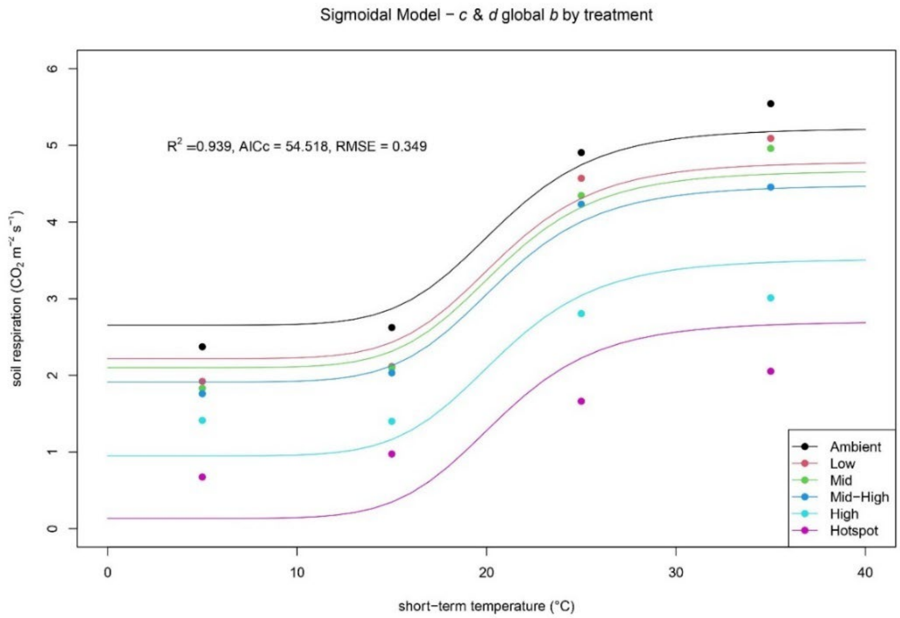

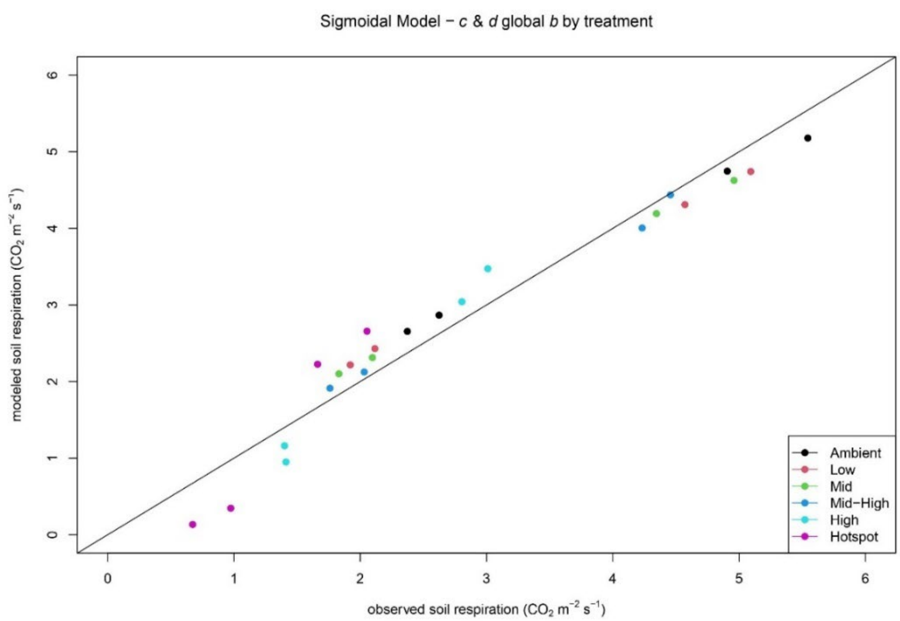

Figure S22. Sigmoidal model 2 with *b* adjusted by decadal warming level, *c* and *d* adjusted globally and *a* as a global constant, fit to soil respiration in μmol CO_2 m^{-2} s^{-1} against short-term temperature in °C (above). Model fit R^2, RMSE, and AICc found in top-right corner of top sub-plot. Mean modeled soil respiration in μmol CO_2 m^{-2} s^{-1} against mean observed respiration in μmol CO_2 m^{-2} s^{-1} (below). Ambient in black, low in red, mid in green, mid-high in blue, high in cyan, and hotspot in magenta for decadal warming levels.

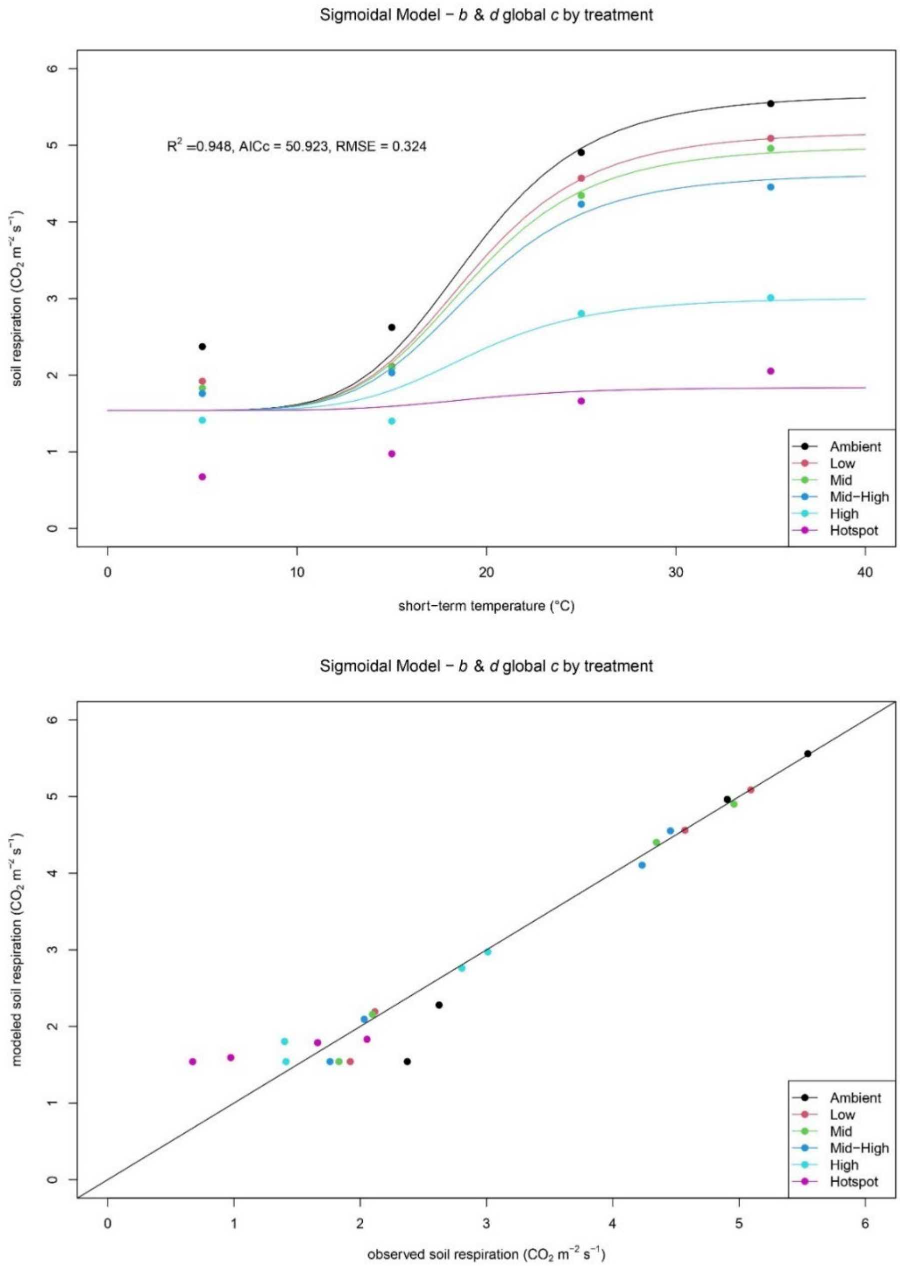

Figure S23. Sigmoidal model 3 with *c* adjusted by decadal warming level, *b* and *d* adjusted globally and *a* as a global constant, fit to soil respiration in μmol CO_2 m^{-2} s^{-1} against short-term temperature in °C (above). Model fit R^2, RMSE, and AICc found in top-right corner of top sub-plot. Mean modeled soil respiration in μmol CO_2 m^{-2} s^{-1} against mean observed respiration in μmol CO_2 m^{-2} s^{-1} (below). Ambient in black, low in red, mid in green, mid-high in blue, high in cyan, and hotspot in magenta for decadal warming levels.

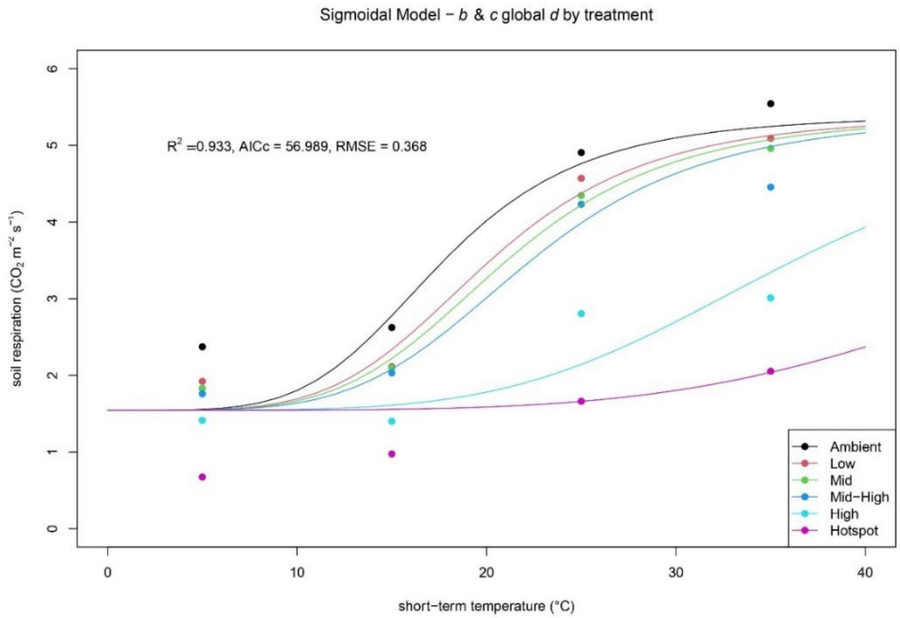

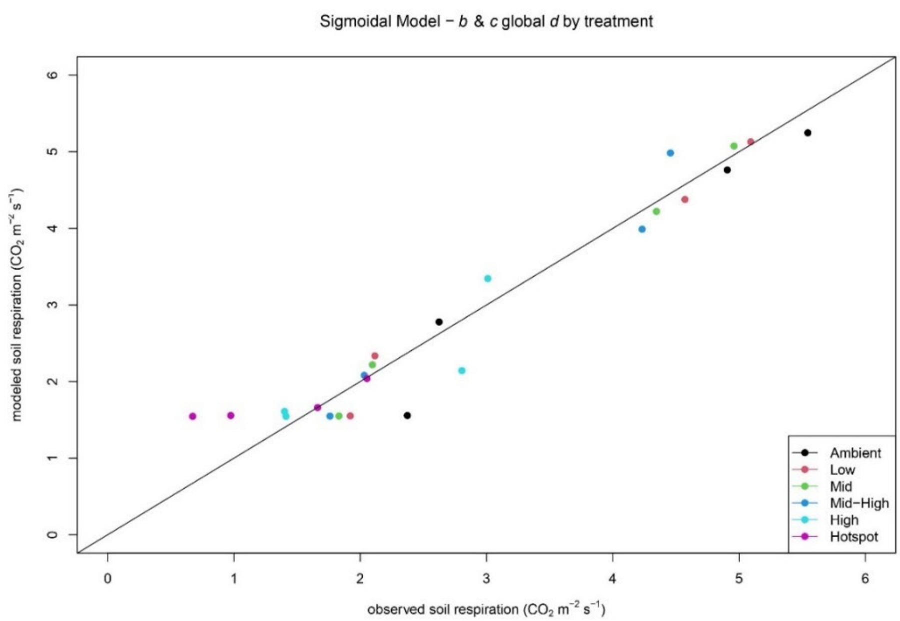

Figure S24. Sigmoidal model 4 with *d* adjusted by decadal warming level, *b* and *c* adjusted globally and *a* as a global constant, fit to soil respiration in μmol CO_2 m^{-2} s^{-1} against short-term temperature in °C (above). Model fit R^2, RMSE, and AICc found in top-right corner of top sub-plot. Mean modeled soil respiration in μmol CO_2 m^{-2} s^{-1} against mean observed respiration in μmol CO_2 m^{-2} s^{-1} (below). Ambient in black, low in red, mid in green, mid-high in blue, high in cyan, and hotspot in magenta for decadal warming levels.

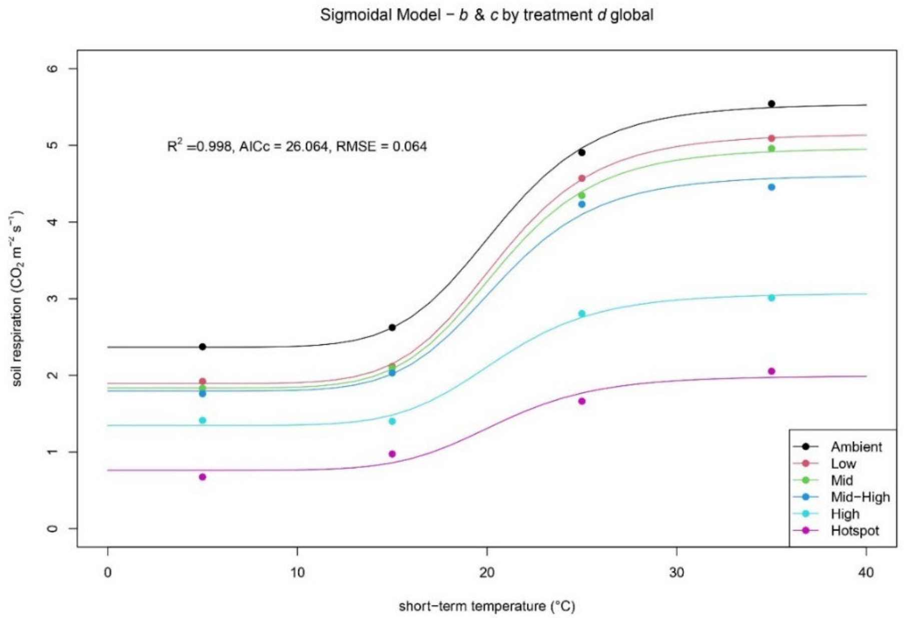

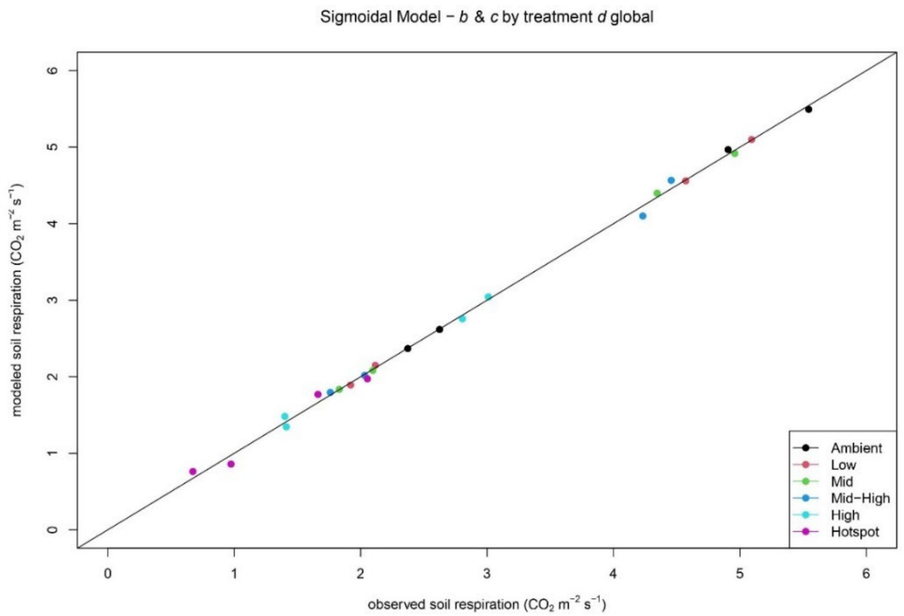

Figure S25. Sigmoidal model 5 with *b* and *c* adjusted by decadal warming level, *d* adjusted globally and *a* as a global constant, fit to soil respiration in μmol CO_2 m^{-2} s^{-1} against short-term temperature in °C (above). Model fit R^2, RMSE, and AICc found in top-right corner of top sub-plot. Mean modeled soil respiration in μmol CO_2 m^{-2} s^{-1} against mean observed respiration in μmol CO_2 m^{-2} s^{-1} (below). Ambient in black, low in red, mid in green, mid-high in blue, high in cyan, and hotspot in magenta for decadal warming levels.

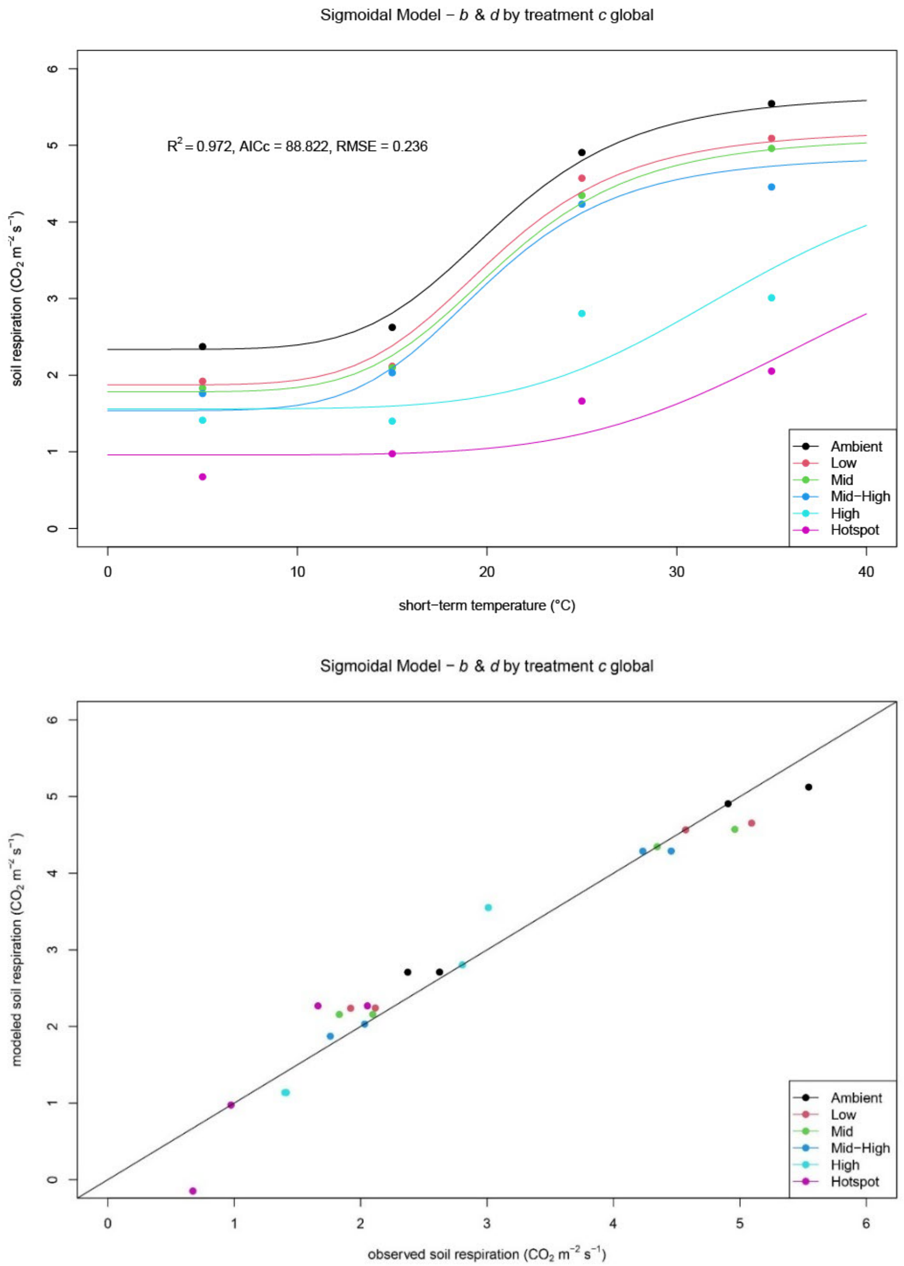

Figure S26. Sigmoidal model 6 with *b* and *d* adjusted by decadal warming level, *c* adjusted globally and *a* as a global constant, fit to soil respiration in µmol CO_2 m^{-2} s^{-1} against short-term temperature in °C (above). Model fit R^2, RMSE, and AICc found in top-right corner of top sub-plot. Mean modeled soil respiration in µmol CO_2 m^{-2} s^{-1} against mean observed respiration in µmol CO_2 m^{-2} s^{-1} (below). Ambient in black, low in red, mid in green, mid-high in blue, high in cyan, and hotspot in magenta for decadal warming levels.

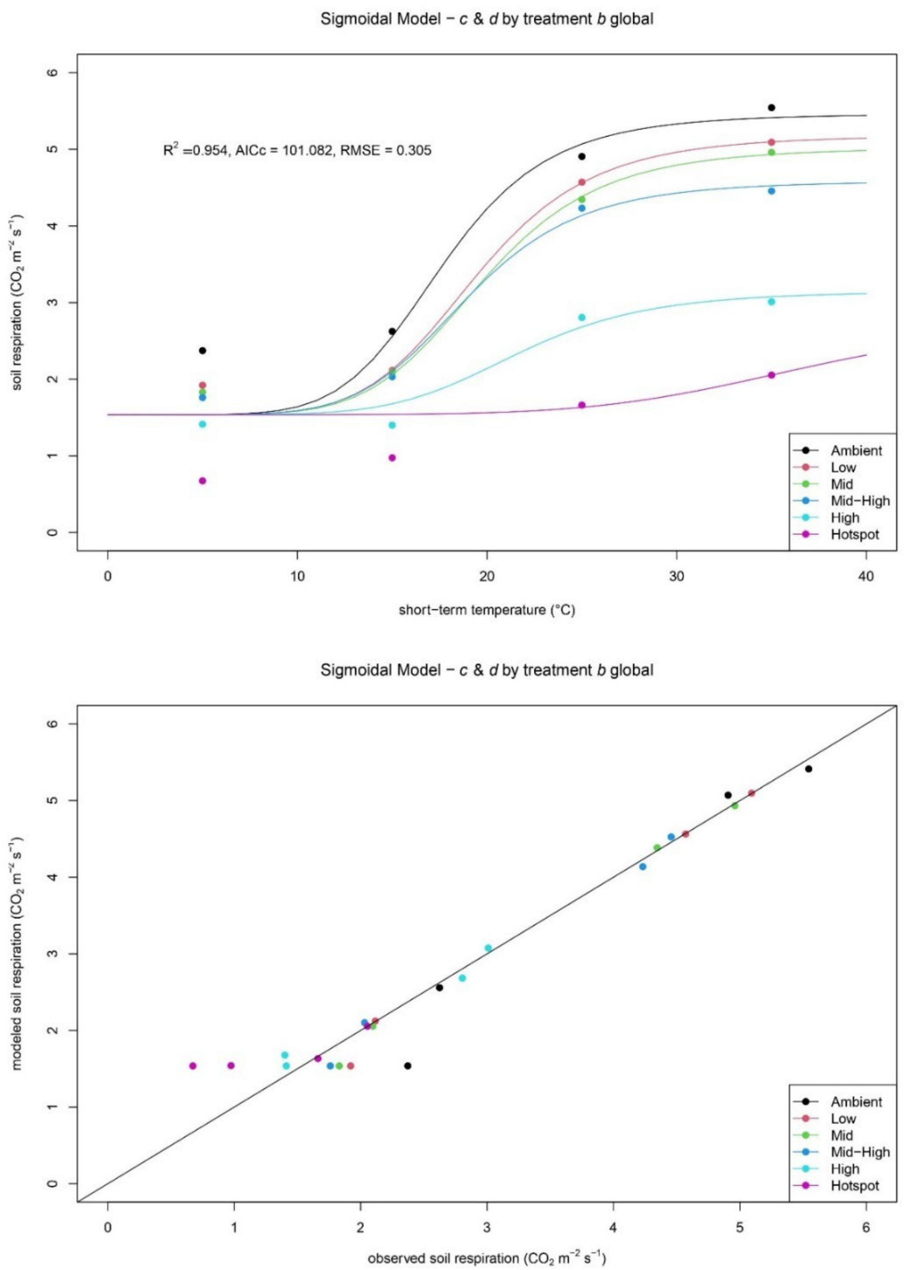

Figure S27. Sigmoidal model 7 with *c* and *d* adjusted by decadal warming level, *b* adjusted globally and *a* as a global constant, fit to soil respiration in μmol CO_2 m^{-2} s^{-1} against short-term temperature in °C (above). Model fit R^2, RMSE, and AICc found in top-right corner of top sub-plot. Mean modeled soil respiration in μmol CO_2 m^{-2} s^{-1} against mean observed respiration in μmol CO_2 m^{-2} s^{-1} (below). Ambient in black, low in red, mid in green, mid-high in blue, high in cyan, and hotspot in magenta for decadal warming levels.

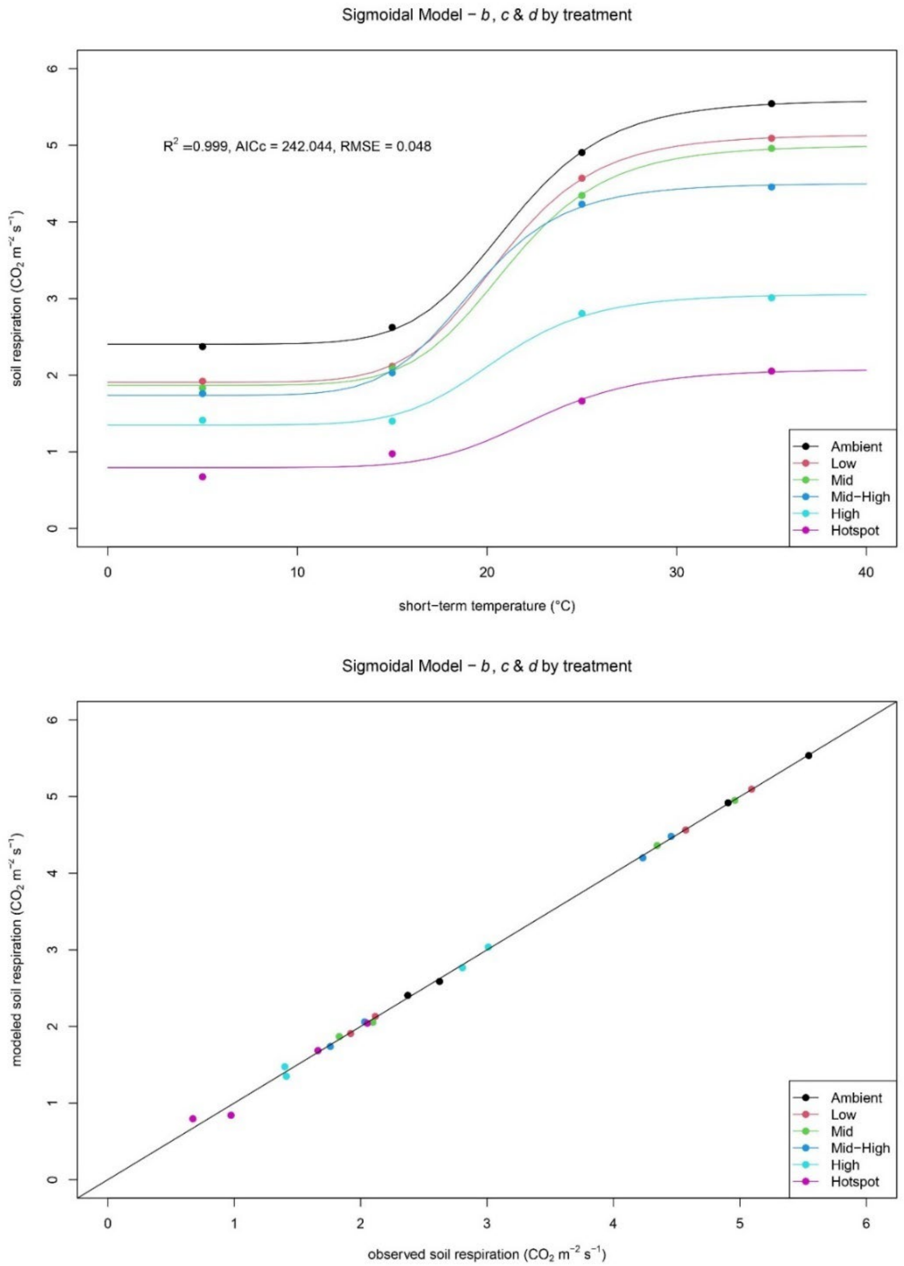

Figure S28. Sigmoidal model 8 with *b*, *c* and *d* adjusted by decadal warming level and *a* as a global constant, fit to soil respiration in µmol CO_2 m^{-2} s^{-1} against short-term temperature in °C (above). Model fit R^2, RMSE, and AICc found in top-right corner of top sub-plot. Mean modeled soil respiration in µmol CO_2 m^{-2} s^{-1} against mean observed respiration in µmol CO_2 m^{-2} s^{-1} (below). Ambient in black, low in red, mid in green, mid-high in blue, high in cyan, and hotspot in magenta for decadal warming levels.

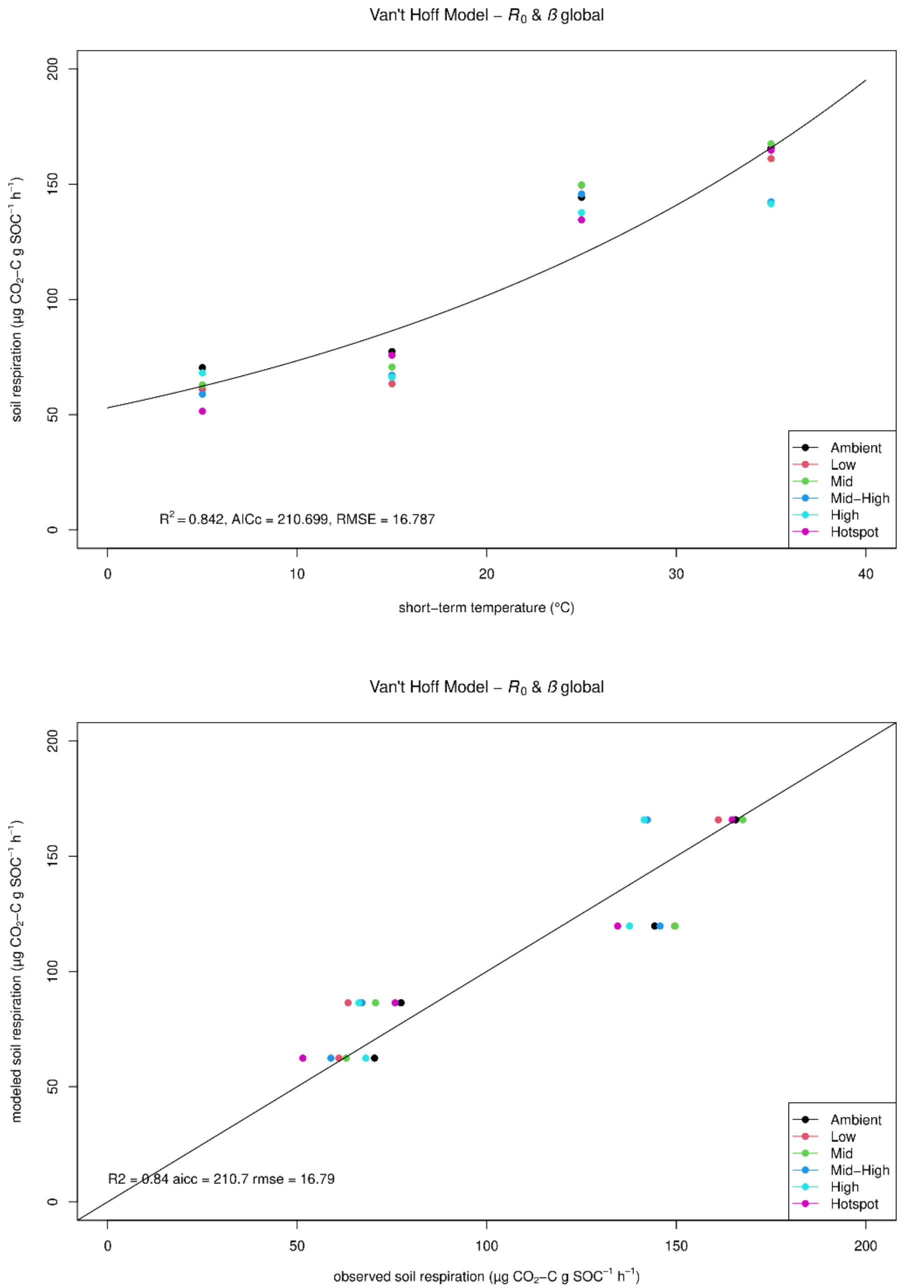

Figure S29. Van't Hoff model 1 with R_0 and β parameters adjusted globally, fit to soil respiration in µg CO_2-C g SOC^{-1} h^{-1} against short-term temperature in °C (above). Model fit R^2, RMSE, and AICc found in top-right corner of top sub-plot. Mean modeled soil respiration in µg CO_2-C g SOC^{-1} h^{-1} against mean observed respiration in µg CO_2-C g SOC^{-1} h^{-1} (below). Ambient in black, low in red, mid in green, mid-high in blue, high in cyan, and hotspot in magenta for decadal warming levels.

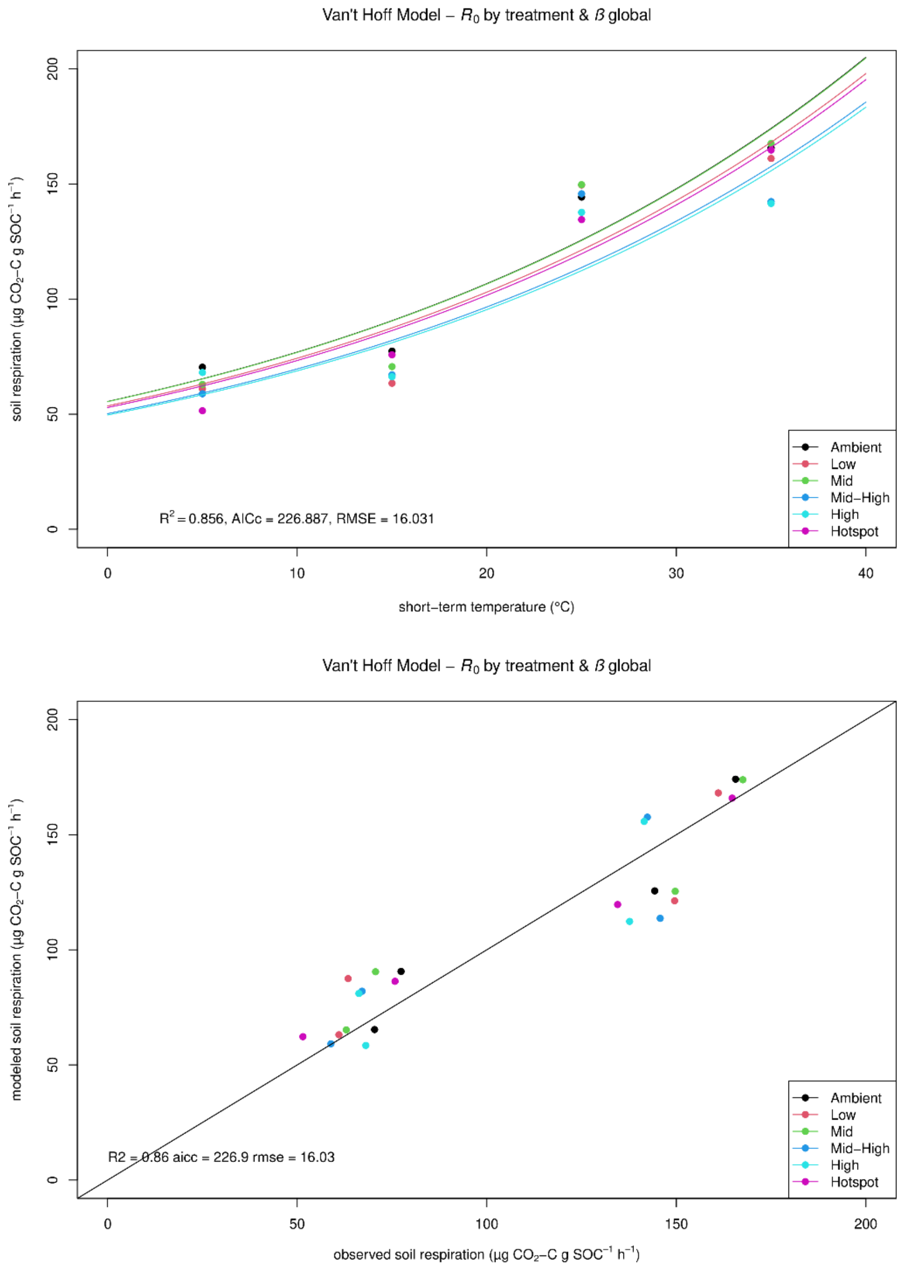

Figure S30. Van't Hoff model 2 with R_0 adjusted by decadal warming level and β adjusted globally, fit to soil respiration in µg CO_2-C g SOC^{-1} h^{-1} against short-term temperature in °C (above). Model fit R^2, RMSE, and AICc found in top-right corner of top sub-plot. Mean modeled soil respiration in µg CO_2-C g SOC^{-1} h^{-1} against mean observed respiration in µg CO_2-C g SOC^{-1} h^{-1} (below). Ambient in black, low in red, mid in green, mid-high in blue, high in cyan, and hotspot in magenta for decadal warming levels.

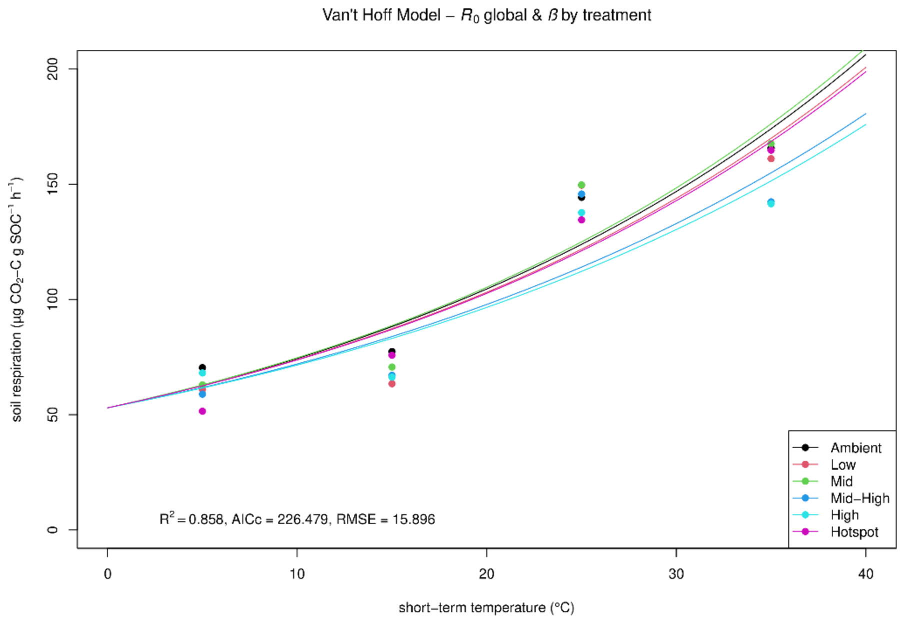

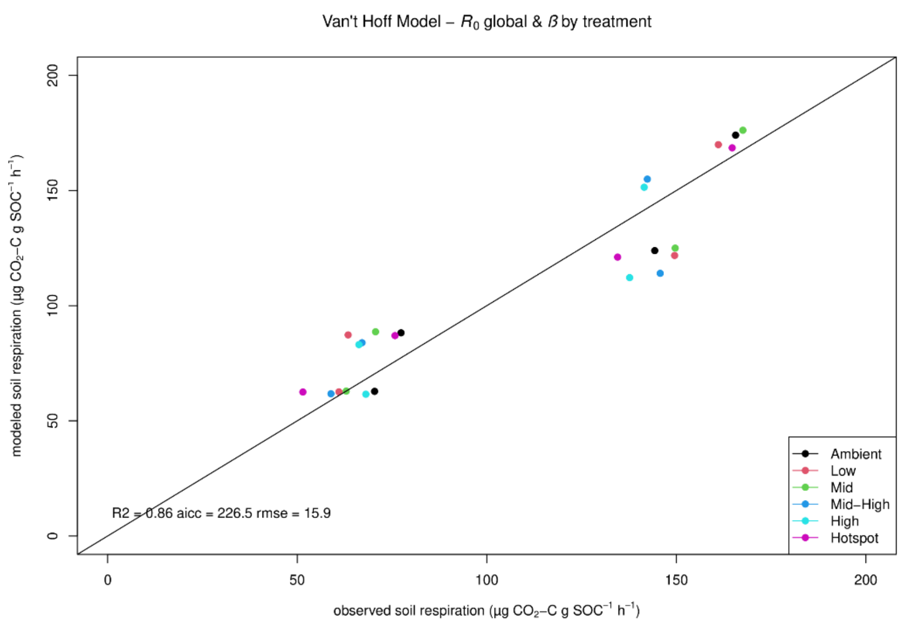

Figure S31. Van't Hoff model 3 with β adjusted by decadal warming level and R_0 adjusted globally, fit to soil respiration in μg CO_2-C g SOC^{-1} h^{-1} against short-term temperature in °C (above). Model fit R^2, RMSE, and AICc found in top-right corner of top sub-plot. Mean modeled soil respiration in μg CO_2-C g SOC^{-1} h^{-1} against mean observed respiration in μg CO_2-C g SOC^{-1} h^{-1} (below). Ambient in black, low in red, mid in green, mid-high in blue, high in cyan, and hotspot in magenta for decadal warming levels.

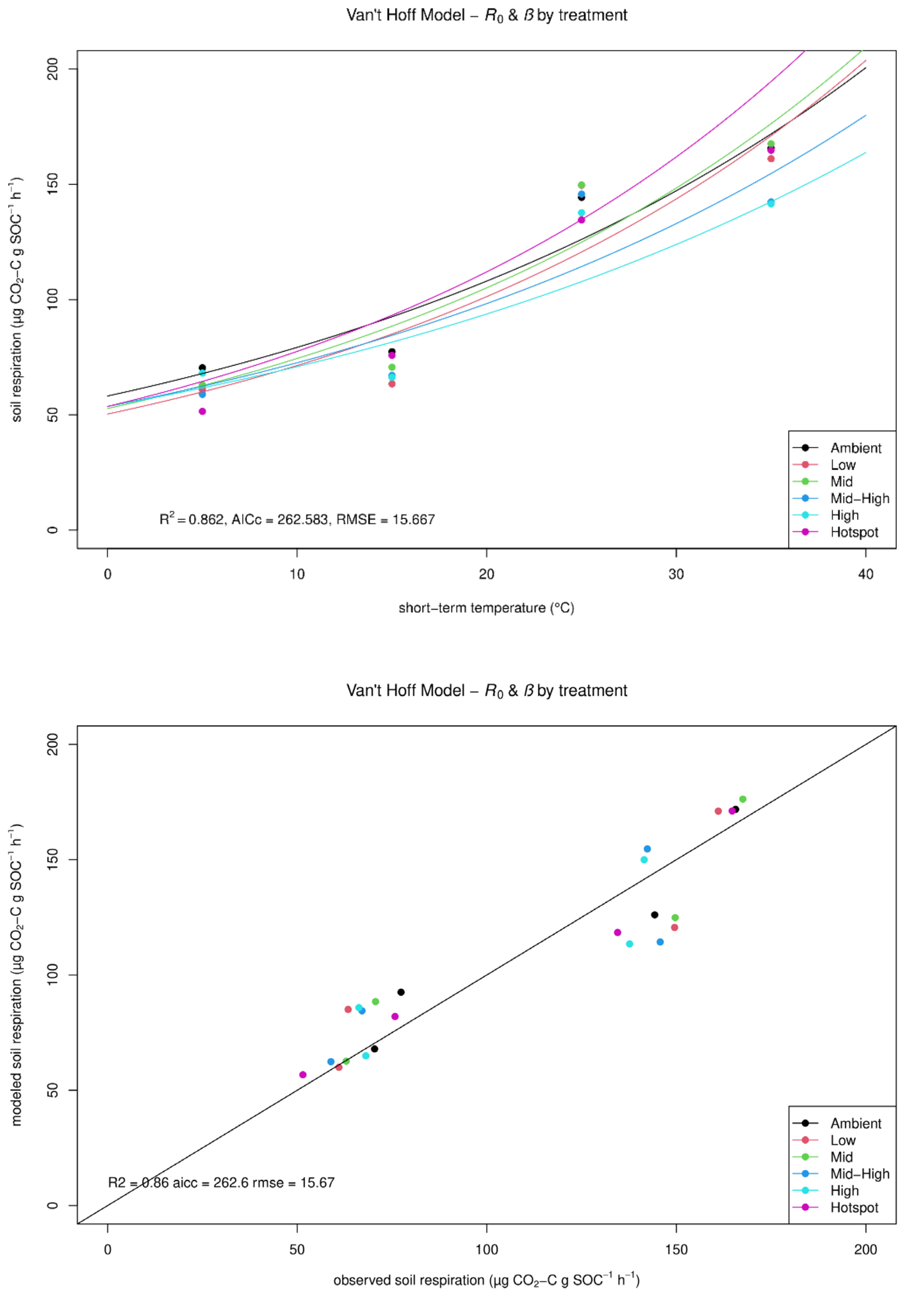

Figure S32. Van't Hoff model 4 with R_0 and β adjusted by decadal warming level, fit to soil respiration in µg CO_2-C g SOC^{-1} h^{-1} against short-term temperature in °C (above). Model fit R^2, RMSE, and AICc found in top-right corner of top sub-plot. Mean modeled soil respiration in µg CO_2-C g SOC^{-1} h^{-1} against mean observed respiration in µg CO_2-C g SOC^{-1} h^{-1} (below). Ambient in black, low in red, mid in green, mid-high in blue, high in cyan, and hotspot in magenta for decadal warming levels.

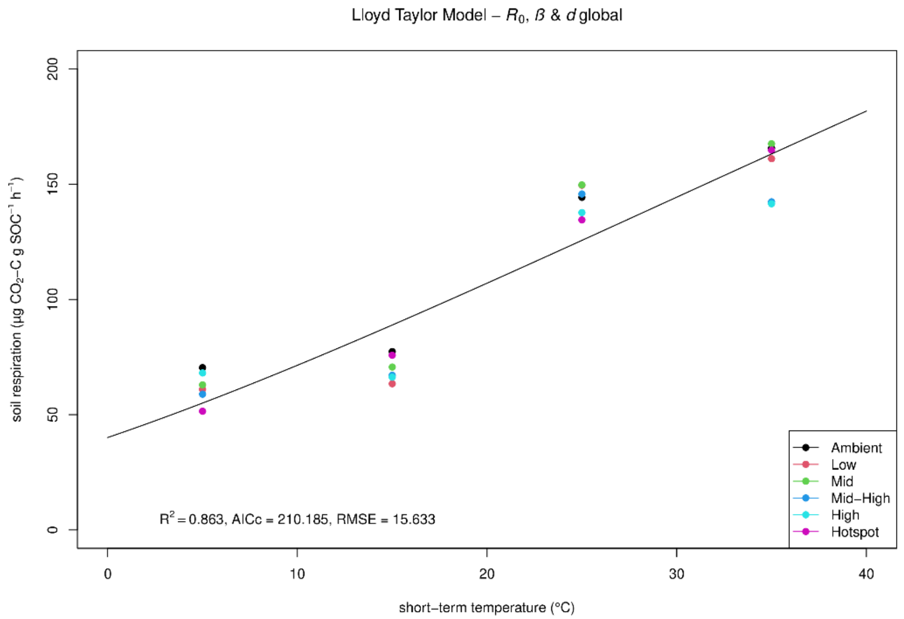

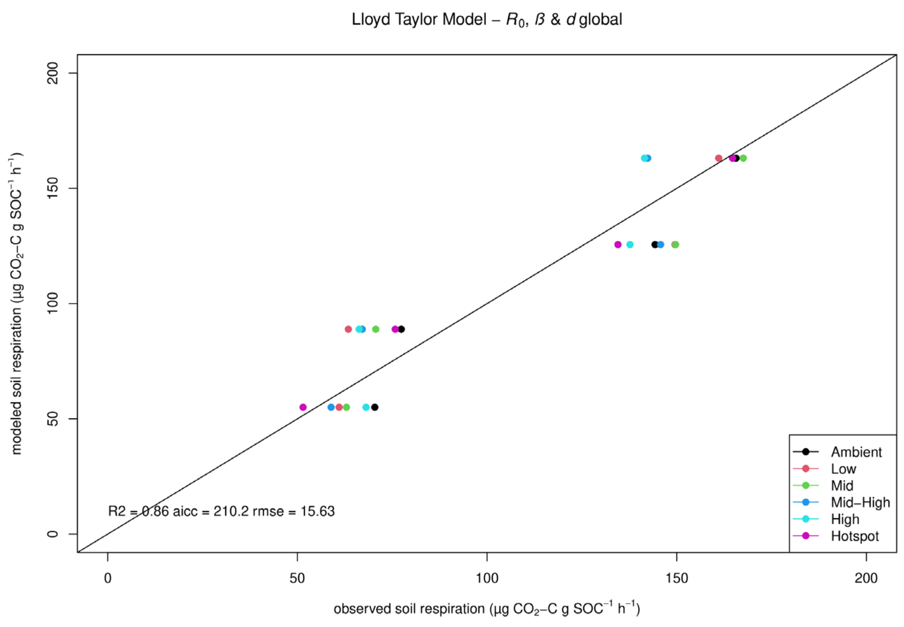

Figure S33. Lloyd-Taylor model 1 with R_0, β, and d parameters adjusted globally, fit to soil respiration in µg CO_2-C g SOC^{-1} h^{-1} against short-term temperature in °C (above). Model fit R^2, RMSE, and AICc found in top-right corner of top sub-plot. Mean modeled soil respiration in µg CO_2-C g SOC^{-1} h^{-1} against mean observed respiration in µg CO_2-C g SOC^{-1} h^{-1} (below). Ambient in black, low in red, mid in green, mid-high in blue, high in cyan, and hotspot in magenta for decadal warming levels.

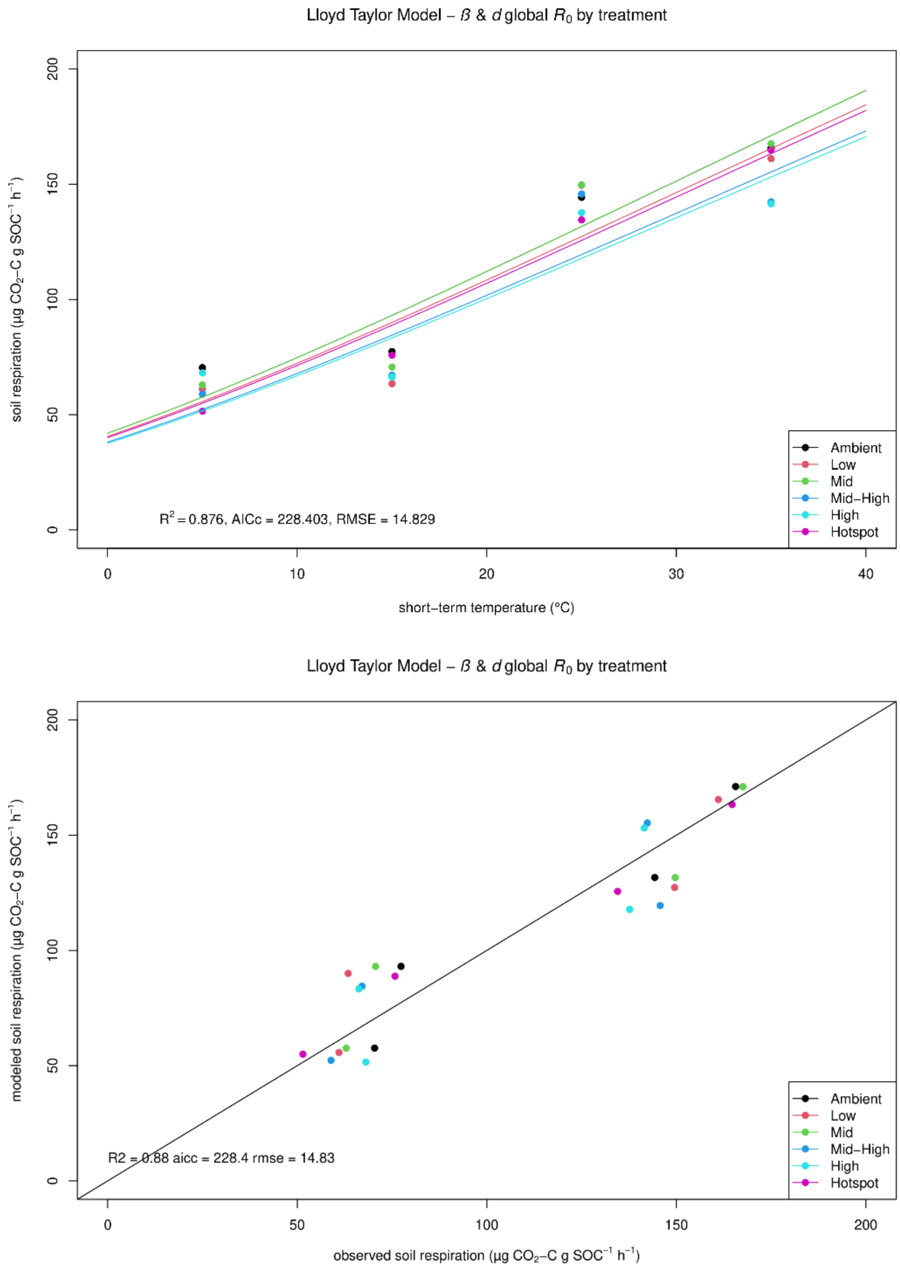

Figure S34. Lloyd-Taylor model 2 with R_0 adjusted by decadal warming level β and d adjusted globally, fit to soil respiration in µg CO_2-C g SOC^{-1} h^{-1} against short-term temperature in °C (above). Model fit R^2, RMSE, and AICc found in top-right corner of top sub-plot. Mean modeled soil respiration in µg CO_2-C g SOC^{-1} h^{-1} against mean observed respiration in µg CO_2-C g SOC^{-1} h^{-1} (below). Ambient in black, low in red, mid in green, mid-high in blue, high in cyan, and hotspot in magenta for decadal warming levels.

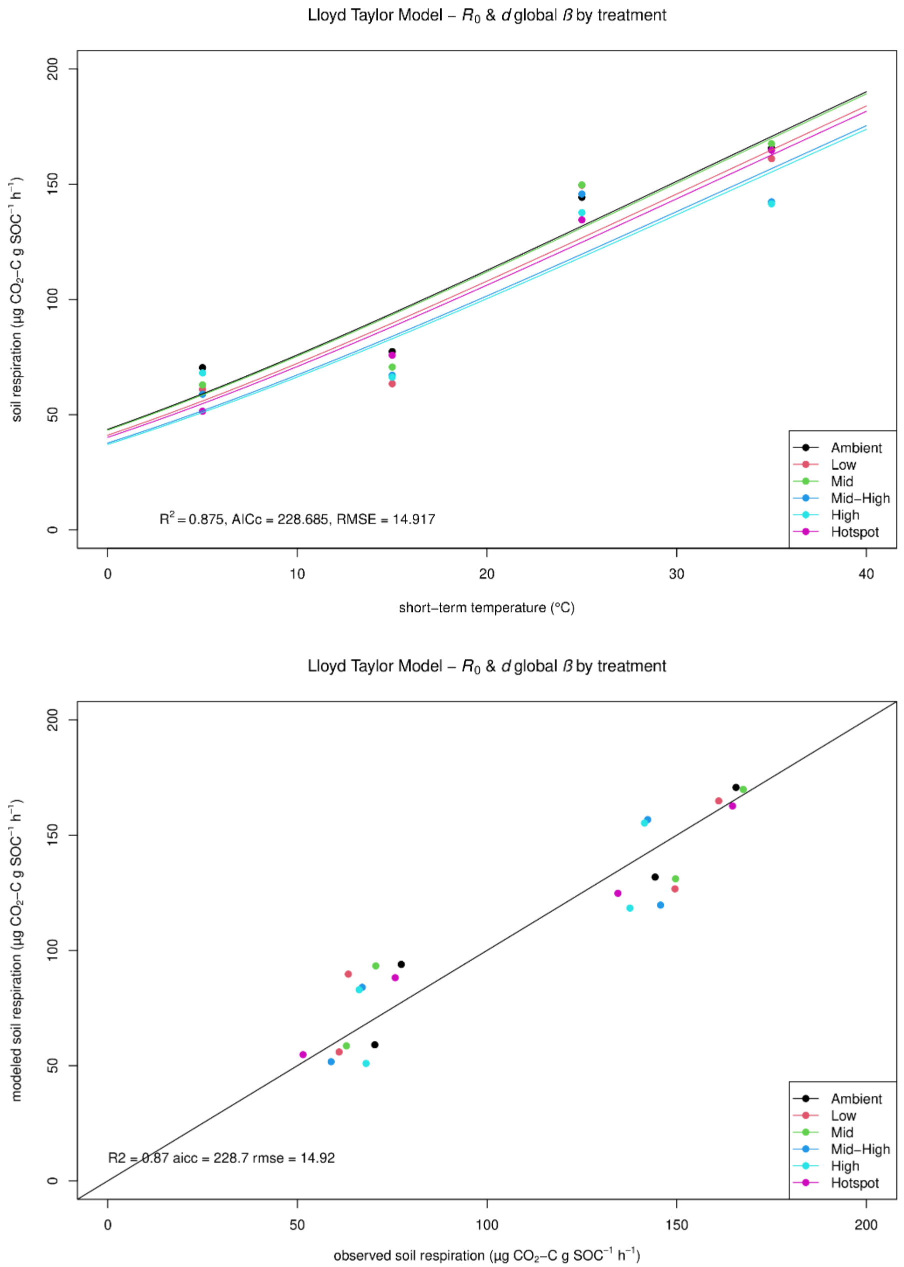

Figure S35. Lloyd-Taylor model 3 with β adjusted by decadal warming level R_0 and d adjusted globally, fit to soil respiration in µg CO_2-C g SOC^{-1} h^{-1} against short-term temperature in °C (above). Model fit R^2, RMSE, and AICc found in top-right corner of top sub-plot. Mean modeled soil respiration in µg CO_2-C g SOC^{-1} h^{-1} against mean observed respiration in µg CO_2-C g SOC^{-1} h^{-1} (below). Ambient in black, low in red, mid in green, mid-high in blue, high in cyan, and hotspot in magenta for decadal warming levels.

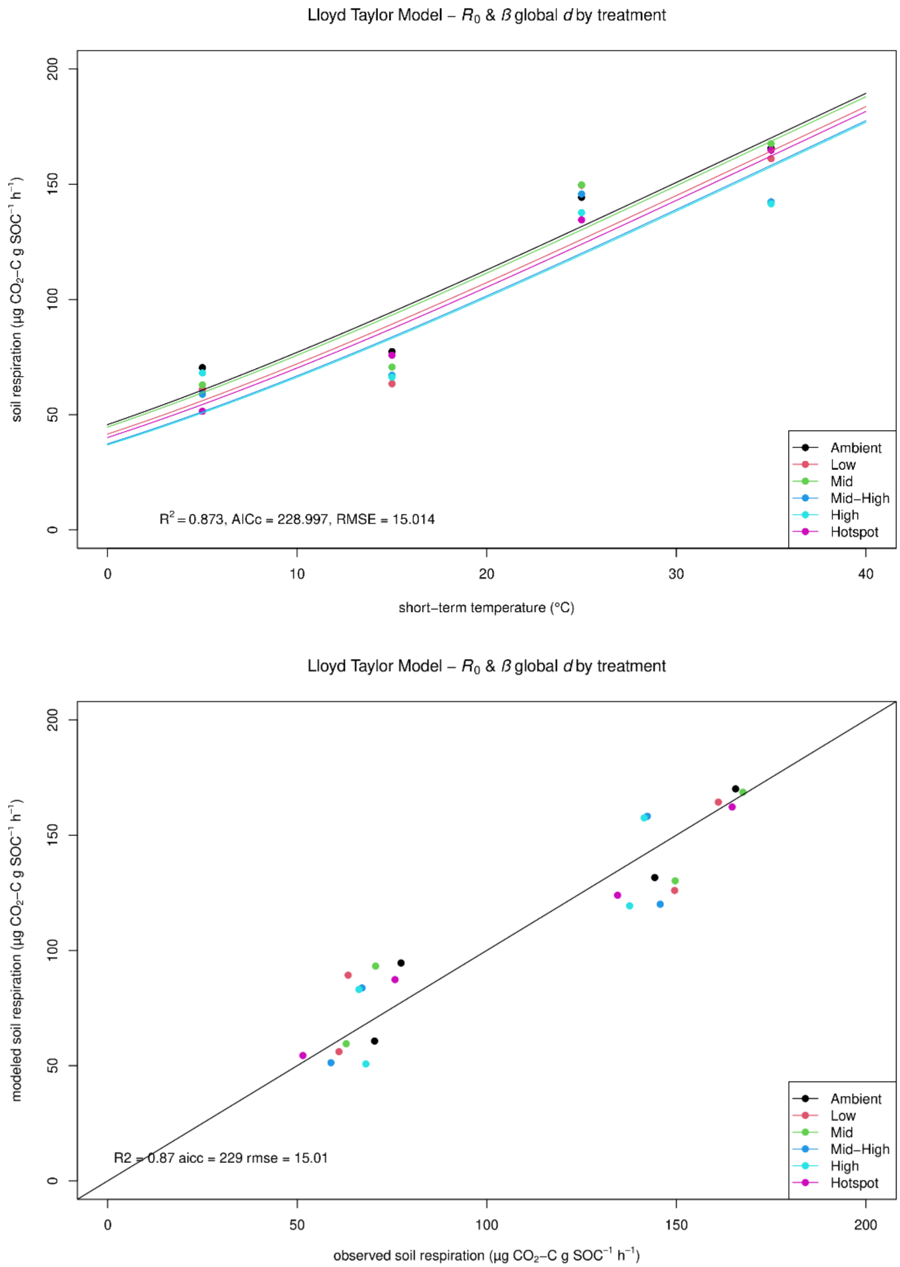

Figure S36. Lloyd-Taylor model 4 with *d* adjusted by decadal warming level R_0 and β adjusted globally, fit to soil respiration in µg CO_2-C g SOC^{-1} h^{-1} against short-term temperature in °C (above). Model fit R^2, RMSE, and AICc found in top-right corner of top sub-plot. Mean modeled soil respiration in µg CO_2-C g SOC^{-1} h^{-1} against mean observed respiration in µg CO_2-C g SOC^{-1} h^{-1} (below). Ambient in black, low in red, mid in green, mid-high in blue, high in cyan, and hotspot in magenta for decadal warming levels.

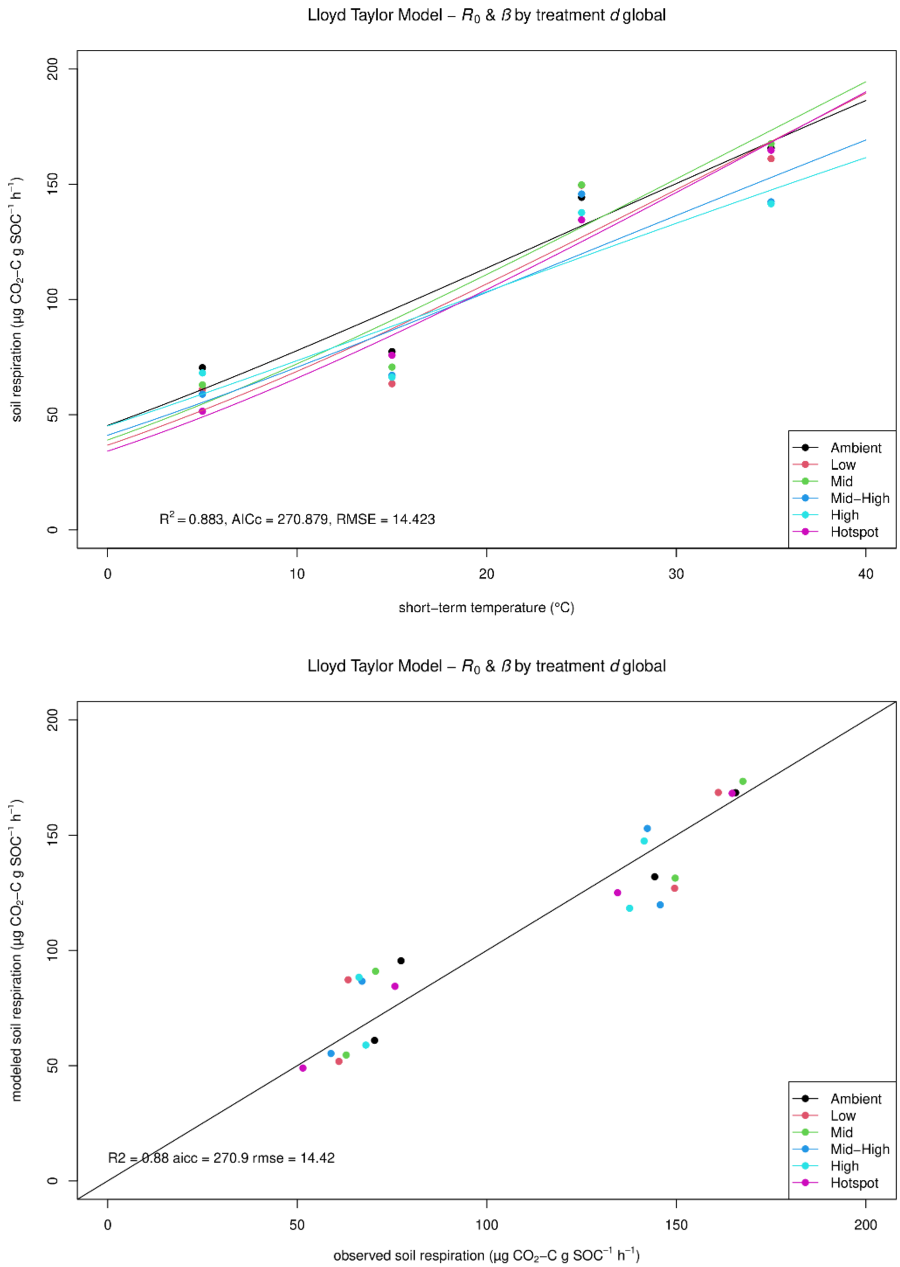

Figure S37. Lloyd-Taylor model 5 with R_0 and β adjusted by decadal warming level d adjusted globally, fit to soil respiration in µg CO_2-C g SOC^{-1} h^{-1} against short-term temperature in °C (above). Model fit R^2, RMSE, and AICc found in top-right corner of top sub-plot. Mean modeled soil respiration in µg CO_2-C g SOC^{-1} h^{-1} against mean observed respiration in µg CO_2-C g SOC^{-1} h^{-1} (below). Ambient in black, low in red, mid in green, mid-high in blue, high in cyan, and hotspot in magenta for decadal warming levels.

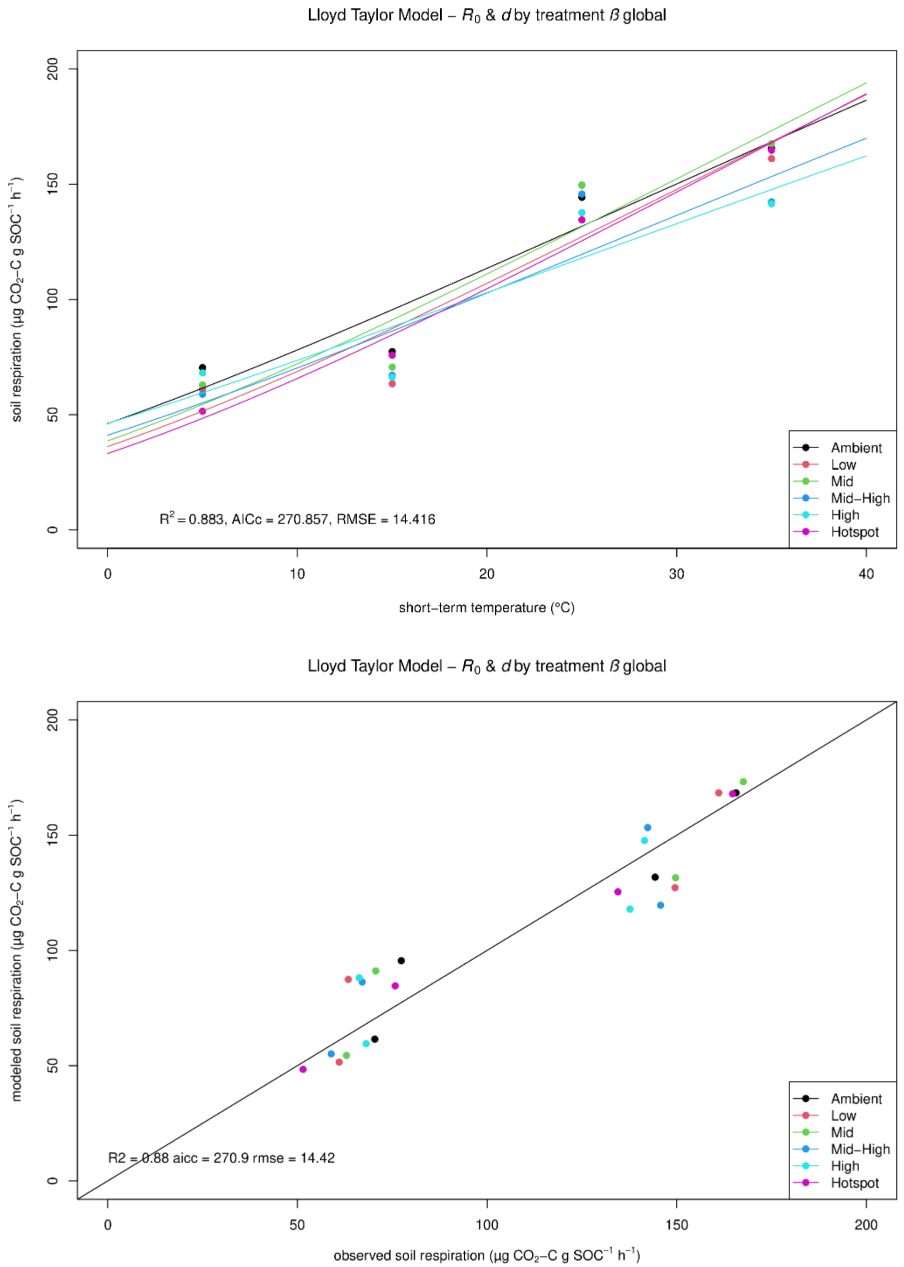

Figure S38. Lloyd-Taylor model 6 with R_0 and d adjusted by decadal warming level β adjusted globally, fit to soil respiration in µg CO_2-C g SOC^{-1} h^{-1} against short-term temperature in °C (above). Model fit R^2, RMSE, and AICc found in top-right corner of top sub-plot. Mean modeled soil respiration in µg CO_2-C g SOC^{-1} h^{-1} against mean observed respiration in µg CO_2-C g SOC^{-1} h^{-1} (below). Ambient in black, low in red, mid in green, mid-high in blue, high in cyan, and hotspot in magenta for decadal warming levels.

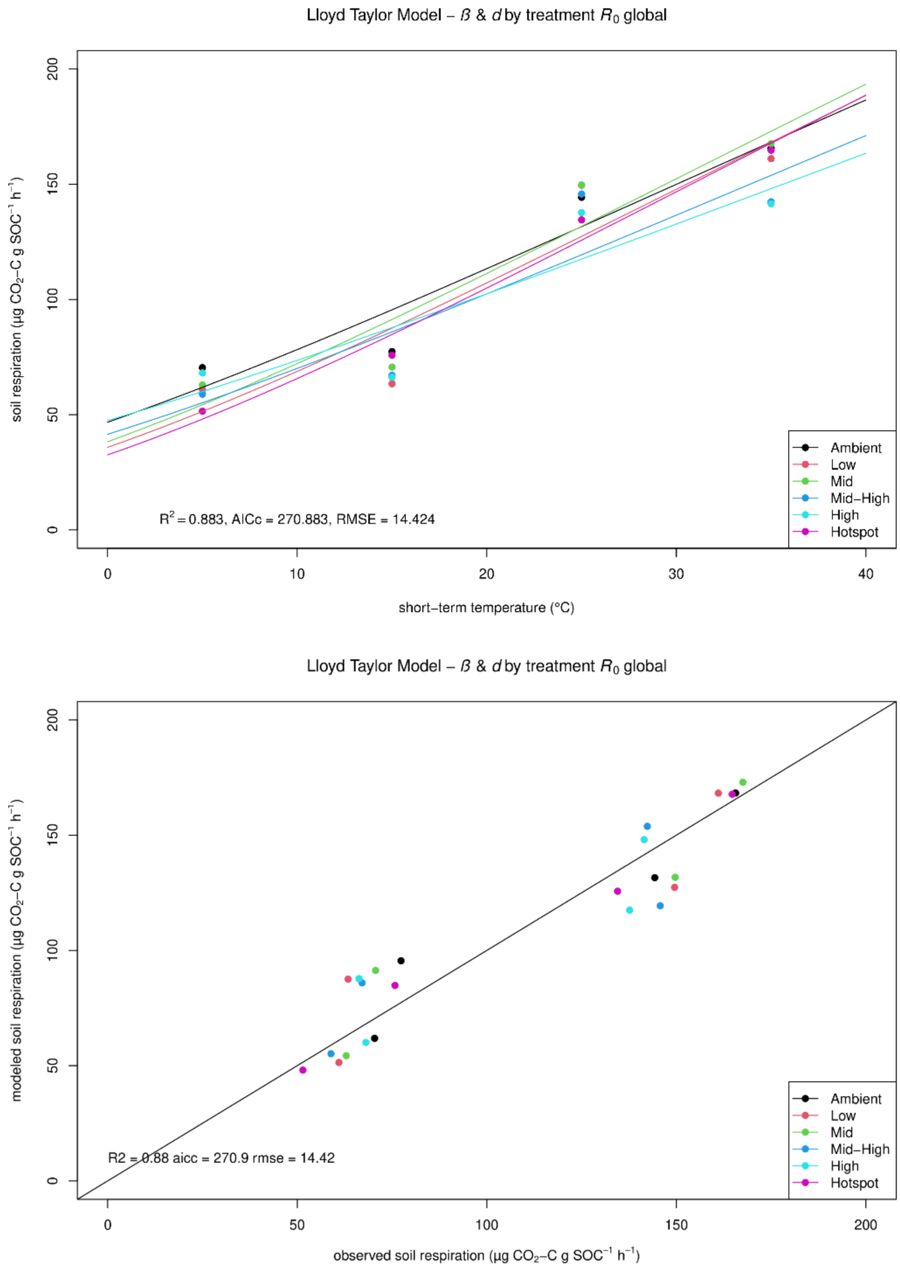

Figure S39. Lloyd-Taylor model 7 with *β* and *d* adjusted by decadal warming level R_0 adjusted globally, fit to soil respiration in µg CO_2-C g SOC^{-1} h^{-1} against short-term temperature in °C (above). Model fit R^2, RMSE, and AICc found in top-right corner of top sub-plot. Mean modeled soil respiration in µg CO_2-C g SOC^{-1} h^{-1} against mean observed respiration in µg CO_2-C g SOC^{-1} h^{-1} (below). Ambient in black, low in red, mid in green, mid-high in blue, high in cyan, and hotspot in magenta for decadal warming levels.

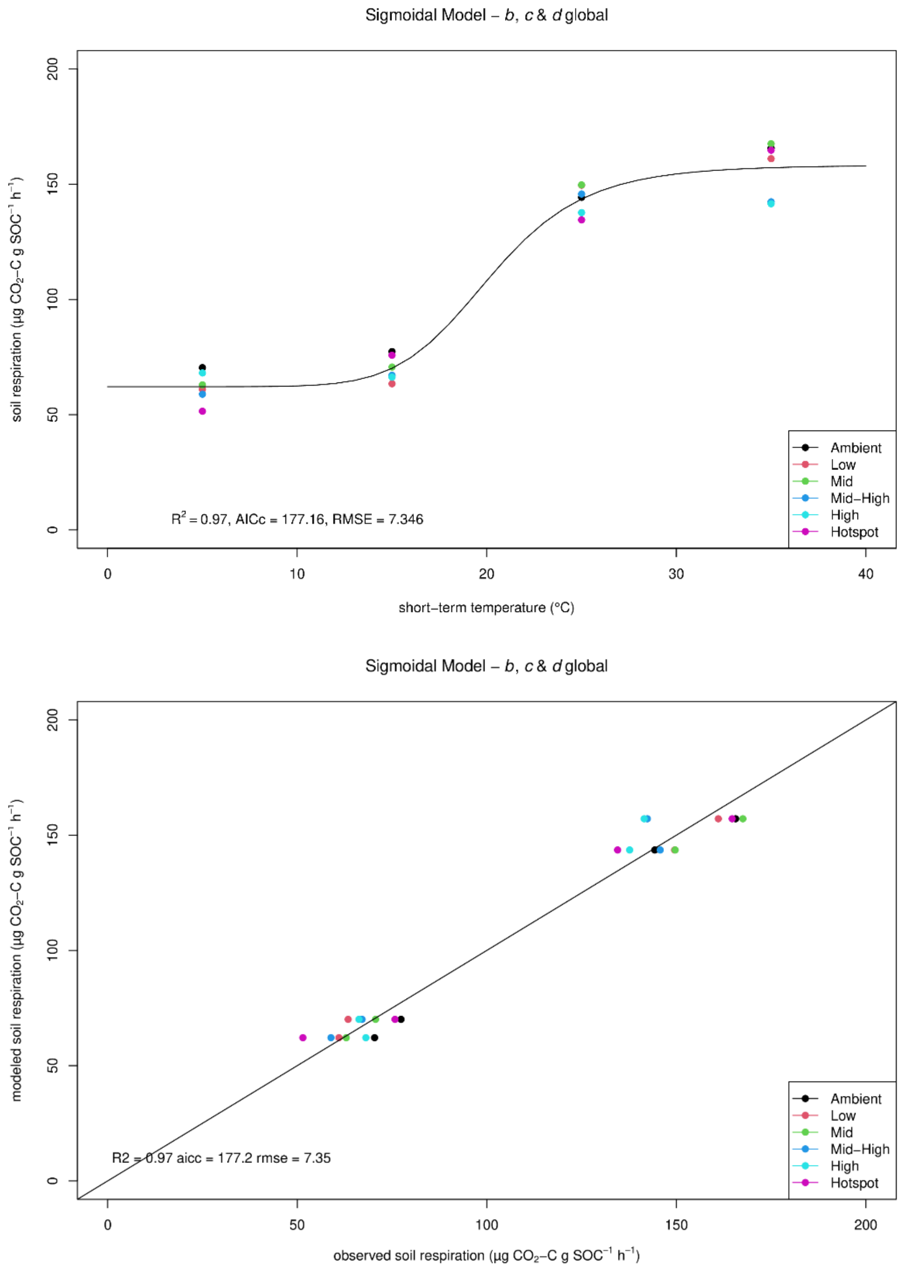

Figure S40. Sigmoidal model 1 with *b*, *c*, and *d* parameters adjusted globally and *a* as a global constant, fit to soil respiration in µg CO_2-C g SOC^{-1} h^{-1} against short-term temperature in °C (above). Model fit R^2, RMSE, and AICc found in top-right corner of top sub-plot. Mean modeled soil respiration in µg CO_2-C g SOC^{-1} h^{-1} against mean observed respiration in µg CO_2-C g SOC^{-1} h^{-1} (below). Ambient in black, low in red, mid in green, mid-high in blue, high in cyan, and hotspot in magenta for decadal warming levels.

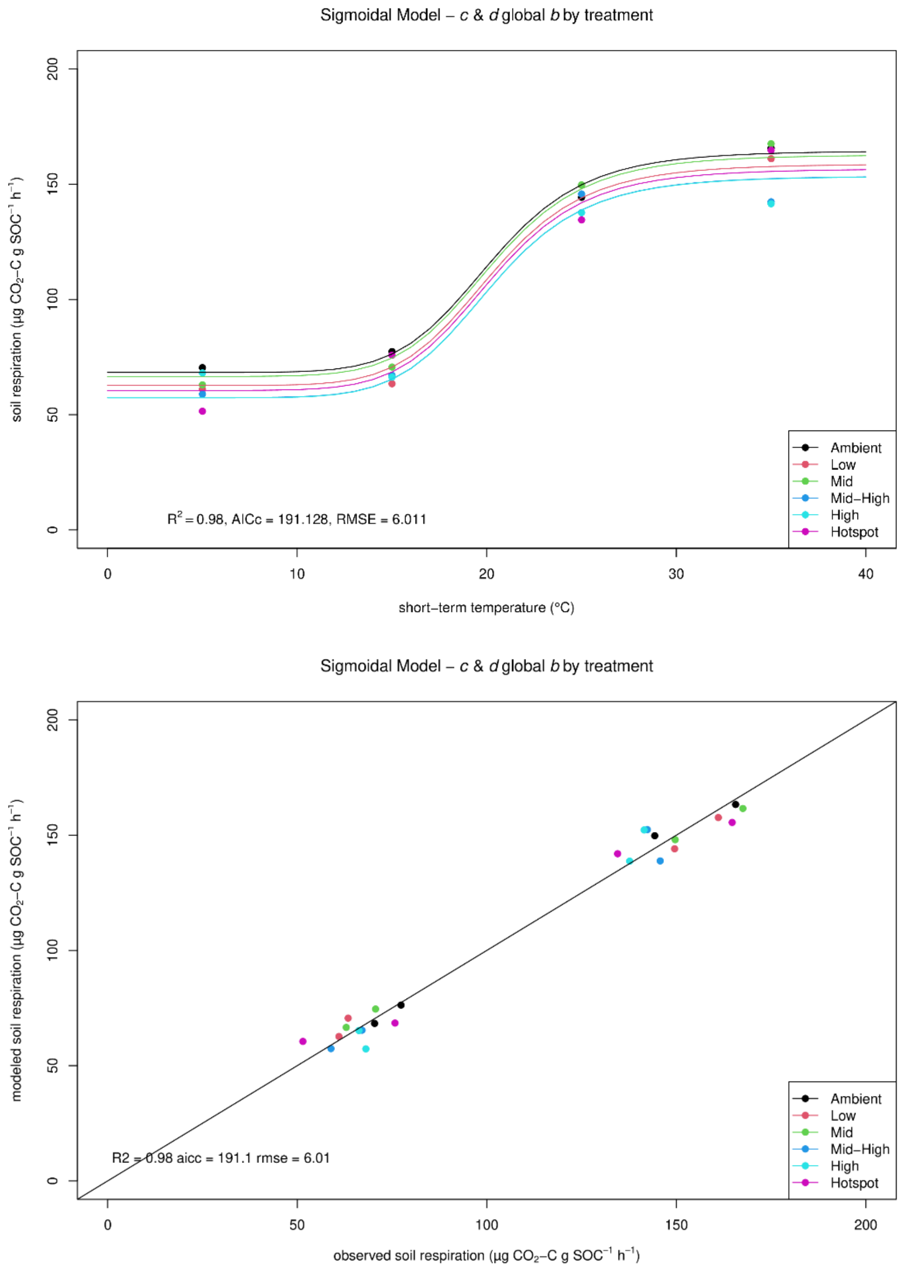

Figure S41. Sigmoidal model 2 with *b* adjusted by decadal warming level, *c* and *d* adjusted globally and *a* as a global constant, fit to soil respiration in μg CO_2-C g SOC^{-1} h^{-1} against short-term temperature in °C (above). Model fit R^2, RMSE, and AICc found in top-right corner of top sub-plot. Mean modeled soil respiration in μg CO_2-C g SOC^{-1} h^{-1} against mean observed respiration in μg CO_2-C g SOC^{-1} h^{-1} (below). Ambient in black, low in red, mid in green, mid-high in blue, high in cyan, and hotspot in magenta for decadal warming levels.

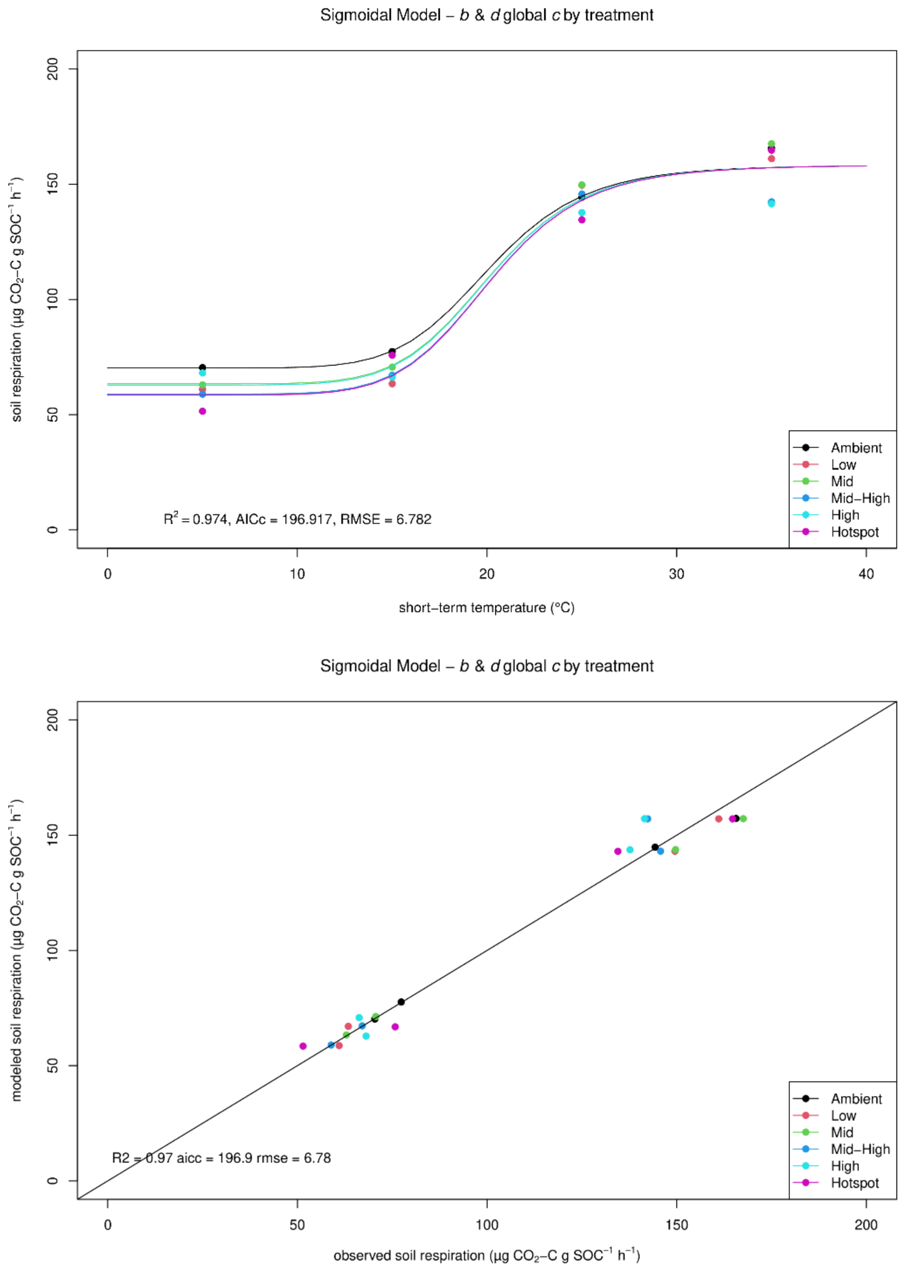

Figure S42. Sigmoidal model 3 with *c* adjusted by decadal warming level, *b* and *d* adjusted globally and *a* as a global constant, fit to soil respiration in µg CO_2-C g SOC^{-1} h^{-1} against short-term temperature in °C (above). Model fit R^2, RMSE, and AICc found in top-right corner of top sub-plot. Mean modeled soil respiration in µg CO_2-C g SOC^{-1} h^{-1} against mean observed respiration in µg CO_2-C g SOC^{-1} h^{-1} (below). Ambient in black, low in red, mid in green, mid-high in blue, high in cyan, and hotspot in magenta for decadal warming levels.

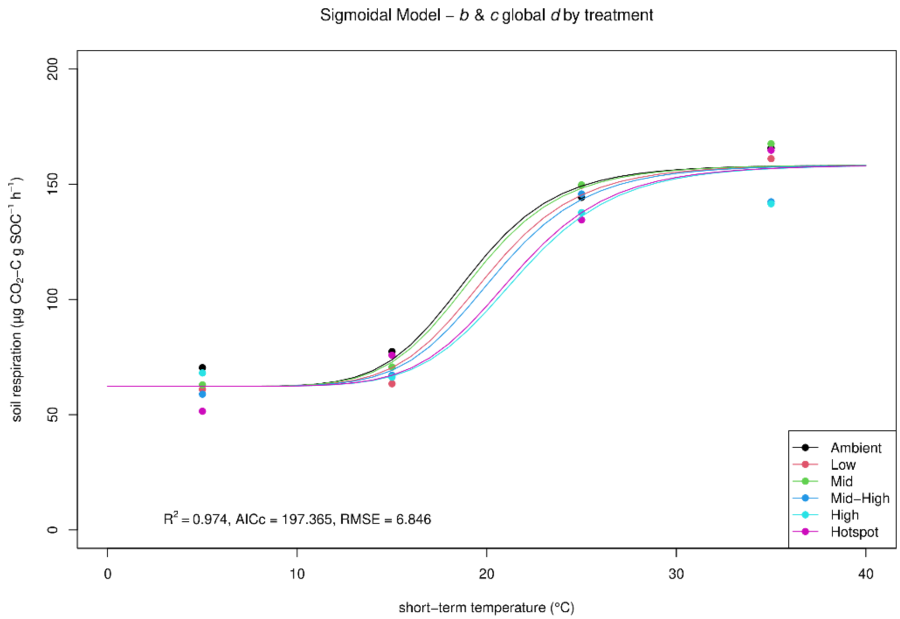

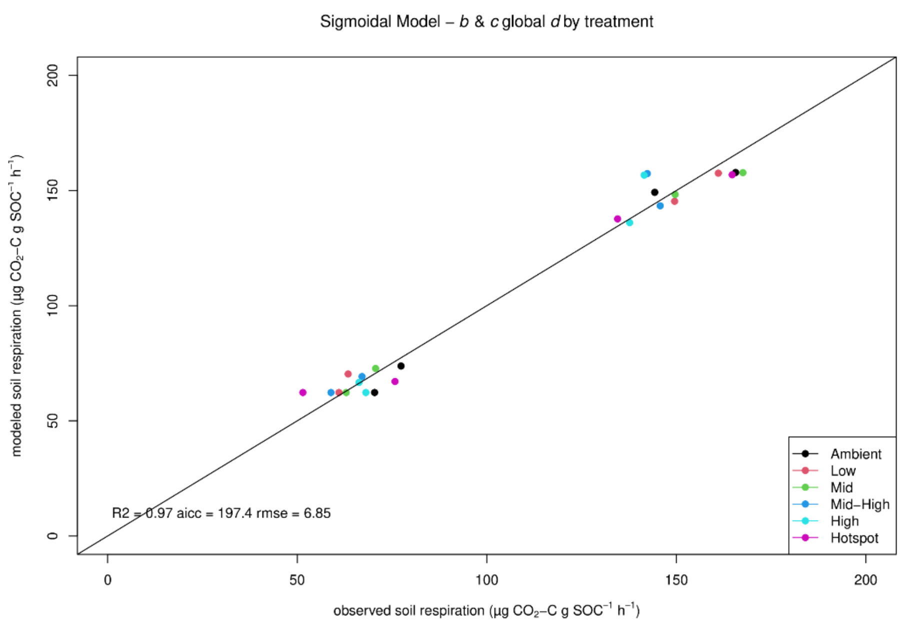

Figure S43. Sigmoidal model 4 with *d* adjusted by decadal warming level, *b* and *c* adjusted globally and *a* as a global constant, fit to soil respiration in µg CO_2-C g SOC^{-1} h^{-1} against short-term temperature in °C (above). Model fit R^2, RMSE, and AICc found in top-right corner of top sub-plot. Mean modeled soil respiration in µg CO_2-C g SOC^{-1} h^{-1} against mean observed respiration in µg CO_2-C g SOC^{-1} h^{-1} (below). Ambient in black, low in red, mid in green, mid-high in blue, high in cyan, and hotspot in magenta for decadal warming levels.

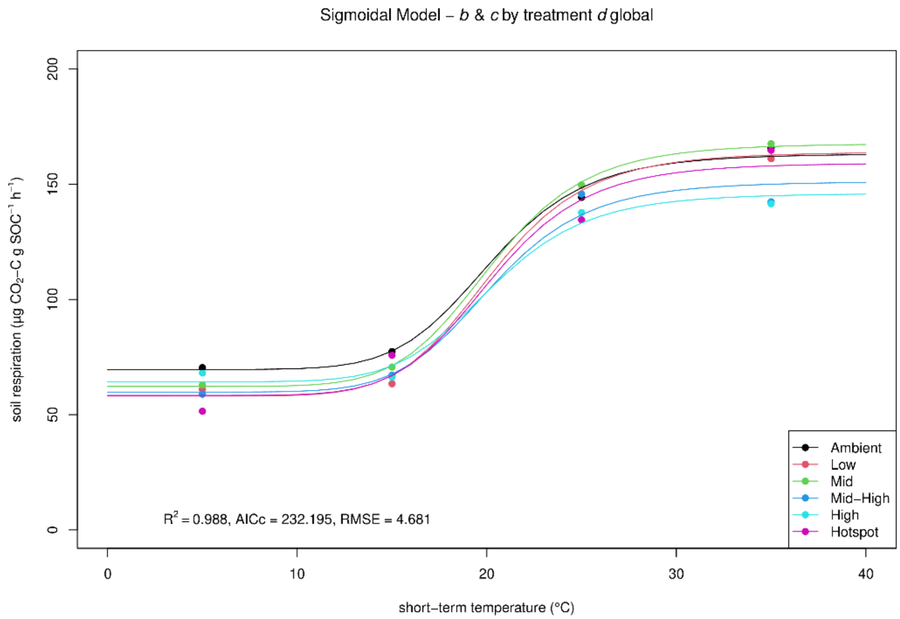

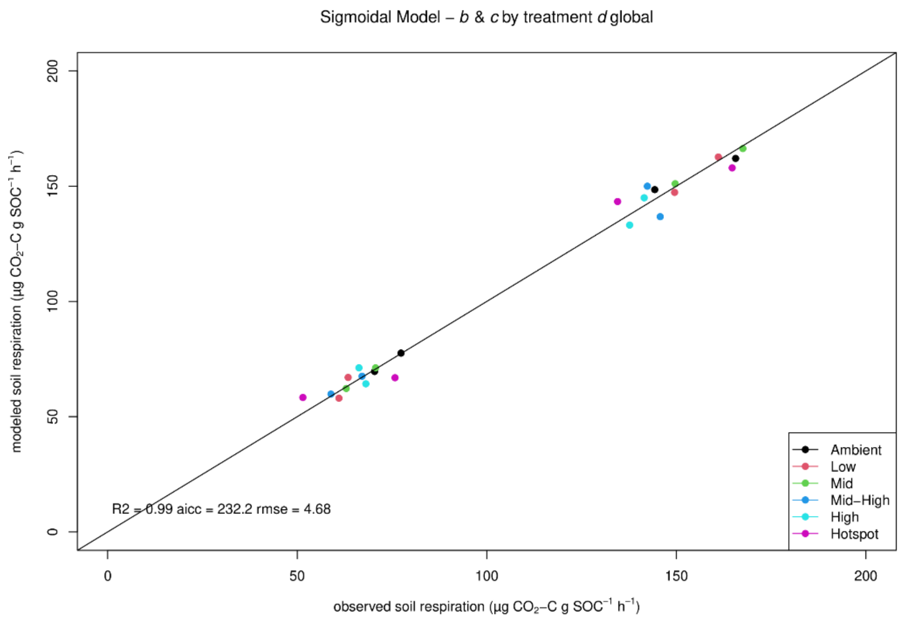

Figure S44. Sigmoidal model 5 with *b* and *c* adjusted by decadal warming level, *d* adjusted globally and *a* as a global constant, fit to soil respiration in µg CO_2-C g SOC^{-1} h^{-1} against short-term temperature in °C (above). Model fit R^2, RMSE, and AICc found in top-right corner of top sub-plot. Mean modeled soil respiration in µg CO_2-C g SOC^{-1} h^{-1} against mean observed respiration in µg CO_2-C g SOC^{-1} h^{-1} (below). Ambient in black, low in red, mid in green, mid-high in blue, high in cyan, and hotspot in magenta for decadal warming levels.

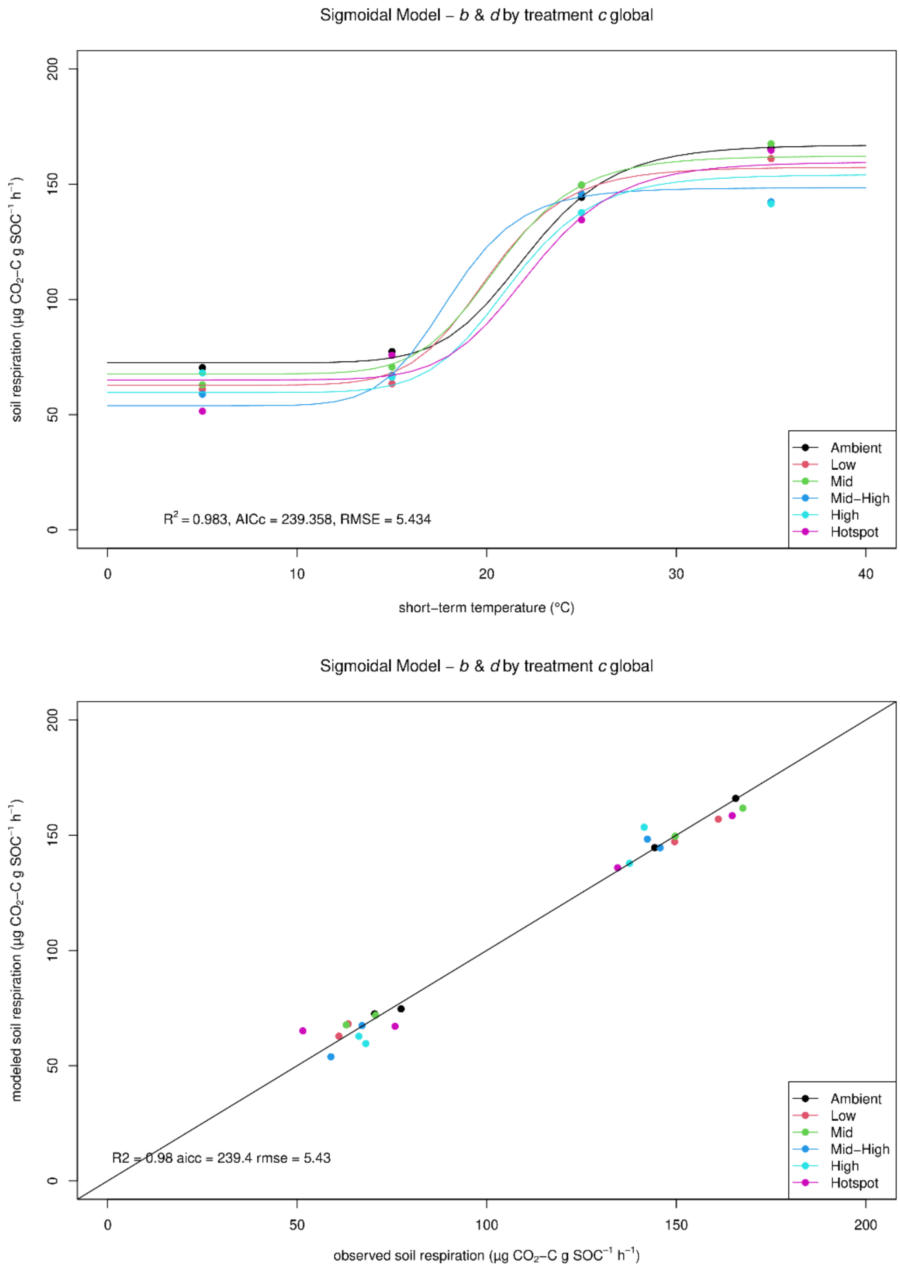

Figure S45. Sigmoidal model 6 with *b* and *d* adjusted by decadal warming level, *c* adjusted globally and *a* as a global constant, fit to soil respiration in µg CO_2-C g SOC^{-1} h^{-1} against short-term temperature in °C (above). Model fit R^2, RMSE, and AICc found in top-right corner of top sub-plot. Mean modeled soil respiration in µg CO_2-C g SOC^{-1} h^{-1} against mean observed respiration in µg CO_2-C g SOC^{-1} h^{-1} (below). Ambient in black, low in red, mid in green, mid-high in blue, high in cyan, and hotspot in magenta for decadal warming levels.

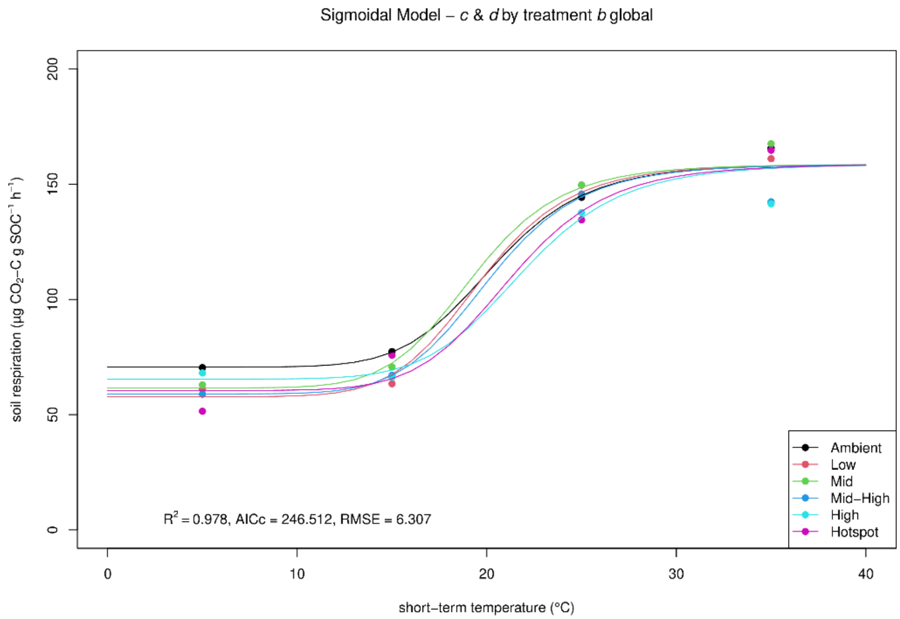

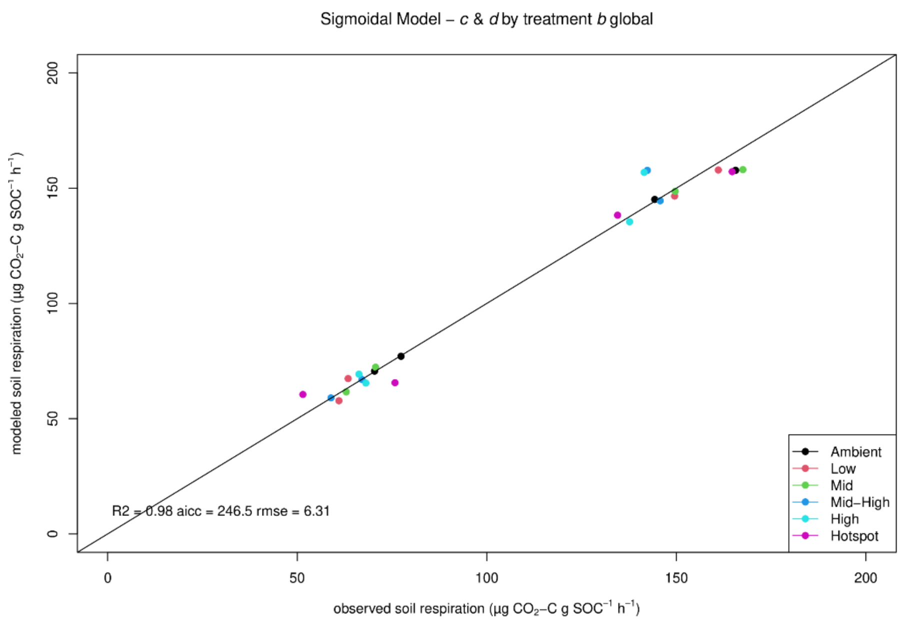

Figure S46. Sigmoidal model 7 with *c* and *d* adjusted by decadal warming level, *b* adjusted globally and *a* as a global constant, fit to soil respiration in µg CO_2-C g SOC^{-1} h^{-1} against short-term temperature in °C (above). Model fit R^2, RMSE, and AICc found in top-right corner of top sub-plot. Mean modeled soil respiration in µg CO_2-C g SOC^{-1} h^{-1} against mean observed respiration in µg CO_2-C g SOC^{-1} h^{-1} (below). Ambient in black, low in red, mid in green, mid-high in blue, high in cyan, and hotspot in magenta for decadal warming levels.

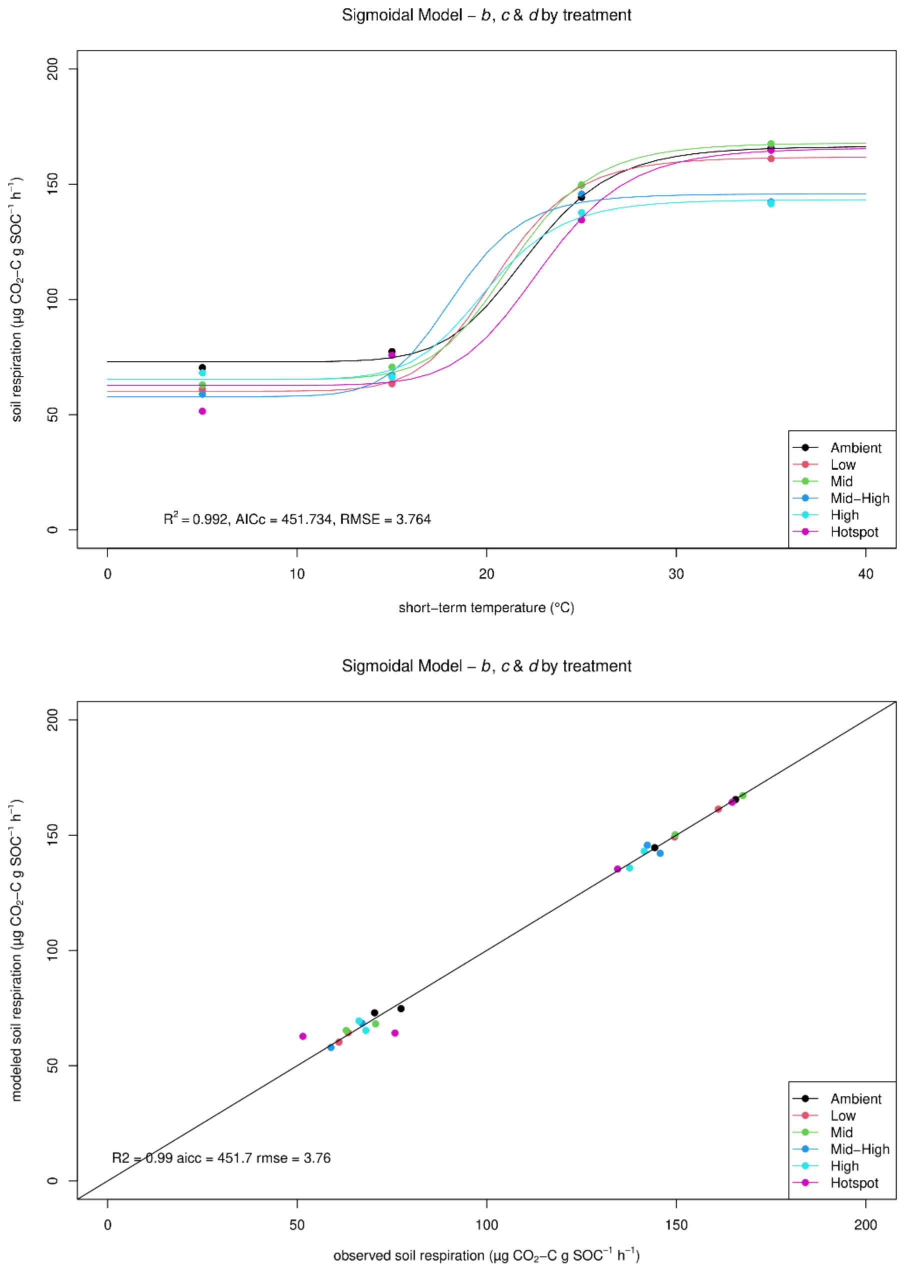

Figure S47. Sigmoidal model 8 with *b*, *c* and *d* adjusted by decadal warming level and *a* as a global constant, fit to soil respiration in µg CO_2-C g SOC^{-1} h^{-1} against short-term temperature in °C (above). Model fit R^2, RMSE, and AICc found in top-right corner of top sub-plot. Mean modeled soil respiration in µg CO_2-C g SOC^{-1} h^{-1} against mean observed respiration in µg CO_2-C g SOC^{-1} h^{-1} (below). Ambient in black, low in red, mid in green, mid-high in blue, high in cyan, and hotspot in magenta for decadal warming levels.